Investigations on Possible Realization of Log Periodic Dielectric Resonator Antenna

Runa Kumari

Department of Electronics and Communication Engineering
National Institute of Technology Rourkela
Rourkela-769 008, Odisha, India

Investigations on Possible Realization of Log Periodic Dielectric Resonator Antennas

Thesis submitted in partial fulfillment
of the requirements for the degree of

Doctor of Philosophy

in

Electronics and Communication Engineering

by

Runa Kumari
(Roll: 509EC103)

under the guidance of

Dr. Santanu Kumar Behera

Department of Electronics and Communiation Engineering
National Institute of Technology Rourkela
Rourkela-769 008, Odisha, India

2013

Dedicated to my Parents without whom none of my success would be possible.

Department of Electronics and Communication Engg.
National Institute of Technology Rourkela
Rourkela-769 008, Odisha, India.

July 8, 2014

CERTIFICATE

This is to certify that the thesis titled ***Investigations on Possible Realization of Log Periodic Dielectric Resonator Antenna*** by ***Runa Kumari*** is a record of an original research work carried out under my supervision and guidance in partial fulfillment of the requirements for the award of the degree of Doctor of philosophy in ***Electronics and Communication Engineering*** during the session 2013-2014. I believe that the thesis fulfills part of the requirements for the award of degree of Doctor of Philosophy. Neither this thesis nor any part of it has been submitted for any degree or academic award elsewhere.

Dr. Santanu Kumar Behera
Asso. Professor
Dept. of ECE
National Institute of Technology, Rourkela
Odisha, India - 769 008

Acknowledgement

"It is a myth that a dissertation is the soul-wrenching creation solely of its author's time, toil and tenacity. Many people conspire and encourage the author to achieve the goal."

I thank these people for conspiring to do so...

I am thankful to Prof. S. K. Behera, my advisor, for giving me guidance, counsel, and for having faith and confidence in me. I thank him for his support, patience, and encouragement throughout my research work. His technical and editorial advice was essential to the completion of this dissertation. His patience in reading draft after draft of every paper, proposal and chapters of thesis continues to amaze me. I am indebted to him for the valuable time he has spared for me during this work.

I am grateful to Prof. S. K. Sarangi, Director, NIT Rourkela for providing me adequate infrastructure to carry out the present investigations.

I am grateful to my DSC members Prof. S. K. Patra, Prof. S. K. Jena and Prof. P. K. Sahu for their valuable comments. I have benefitted greatly from their suggestions. I would like to thank Professor S. Meher, Head of Department, ECE for providing the opportunity to work on this research area. I thank from bottom of my heart Prof. R. K. Mishra, Dept. of Electronic science, Berhampur University, Orissa, for his support and good will through all these years.

My thanks go to Prof. R. K. Mishra and Prof. S .Meher for reading the drafts of research papers and dissertation and providing many valuable comments that improved the presentation and contents of this dissertation. Their incisive comments made me re-think to present my ideas. Any errors that remain in this presentation are attributable to my negligence.

I am obliged to Prof. S. K. Sharma, Dept. of ECE, SDSU, USA, for providing a solid background for my research work, whose involvement gave a new breath to my research. He has taught me innumerable lessons and insights on the workings of research in general.

I express my indebtedness and gratefulness to Prof. Amalendu Patnaik, IIT,

Roorkee for providing measurement facility in his Advanced Microwave Lab. Also, thanks to Rajaram Sir for their support during the measurement of antennas.

My sincere thanks to Prof. U. C. Pati, Prof. D. P. Acharya, Prof. S. K. Das, Prof. K. K. Mahapatra, Prof. A. K. Sahoo, and Prof. A. Swain, for their infallible motivation and moral support. I thank to all the non-teaching staff and technical staff at the Dept. of ECE, especially Mr. Kujur and Mr. B. Das for their support.

It has been a great pleasure to working with the research scholars of antenna and microwave laboratory, in particular, S. Natarajamani and Yogesh Choukiker as many of the ideas in my work originated in discussions with them. Thanks to the entire antenna and microwave research group's members for their valuable friendship, help and support. I am deeply grateful to Trilochan Sir, Manab Sir, Deepak Sir, Kanhu Sir, Madhu mam, Raseswari mam, Achala, Smita Tapaswini, Sankat, Bhaskar sir and Deepak Panda sir for investing time and energy in discussing ideas with me and tolerating my many opinionated digressions. I always cherished the company of Kapil, Imran, Ayaskant, Sweta, Meena, Subhashree, Saswati, Sanghamitra, Aprajita and Preetisudha for many good times.

I would like to acknowledge the people who mean world to me, my family: parents, parents-in-law, sisters, sister-in-law, brothers-in-law and nephews who have been a continual source of support, strength and motivation, for that I am forever grateful to them. I wish to thank my parents, Biswanath Singh and Asha Singh. They have always supported and encouraged me to do my best in all matters of life.

This dissertation would not have been possible without Rudra, my husband and friend. His understanding, support and encouragement have seen me through tumultuous times.

Finally, my greatest regards to the Almighty for giving me the strength and patience to work through all these years and complete my doctoral research work successfully.

Runa Kumari

Abstract

Over the last few decades, a tremendous growth has been seen in the wideband high-frequency communication systems. In addition to other necessary requirements, a compact size, high-efficiency antenna design with low conductor loss is mandatory for enabling high data rate communication. In recent years, Dielectric Resonator Antenna (DRA) has proven to be of exceptional low profile, light weight antenna, which provide wide bandwidth with low dissipation loss compared with microstrip antennas. The gain, bandwidth, and radiation characteristic of DRA can be improved by using array instead of single element DRA. The radiation performance of DRA array can be further enhanced by using log periodic technique.

With the growing demand of high speed data transfer and internet access, the communication systems operating in the X, Ku, K and Ka-bands are becoming more prevalent. In this thesis, some DRA array designs based on log periodic technique are investigated experimentally for high frequency wideband applications such as X, Ku, and NATO K-band (K and Ka band jointly known as NATO K-band).

The Log Periodic Dielectric Resonator Antenna (LPDRA) array relies on recent developments of wideband DRA array and multi-frequency log periodic technique. The design of LPDRA array is proposed to achieve significant multi-resonant wide bandwidth, with low conductor loss for high frequency applications.

The present work deals with the design and analysis of some log-periodic DRA with different feeding methods: Branch microstrip line fed LPDRA; Capacitive coupled LPDRA; Electromagnetically coupled LPDRA and Nine elements LPDRA with dielectric resonators of high relative permittivity as well as with low relative permittivity material.

An assay on k-β diagram has also been presented to verify the propagation characteristics of the designed LPDRA array.

The proposed LPDRAs offer continuous operation over a wide bandwidth. It provides high efficiency with low cross polarization level and sufficient gain for practical applications. Due to the inherited advantages of Log Periodic DRA array over single

DRAs, the LPDRA designs can have applications at microwave and millimetre wave communication like satellite and radar systems.

Contents

List of Figures

List of Tables

List of Abbreviations

AR	Axial Ratio
AUT	Antenna Under Test
BW	Bandwidth
CAD	Computer Aided Design
CDR	Cylindrical Dielectric Resonator antenna
CPW	Coplanar Waveguide
CP	Circular Polarization
CST	Computer Simulation Technology
DCS	Defense Communication System
DOF	Degree Of Freedom
DR	Dielectric Resonator
DRA	Dielectric Resonator Antenna
DTV	Direct Television
dB	Decibel
dBi	Decibel isotropic
EBG	Electromagnetic Band-Gap
EIRP	Effective Isotropic Radiated Power
EM	Electromagnetic
EHF	Extremely High Frequency
F/B ratio	Front to Back ratio
FCC	Federal Communication Commission
FDTD	Finite Differentiation Time Domain
FEM	Finite Element Method
FIT	Finite Integration Technique
GaAs	Gallium Arsenide
GPS	Global Position System
GPRS	General Packet Radio Services
GSM	Global System for Mobile Communication
IE	Integral Equations

LHCP	Left Hand Circular Polarization
LPDRA	Log Periodic Dielectric Resonator Antenna
MIC	Microwave Integrated Circuit
MIMO	Multiple Input Multiple Output
MMIC	Millimeter-wave Monolithic Integrated Circuit
MoM	Method of Moment
MPA	Microstrip Patch Antenna
PCB	Printed Circuit Board
PCS	Personal Communication System
PDA	Personal Digital Assistant
RADAR	RAdio Detection And Ranging
RF	Radio Frequency
RHCP	Right Hand Circular Polarization
RL	Return Loss
RSGB	Radio Society of Great Britain
SAP	Shorted Annular Patch
SLL	Side Lobe Level
T/R	Transmitter and Receiver
TSDR	Two-Segments Dielectric Resonator antenna
UHF	Ultra High Frequency
UMTS	Universal Mobile Telecommunication System
UWB	Ultra Wide Band
VSWR	Voltage Standing Wave Ratio
VNA	Vector Network Analyzer
WiMax	Worldwide Interoperability for Microwave Access
WLAN	Wireless Local Area Network

List of Symbols

ϵ_s	Dielectric constant of substrate
ϵ_r	Dielectric constant of resonator
ρ_e	Envelope correlation coefficient
λ	Wavelength
λ_0	Free-space Wavelength
λ_g	Guided Wavelength
τ	Scaling Factor
σ	Relative Spacing
σ_i	Ideal value of Relative Spacing
α_d	Design Parameter
$tan\delta$	Loss tangent
c	Speed of light in free space
γ	Propagation Constant
α	Attenuation Constant
β	Phase Constant
k	Free space wave number
k_c	cut-off wave number
ψ_R	Envelope correction coefficient
ρ	Receiving antenna correlation matrix
φ_f	Phase of radiated signal
$W(A)$	Hutchinson operator.
$\vec{E}$	Electric field intensity
$\vec{H}$	Magnetic field intensity
$\vec{D}$	Electric flux density
$\vec{B}$	Magnetic flux density
φ_E	Scalar quantities of electric flux
φ_B	Scalar quantities of magnetic flux
$\bar{x}$	Electric field vector
Δt	Maximum time step

f_c	Centre frequency
G_t	Gain of the transmitting antenna
G_r	Gain of the receiving antenna
P_t	Transmitted power
P_r	Received power

CHAPTER 1

Introduction

"***Wireless communication has turned imagination of past research ideas into today's reality***". Many new applications, such as automated highways and factories, wireless sensor networks, remote telemedicine etc., have emerged in this area recently. It is the fastest growing section of the communication industry. Wireless systems have become part of everyday life in most of the countries, around the world and are superseding the existing wireless systems in companies, homes and campuses [1].

Wireless networks were first developed in the pre-industrial era, when the signals were transmitted using smoke, torch or flashing mirrors. However, the transmission of the information was over line-of-sight distances. These earliest means of communication eventually got replaced by telegraph network (invented by Samuel Morse in 1838) and later by telephone (in 1895 Marconi demonstrated first radio transmission). The rapid growth of radio technology enabled transmission over long distances with less power, better quality, small and cheaper devices, thereby encouraging public and private communication through wireless techniques. The next major step in communication revolution was the evolution of satellite communication, which use microwave to operate. In early 1930s microwaves were first used for communication. Broadcasting of video and audio over a large geographic area is the most appealing application of satellites.

Satellite communication systems provide flexibility as well as high speed data transfer at high frequencies. With the increasing demand to support satellite communication system for simultaneous transmission and reception of high quality data,

both wideband and multiband antennas are in boom. In all communication systems, antenna is the most crucial component. The communication systems for RADAR-band applications are preferred well improved antenna designs which entails low cost, low profile, wideband with high gain and less metallic losses.

Recently, dielectrically loaded antennas have received extensive attention in wireless and satellite communication due to their small dimensions, light weight, low profile, controllable properties, high dielectric strength, higher power handling capacity, large bandwidth, low metallic losses and perfect protection from damages even in case of explosions [2,3]. Due to these inherited advantages of Dielectric Resonator Antenna (DRA), it can be a suitable choice for microwave and millimeter wave applications. Microstrip patch antennas (MPA) and DRA, both are most popular and adaptable but as compared to microstrip antenna, the DRA has a much wider impedance bandwidth with high efficiency.

In case of satellite communication systems, a robust DRA array is essential for high frequency applications. The gain, bandwidth and radiation performance of DRA array can be modified by using log periodic technique. Log Periodic antennas are broadly used for wideband applications. The class of antennas that have resulted from applying log periodic techniques to DRA array is named as frequency independent or Log Periodic Dielectric Resonator Antenna (LPDRA) array which substantially extends the useful applications of DRA.

1.1 Satellite Communications

Microwaves are radio waves with wavelengths ranging from one meter to one millimeter (frequencies from 300 MHz to 300 GHz) [4,5]. The microwave spectrum is usually defined as electromagnetic energy ranging from approximately 1 GHz to 100 GHz in frequency, but older usage includes lower frequencies. Most common applications are within the 1 to 40 GHz range. One set of microwave frequency band designated by the Radio Society of Great Britain (RSGB) are given in Table 1.1.

Table 1.1: IEEE microwave frequency bands.

IEEE frequency bands	**Frequency Range**	**Wavelength Range**	**Applications**
L band	1 to 2 GHz	15 cm to 30 cm	Military telemetry, GPS, mobile phones (GSM).
S band	2 to 4 GHz	7.5 cm to 15 cm	Weather RADAR, surface ship radar, communication satellites, Wireless LAN, Bluetooth, Zig bee, GPS.
C band	4 to 8 GHz	3.75 cm to 7.5 cm	Long-distance radio telecommunications.
X band	8 to 12 GHz	25 mm to 37.5 mm	Satellite communications, radar, terrestrial broadband, space communication.
Ku band	12 to 18 GHz	16.7 mm to 25 mm	Satellite communications.
K band	18 to 26.5 GHz	11.3 mm to 16.7 mm	Radar, Satellite communications.
Ka band	26.5 to 40 GHz	5.0 mm to 11.3 mm	Satellite communications.

Depending upon the requirements of swift transmission of digital data via satellites, different IEEE RADAR bands such as X-band, Ku band, NATO-K band can be preferred, which can provide the desirable bandwidth.

X-band meets the need of its users for several applications. It is successfully used for military communications for decades. Commercial X-band advantages include freedom from the clutter of commercial users, rain fade resistance, and maximized throughput.

In the 1980s and 90s, the adoption of Ku-band is providing more capacity and bandwidth. Ku-band enables focused bandwidth and high-quality communications across larger geographical locations. NATO-K band is a frequency band which can be used for a wide variety of applications, just like C- and Ku-band. It provides increased spectrum compared to C-band and Ku-band enabling greater volumes of traffic for communication. Satellites using NATO-K band frequencies can deliver the same services that are delivered at C- and Ku-band for broadband communications.

1.2 Log Periodic Technique

The Log Periodic technique is initially adopted for bandwidth enhancement of antenna, which has been evolved from the initial work of a number of researchers at the University of Illinois. In 1960's, Isbel introduced a log periodic antenna design to achieve wide bandwidth with superior performances [6]. It is also known as frequency independent antenna. A conventional log periodic antenna is shown in Figure 1.1.

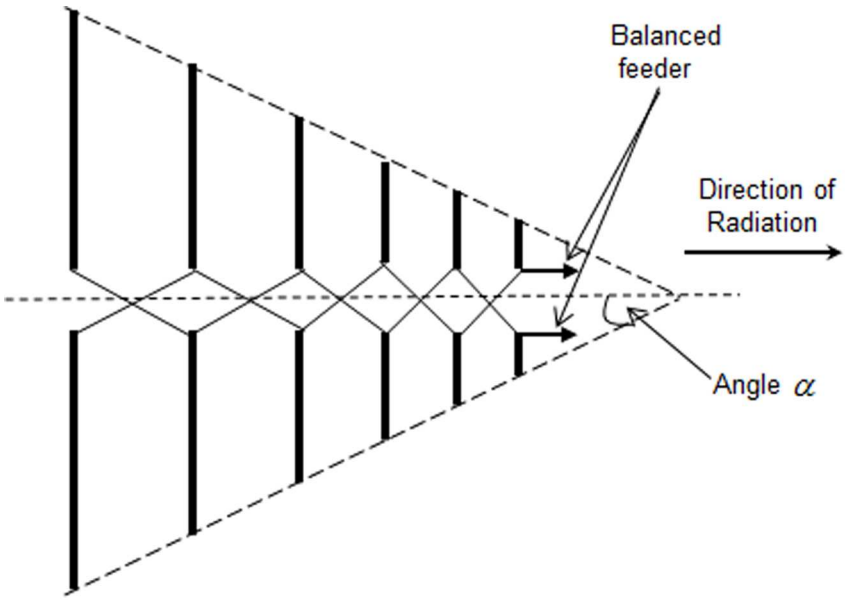

Figure 1.1: Conventional Log periodic antenna.

The design principle of log periodic structure requires scaling of dimensions from period to period so that performance is periodic with the logarithm of the frequency. In case of log periodic structure, if the input impedance as a function of frequency is plotted, the variation will be found to be repetitive. If the plot is taken against the logarithm of the frequency rather than the frequency itself, this variation will be periodic and the impedance will go through cycles of variation in such a way that each cycle is exactly like the preceding one. Here, the impedance is a logarithmically periodic function of the frequency [7]. This behavior of the structure gives rise to the name log periodic. Moreover, all the electrical properties of the antenna undergo a similarly periodic variation [8].

The concept of log periodic antenna is of building a structure, that scales into itself periodically as the frequency and hence wavelength changes. The physical structure of log periodic antenna is repetitive, which results in repetitive behaviour in its electrical characteristic [7, 9–11]. In this type of antenna, it is normal to drive alternating element with 180^0 of phase shift from one another.

The log periodic antenna achieves bandwidths of 10:1 with ease, and much larger values are possible with careful design [12]. By applying log periodic technique to antenna array, a negligible variation in electrical characteristics (i.e. input impedance, patterns etc.) of the antenna is obtained over wideband frequency, which is within the design limits of the antenna.

The design of a log periodic antenna consists of a basic geometric pattern that repeats, apart from a different size pattern which results in repetitive behaviour in its electrical characteristics [13]. The length, width and spacing between the adjacent elements of a log periodic antenna increases logarithmically from one end to the other [14]. This self-scaling property implies that the array will have the same radiating properties at all frequencies that are related by a factor 'τ'. The magnitude of the log-frequency periods is determined by the design ratio, τ , and has a magnitude log $(1/\tau)$. That is, the two maxima of the impedance or pattern variation occurs at frequencies f_1 and f_2 having log frequency period, $\log(1/\tau)$ and they are related by the Equation (1.1),

$$\log f_1 - \log f_2 = \log \frac{f_1}{f_2} = \log \frac{1}{\tau} \tag{1.1}$$

where,

$$\frac{f_1}{f_2} = \frac{1}{\tau}, or f_2 = \tau f_1 \tag{1.2}$$

If the log-periodic antenna has certain measured properties (e.g. impedance, gain) at any particular frequency f, it follows that it will have exactly the same properties at frequencies τf,$\tau^2 f$, $\tau^3 f$ and so on and also at f, f/τ, f/τ^2, f/τ^3,...., provided that these frequencies are all within the cutoff limits. The log-periodic antenna is frequency independent in which the electrical properties such as the mean resistance level R_0, the characteristic impedance of the feed line Z_0, and driving-point admittance Y_0,

vary periodically with the logarithm of the frequency [11]. In the recent era, the log periodic technique has been employed to achieve wideband characteristics with a negligible variation in electrical parameters such as input impedance, and radiation patterns of the antenna. The Log periodic technique is a very sophisticated and effective approach to achieve wideband, high frequency antenna design.

1.3 Motivation

With the growing demand of high speed data transfer and internet access, the communication systems with wideband applications are becoming more prevalent. The rapid increase in the demand for wireless applications in the microwave range has led the research community to focus their attention on highly efficient antennas, which exhibit wide bandwidth, good radiation characteristics and low metallic losses with small size. The DRAs could be used for above applications due to their many useful features. Microstrip antennas have some limitations compared to DRAs as narrow bandwidth, lower gain, low power handling capacity etc. For these reasons, DRAs are preferred over microstrip and conventional antennas. Bandwidth enhancement is one of the major design considerations for most practical applications of DRAs. In recent few decades, research scientists have developed several techniques to increase the bandwidth and obtain a wideband response for the DRA. Using DRA array with different types of feeding technique is one of the most popular bandwidth enhancement approach. The gain, bandwidth and radiation performances of DRA array can be enhanced by using log periodic technique. Log Periodic antennas are widely used for applications where a large frequency band is desired. The recent advancements in wireless communication industry, especially the area of mobile communication, wireless data communication and satellite communication have led to the increased demand for high gain, high efficiency, wideband antennas which motivated the study and design of LPDRA array.

1.4 Problem Statement

With the motivation mentioned in section 1.3, we take up a problem for the doctoral research, which is stated as follows.
To design and develop Log Periodic Dielectric Resonator Antenna (LPDRA) array for:

- Ku band applications using the branched microstrip feed line,
- X band applications using the capacitive coupled microstrip feed line,
- Wideband applications using the overlaid microstrip feed line,
- NATO-K band and X band applications using dielectric resonators with different relative permittivity.

1.5 Thesis organization

The **FIRST** chapter of this thesis presents, a brief introduction of the log periodic technique. The motivation and problem statement of the present research structure are included in this chapter. The chapter wise presentation of the thesis is also dealt here. Finally, the chapter is summarized.

The **SECOND** chapter is dedicated to the background of DRA, bandwidth enhancement in DRA, DRA array and log periodic dielectric resonator antenna array. The literature of the present and previous works on DRA and log periodic antennas are reported and summarized. It includes reviews on DRA, wideband DRA, DRA array, log periodic dipole array, log periodic microstrip antenna etc.

The **THIRD** chapter is based on a seven element LPDRA array with the branched microstrip line feeding. The k-β analysis for log periodic DRA array is presented in this chapter. The design methodology of the DRA array using log periodic technique is discussed and the detailed results of the proposed antenna are investigated in this chapter. This LPDRA array can be a good choice for Ku band (12-18 GHz) applications.

The **FOURTH** chapter contributes a seven element LPDRA array excited by capacitive coupled microstrip line series feeding. The dielectric resonators are engraved on the same substrate as the feed line and directly or capacitive coupled to it. The designed LPDRA array is fabricated and the measured results are compared to the simulated results. The array can be used for X-band applications.

The **FIFTH** chapter deals with the design of a seven element frequency independent LPDRA array to acquire a light weight, physically small sized antenna. The LPDRA array with an overlaid microstrip line feeding has been designed, simulated and experimentally tested. This feeding circuit is providing sufficient isolation between the dielectric resonator (DR) and the feed circuits which reduces the surface wave losses. The proposed antenna is suitable for wideband applications in satellite and RADAR communications.

In the **SIXTH** chapter, the design and analysis of nine element LPDRA array with overlaid microstrip line feeding for different dielectric material are proposed. The first design describes an analysis on LPDRA with dielectric resonators having a high relative permittivity value for NATO-K band applications. For ease of fabrication, another LPDRA is designed with resonators of Teflon based low cost dielectric material having low relative permittivity for X- band applications.

Finally,the **SEVENTH** chapter outlines the overall contributions of the thesis. The achievements and limitations of the results are also discussed. The details of further research work in the same area are also included in this chapter.

The detailed descriptions of design methodology used for designing LPDRA array are described in the **APPENDIX A**. Here, Electromagnetic (EM) numerical modelling techniques for Computer Simulation Technology (CST) microwave studio simulation programs are discussed.

1.6 Summary

In this chapter, a brief introduction on satellite communication and log Periodic technique are discussed. The Log periodic technique is introduced to achieve significant multi resonant wide bandwidth for high frequency applications. This chapter also sys-

tematically outlines the motivation behind this work and the problem statement of the thesis. A concise presentation of research work carried out in each chapter has been dealt. In essence, this chapter provides an overview of the thesis in a comprehensive manner.

CHAPTER 2

Dielectric Resonator Antennas: A state-of-the-art

2.1 Introduction

The recent explosions in wireless communication industry have led to the increased demand for compact antenna designs. The main purpose of designing an antenna is to obtain a wide range of bandwidth. Microstrip Patch antennas (MPA) have some limitations like narrow bandwidth, lower gain, low power handling capacity, poor polarization purity etc. To overcome these problems, DRAs are preferred over microstrip and conventional antennas. The DRAs are good replacement of the microstrip antenna. It provides wider impedance bandwidth with high power handling capability due to its many advantageous features. These include the compact size, simple structure, ease of fabrication and the versatility in their shape and feeding mechanism described by Mongia and Bhartia in 1994 and later on by Petosa in 2007 [2, 3, 15].

DRAs become very popular in the core sectors like defense, military, satellite, radar and especially for high frequency applications. It has received extensive attention due to its several features such as light weight, low profile, low-dissipation loss, high-dielectric strength, and higher power handling capacity. Due to the flexibility in DRAs, it can be designed with different shapes as per the requirements depending upon the applications in the wireless communications world. DRAs can be excited with several feeding methods, such as probes, microstrip lines, slots, co-planar lines and image waveguide [16].

DRA can be fabricated from low-loss and high relative dielectric constant material of various shapes whose resonant frequencies are functions of the size, shape

and permittivity of the material. The DRA has some additional properties such as frequency stability with temperature, ease of integration with other hybrid MIC circuitries, simple construction and the ability to withstand harsh environments. Due to these numerous benefits of DRAs, it is very promising for applications in wireless communications.

2.2 Dielectric Resonator

Microwave resonators in the form of dielectric spheres and toroids were first theoretically demonstrated in 1939 by Richtmeyer [17]. In the early 1960s, the modes of the resonators were first analyzed by Okaya and Barash [18]. Development of low-loss ceramic materials opened the way for the use of these resonators as high-Q (quality factor) elements for circuit applications such as filters and oscillators, offering a more compact alternative to the waveguide cavity resonator. For these applications, dielectric resonators are typically machined into different shapes out of materials having a high relative permittivity ($\epsilon_r \geq 35$) to maintain compactness. Dielectric Resonators (DRs) made of low loss dielectric materials are widely used in shielded microwave circuits such as filters and oscillators as a tuning element. They could be excited using different transmission lines.

DRs generally consist of puck of ceramics that has a high permittivity and low dissipation factor [19]. These are good alternatives to metallic cavities where they offer a reduction in size without degradation in performance. Dielectric materials with dielectric constant (ϵ_r) in the range of 2-100 have been used in high microwave frequency applications. The high relative permittivity at the interfaces of DR and free space provide a standing electromagnetic wave inside the resonator.

In 1983, S. A. Long has introduced DR as a radiating element [20]. The study of DRs as an antenna began in the early 1980s with the examination of the characteristics of basic shapes such as cylindrical, rectangular and hemispherical. An antenna consists of a rectangular parallelepiped dielectric on top of the ground plane is described by McAllister in 1983 [21]. In 1989, Mongia has placed a half split DR on metallic plane for antenna applications and proposed the structure as a practical dielectric

resonator antenna for use at microwave and millimetre-wave frequencies [**?**, ref107] The necessity of smaller size antenna with higher frequency applications is boosted the research in the area of DRA.

2.3 Dielectric Resonator Antenna

The DRA is constructed from dielectric resonator, substrate and ground with different excited feeding techniques. DRA consists of dielectric materials as its radiating patch also called as DR on one side of the substrate and has a ground plane (metal) on the other side.

DRA is a resonant antenna, fabricated from low-loss microwave dielectric material. A high permittivity DRA can be used as a small and low profile antenna. Moreover, the size of DRA can easily be controlled by the dielectric constant of the materials. A wide range of dielectric permittivity values (2 to 100) can be used, allowing the designer to have control over size and bandwidth i.e., wide bandwidth is achievable using low permittivity and compact size is achievable with high permittivity.

DRAs possess some peculiar properties which render them very promising, especially for microwave and millimeter wave applications. DRA can be designed with various geometries including cylindrical, rectangular, spherical, half-split cylindrical, disk, hemispherical, and triangular shapes to accommodate various design requirements as shown in Figure 2.1 [2, 3].

The DRA has attracted much attention in recent years. It has many favorable features. The major feature of DRAs are high radiation efficiency due to the absence of conductor or surface-wave losses. In case of DRA, various modes are excited to produce a broadside or omnidirectional radiation pattern for different coverage requirements. The DRAs are characterized by low phase noise, compact size, frequency stability with temperature, ease of integration with other hybrid MIC circuitries, simple construction and the ability to withstand harsh environments. It has some interesting characteristics like light weight, high permittivity, wide impedance bandwidth, low-production cost and ease of excitation [15, 16].

Figure 2.1: Several possible shapes of DRAs.

2.3.1 Feeding Techniques

Feeding techniques are required to energize the antenna i.e. to transfer the power into the antenna. Early microstrip antennas were fed either by a microstrip line or a coaxial probe through the ground plane. DRAs can be excited by using several feeding methods, such as probes feed, slots, microstrip feed lines, dielectric image guides and co-planar lines etc [2, 3, 15, 16, 22]. A number of modified feeding techniques have also been developed [2, 3]. Some of the feeding techniques are easy to fabricate whereas others are difficult. Some of the feeding techniques can enhance the bandwidth of DRA. For example, aperture and proximity feeds are used to increase the bandwidth. In 1997, Mongia proposed the theoretical and experimental investigations on rectangular DRA with various feeds such as probe, microstrip slot and microstrip line to describe the resonant frequencies and radiation Q-factors [23].

Coaxial or Probe Feed

Coaxial or probe feed is a common method of coupling to DRA. The probe usually consists of the center pin of a coaxial transmission line that extends through the ground plane. The center pin can also be soldered to a flat metal strip that is

placed adjacent to the DRA, whose length and width can be adjusted to improve the impedance match [2, 3]. The coaxial connector is attached to the back side of the DRA and the coaxial center conductor after passing through the substrate is drilled into the dielectric resonators.

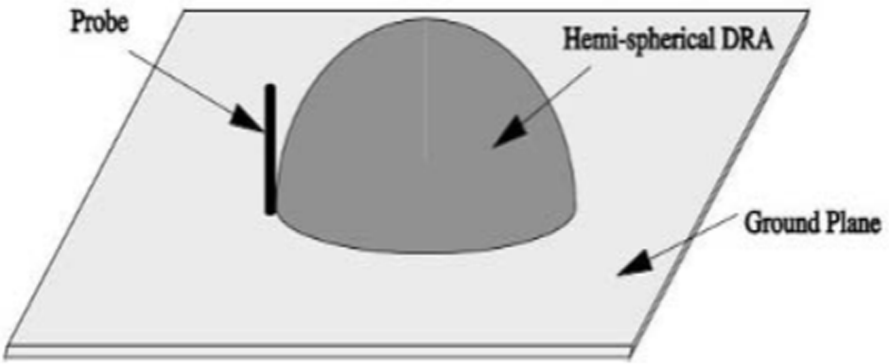

Figure 2.2: A coaxial probe fed hemispherical DRA.

The amount of coupling can be controlled by adjusting the probe height and the DRA location. The probe length is generally chosen to be less than the height of the DRA, to avoid probe radiation as shown in Figure 2.2. Feeding the probe adjacent to the DRA is preferred since it does not require drilling into the DRA. The advantage of the coaxial probe excitation is the direct coupling into a 50 Ω system without the need for a matching network [24, 25].

Microstrip Line Feed

Excitation of the dielectric resonator antenna by a microstrip line on the same substrate is the easiest method of feeding. In this type of feed technique, a conducting strip is connected directly to the edge of the dielectric resonator (DR) or inserted under the DR. A common method of excitation with microstrip line is to use it by proximity coupling. The amount of coupling from the microstrip line to the DRA can be controlled to a certain degree by adjusting the spacing between the DRA and the line for the side-coupled case or the length of the line underneath the DRA for the direct-coupled case [2]. The dielectric constant of the DRA also affects the coupling. Higher the value of dielectric constant, higher will be the value of the coupling. This

feeding technique provides ease of fabrication and simplicity in modeling as well as impedance matching. As the thickness of the dielectric substrate of the DRA increases, surface waves and spurious feed radiation also increase, so the thickness of the substrate should be kept less [2, 3, 26, 27].

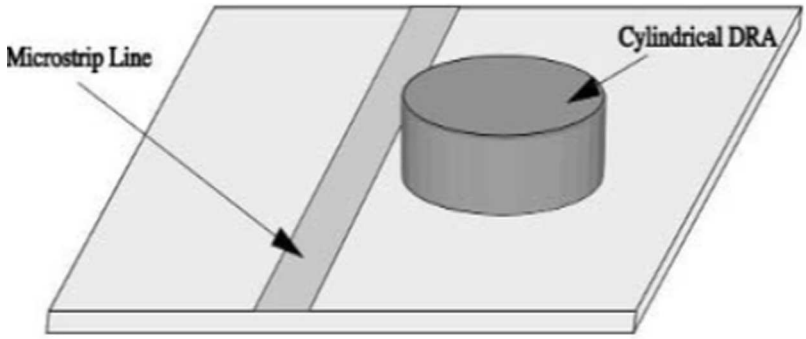

Figure 2.3: A microstrip line fed cylindrical DRA.

An investigation on microstrip transmission line excitation of cylindrical shaped DRA has shown by Kranenburg and Long in 1988. They have reported that a microstrip line can be strongly coupled to the DRA and the coupling results in an efficient and practical antenna system for frequencies within the millimetre wave band [28].

Slot Aperture Feed

In slot aperture method, a DRA is exciting through an aperture in the ground plane upon which it is placed. Aperture coupling is applicable to DRAs of any shapes such as rectangular, cylindrical or hemispherical. The aperture works like a magnetic current running parallel to the size of the slot, which excites the magnetic fields in the DRA. The aperture consists of a slot cut in a ground plane and fed by a microstrip line below the ground plane. For avoiding spurious radiation, feed network is located below the ground plane. Moreover, slot coupling is an attractive technique for integrating DRAs with printed feed structures. The coupling level can be changed by moving the DRA with respect to the slot. Generally, a high dielectric material is used for the substrate and a thick, low dielectric constant material is used for the top dielectric resonator patch to optimize radiation from the antenna [2]. It is difficult to fabricate the DRA

with this feeding technique due to its multiple layers which also increases the thickness of antenna. This feeding method provides narrow bandwidth (up to 21%). In 1990, Martin and Antar designed a circular cylindrical dielectric resonator fed by microstrip feed line through a coupling aperture on the ground plane. The antenna configuration can be used at microwave and millimetre wave frequencies [29].

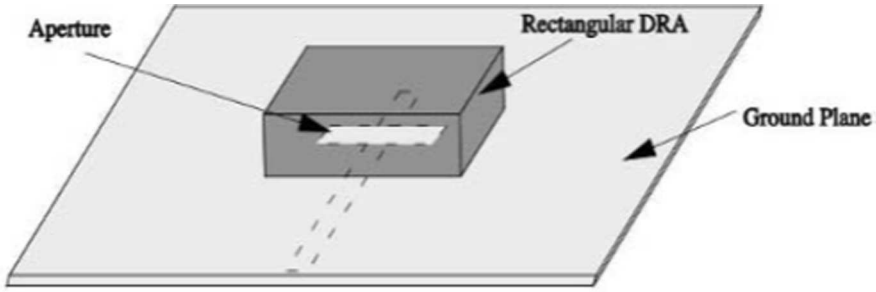

Figure 2.4: A aperture coupled rectangular DRA.

Proximity Coupled Microstrip Feed

In this type of feeding a two layer substrate is used and the DRA is placed on the upper layer. This feed is also known as an electromagnetically coupled feed. To design this feed, two substrates are required and the feed line should be in between the two substrates. The fabrication of the antenna is little bit difficult and the thickness of the antenna is increased due to the presence of the two substrates. By using this feeding technique the bandwidth of the antenna can be improved. The substrate parameters of the two layers can be selected to increase the bandwidth and to reduce spurious radiation. The lower substrate should be kept thin [30, 31]. Proximity-coupled microstrip feed is also known as non-contacting feed.

This feeding method has some advantages such as no physical contact between the feed line and radiating element, no drilling required, less spurious radiation, better for array configurations, good suppression of higher order modes, better high frequency performance etc.

Dielectric Image Guide Feed

This coupling technique is similar to microstrip line coupling but a dielectric material as a feed line is used instead of perfect electric conductor. Dielectric image guides offer advantages over microstrip at millimeter-wave frequencies, since they do not suffer from conductor losses. The coupling can be controlled by adjusting the spacing between the guide and the DRs [2, 3, 32, 33]. The dielectric image guide is thus best utilized as a series feed to a linear array of DRAs.

2.3.2 Modes supported by DRA

Depending on the shape of the resonator, various modes can be excited within the DRA element. These modes can produce different radiation patterns for various coverage requirements. DRAs operating at their fundamental modes radiate like an electric or magnetic dipole, which depends on the mode of excitation and geometry of the bulk dielectric material. Though several geometries have been introduced, the most studied and common structures are the cylindrical and rectangular DRAs because of the simplicity in their design, fabrication, and analysis.

Based on the basic shapes, the excited resonator modes can be classified into three distinct types: Transverse Electric (TE) and Transverse Magnetic (TM) and hybrid. TE and TM must refer to a coordinate axis. In general, TE to an axis implies the Electric field component in that axis vanishes, or equivalently two electric components Transverse (perpendicular) to that axis exist. Similarly for TM, Magnetic is replaced with Electric in the above statement [2, 3, 22].

The fields for TE and TM modes are axisymmetric, whereas hybrid modes are azimuthally dependent. The variation of fields along the azimuthal, radial and Z-direction inside the resonator is denoted by adding mode indices as subscripts to each family of modes. The TE, TM, and hybrid modes are classified as $TE_{mnp+\delta}$, $TM_{mnp+\delta}$ and $HE_{mnp+\delta}$ respectively. The first index denotes the number of full-period field variations in azimuthal direction, the index n (n = 1, 2, 3) denotes the order of variation of the field along the radial direction and the index p + δ (p = 0, 1, 2) denotes the order of variation of the fields along the Z-direction. The actual value

of δ depends on the relative dielectric constant of the resonator and the substrate and on the proximity to the top and bottom conductor planes.

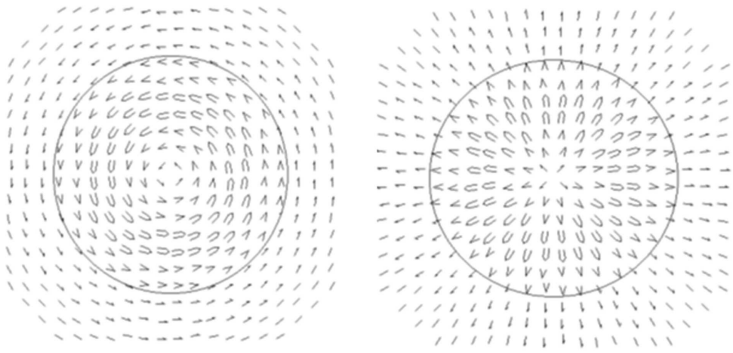

(a)

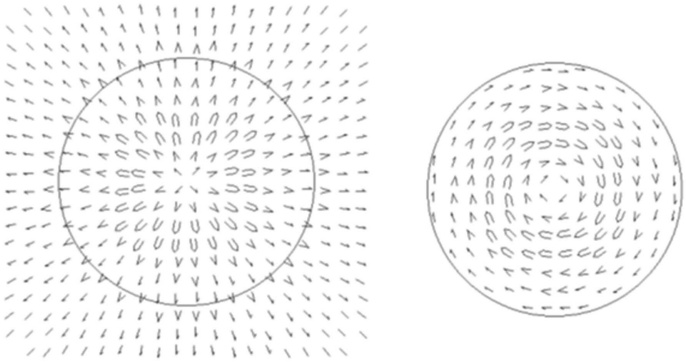

(b)

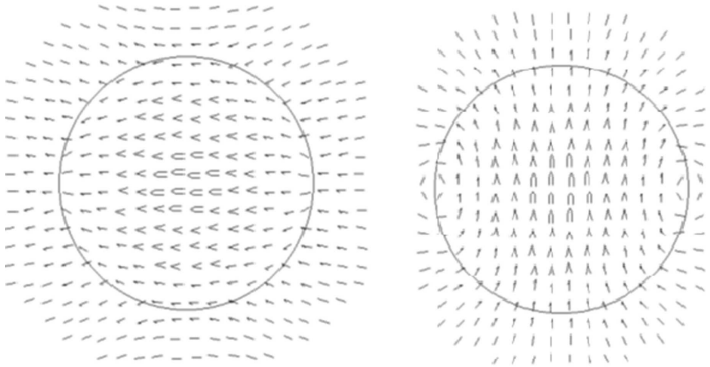

(c)

Figure 2.5: Basic radiating modes in a cylindrical dielectric resonator (Left: E-field, right: H-field) : (a) TE_{01} mode, (b) TM_{01} mode and (c) HEM_{11}mode.

An interesting feature of DR is the variation in field distribution of different modes, because the modes behave like electric and magnetic multipoles such as dipole,

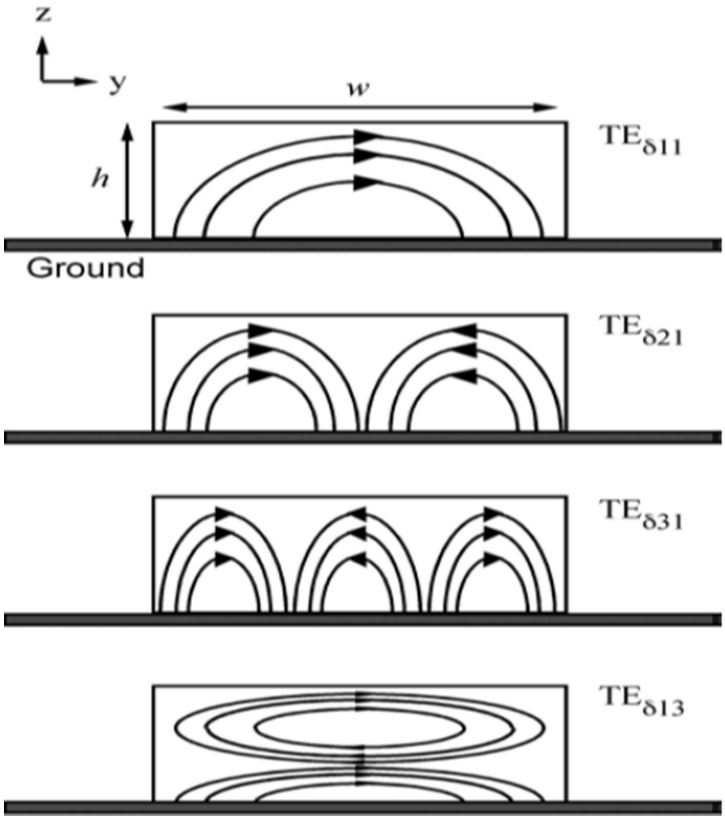

Figure 2.6: Sketches of the E-fields for selected higher-order modes within the rectangular DRA.

quadrupole, octupole, etc. The mode nomenclature makes possible the accurate prediction of far-field radiation of dielectric resonators in their application as antennas. For example, the $TE_{01\delta}$ mode radiates like a short magnetic dipole oriented along its axis, whereas its TM counterpart radiates like a short electric dipole and the $HE_{11\delta}$ mode radiates like a horizontal magnetic dipole.

Figure 2.5 shows the modes in a cylindrical shaped dielectric resonator. The sketches of the electric fields of some of these modes for rectangular shaped DRA are shown in Figure 2.6.

2.3.3 Polarization in DRA

A common method for coupling to dielectric resonators in DRA is by coupling microstrip lines. Microstrip coupling will excite the magnetic fields in the DRA to produce the short horizontal magnetic dipole mode. The level of electromagnetic coupling can be adjusted by the lateral position of the DRA with respect to the mi-

crostrip line and on the relative permittivity of the DRA. For lower permittivity values (necessary for DRAs requiring wide bandwidth), the amount of coupling is generally quite small. Thus, in order to have acceptable radiation efficiency, an array of DRAs is required. Microstrip lines can be used as a series feed for a linear array of DRAs, provided that a sufficient number of elements are used. In this case, the polarisation of the array is dictated by the orientation of the microstrip line. Usually the DRA arrays are linearly polarised [2, 3].

For some of the applications like satellite communications circular polarisation is required which results in the radio path as a line of sight with few reflected paths. The circular polarisation is used to make the received power independent of the angular orientation of the receiver. Circularly polarised (CP) DRA arrays can be constructed using linearly polarised (LP) DRA elements or CP DRA elements. The CP arrays formed using CP DRA elements give better performance in terms of 3dB axial ratio bandwidth, gain and 3dB-gain bandwidth [2].

2.3.4 DRA over Microstrip Patch Antenna

The high-radiation efficiency, wide bandwidth and polarization flexibility of DRAs make them far superior to conventional microstrip antennas. As compared to the Microstrip Patch Antenna (MPA), the DRA provides much wider impedance bandwidth due to their numerous beneficial features [15]. DRA offers wider impedance bandwidth (10% for dielectric constant (ϵ_r) 10). This is because the microstrip antenna radiates only through two narrow radiating slots, whereas the DRA radiates through the entire three dimensional antenna surfaces except the grounded part [2]. DRAs are basically invulnerable to the surface wave power leakage and conductor loss complications, which plagues the MPA and reduces their efficiency. DRAs having an efficiency significantly higher than that of the microstrip antenna, especially at millimeter wave frequencies. With the suitable adjustment of the feed position, the antenna is excited to provide a wide bandwidth with the broadside radiation patterns [15].

2.3.5 Advantages and Limitations of DRA

DRA has various features which make it very versatile elements over a wide frequency range. These features can be adapted to numerous applications by appropriate choice of the design parameters. Due to low loss of the dielectric materials, DRAs offer a high radiation efficiency which is very important in a portable or a mobile unit for saving power. Rectangular DRAs, in comparison to other geometries are more desirable due to two independent aspect ratios which provide more flexibility for antenna design [23]. Bandwidth up to 10% can easily be achieved with simple rectangular DRAs, with relative permittivity values of 10 or less.

The bandwidth of a common DRA is typically below 10%. In order to enhance the bandwidth of DRA, many techniques have been developed for DRAs, such as stacked DRA, embedded DRA, DRA array or various shaped DRA. It is very difficult to get dielectric material of desired dielectric constant, so one has to work with limited available resources. Compared to the printed circuit antennas, the fabrication is generally more complex and more costly.

2.3.6 Applications of DRA

Now-a-days DRA is broadly used in electronic warfare, missile, radar and communication systems. For many of the existing and emerging communication applications, wideband DRA operation is desirable to accommodate the increasing data rates required for services such as video-conferencing, direct digital broadcast, EHF portable satellite communications, local multi-point communications, and indoor wireless. DRAs of relatively simple design have wideband performance and may serve as suitable antenna candidates for various applications such as biomedical radiators and intruder alarms. They find use both in military and commercial applications [34].

Over the past few years, varieties of wideband antennas were investigated. In 2005, Wong et al. had presented a square cylindrical monopole antenna for wideband omnidirectional operation [35]. In the same year, a wideband circularly polarised patch antenna was designed by Lau et al for outdoor GPS communication system [36]. In 2006, Lee et al proposed a planar monopole antenna for ultra-wideband appli-

cations [37]. Ryu and Kishk have described a novel portable DRA design mounted on a vertical ground plane edge with broadside radiation for ultra-wideband wireless applications in 2010 [38]. A novel compact ultra-wideband printed monopole loaded with a DRA is proposed by Ahmed et al. in 2011 [39]. In 2012, Abedian et al. have presented new compact two-segment dielectric resonator antenna (TSDR) for ultra-wideband application [40].

Now-a-days DRAs meet growing interest in wireless and satellite communication systems due to the low loss of dielectric materials [3,4]. For satellite communication in X, Ku, K and Ka bands (8-40 GHz), there is an inherent trade-off between conductor losses and multi frequency broad bandwidth. For high frequency wideband applications, beyond 10 GHz such as X band, Ku band, K band or Ka band, well improved designs of antenna are required. Chair et al. in 2007 had designed a wideband stair shaped DRA for X band applications having impedance bandwidth 54% (7.68-13.4 GHz) [41]. A compact Ka band Lens antenna is presented by Costa et al. in 2008 for Leo satellites which radiates at 26 GHz [42]. In 2009, Arnieri et al. introduced a Shorted Annular Patch (SAP) antenna integrated with a circular radiating waveguide for Ka band applications, which radiates at 20 GHz and 30 GHz providing impedance bandwidth 950 MHz and 630 MHz, respectively [43]. Since DRA has low conductor losses in compared to the typical metal antennas such as microstrip patches, it can be a good choice for satellite communication.

2.4 Bandwidth Enhancement of DRA

The impedance bandwidth of DRA is depending on the dielectric constant of resonator material. For most of the practical applications of DRAs, the major design consideration is the bandwidth enhancement.

In 1994, Mongia and Bhartia have been reported several bandwidth enhancement techniques on modified feed geometries and changing the shape of the DRA including conical, tetrahedron, ring, triangular etc. [15].

By selecting a low dielectric constant and the appropriate dimensionsof DRA, a very low Q-factor can be obtained which implies that it is theoretically possible to

design an isolated cylindrical or rectangular DRA with broad bandwidth [44]. The bandwidth of the DRA can be enhanced by using different techniques e.g. changing the shape of DRA (including conical, tetrahedron, ring, triangular etc.) [16, 45–49], use of modified feed geometries, using multiple DRAs [50–52], optimizing the feeding mechanism etc.

The bandwidth improvement of DRA can also be achieved by using a finite ground plane or introducing an air gap between dielectric resonator (DR) and ground plane [53–56]. The introduction of air gaps between the DR and the ground plane can increase the impedance bandwidth of the antenna significantly [38]. For bandwidth enhancement, some new techniques have been proposed by a number of researchers such as changing the dimensions of the ground or substrate material, varying the parameters of DRA, use of parasitic coupling with different resonators using a number of DRAs or different type of feeds (or excite) to the antenna [38, 52]. The impedance bandwidth of DRAs can be improved by using multiple DRAs (array or stacked or embedded) instead of single DRA [57–60]. The bandwidth of DRA array can further be modified by using Log periodic technique [6–8].

In practice, there are innumerable techniques to enhance the bandwidth of DRA. The most common techniques adopted for wideband DRAs are changing the shapes of the dielectric resonator, use of modified feed geometries, optimizing the feeding mechanism and DRA parameters, stacked DRAs, embedded DRAs and DRA arrays [20, 56, 61, 62].

The performances of DRA can be improved by using stacked or stair shaped DRA [41, 63]. Stacking of DRAs is an efficient technique to raise the gain, bandwidth and radiation performances. In 1989, Kishk et al. have investigated a stacked cylindrical dielectric resonator Antenna. The dielectric resonators of the antenna are made up of different materials and the bandwidth of the stacked antenna was found 25% [64]. An improvement in the bandwidth of the DRA using a stacked elliptical DRA configuration placed above an infinite ground plane was presented by Sharkway et al. in 2004 [65]. The stacked DRA, excited by coaxial probe feed was resulted in an improved bandwidth of 61.5%. In 2006, Walsh and Long proposed an investiga-

tion of stacked and embedded cylindrical DRA to show impedance bandwidth up to 68.1% compared to 21.0% for a homogeneous DRA with the same size and resonant frequency [60].

Leung proposed a new excitation scheme in the year 2000 which employs a conducting conformal strip to excite a hemispherical DRA [66]. In 2005, Tayeb et al. have presented an L-shaped DR antenna with the two equiangular triangles [67], which offered 38% impedance bandwidth. In 2007, Chair et al. have proposed a DRA design using one or two-step stair geometries of dielectric resonators to achieve wideband. The obtained impedance bandwidth is more than 20% for one-step DRA or more than 40% for a two-step DRA design [41].

In 2008, Chang et al. have designed a wideband rectangular-shaped dielectric resonator with a horizontal tunnel to provide an impedance bandwidth of 20% for WLAN applications [68]. In 2009, Chang and Feng have presented a DRA design fed by an L-shaped microstrip monopole yields more than 25% bandwidth [69].

In 2010, Pan and Leung have reported that a wide bandwidth over 20% can be obtained by using a circular polarized trapezoidal DRA excited by a single rectangular slot [70]. A circularly polarized wideband rectangular DRA excited by a concentric open half-loop has been presented by Sulaiman and Khamas in 2011 [71]. The antenna is providing 20% impedance matching bandwidth. In the same year, a wideband rectangular-shaped DRA is designed by Fang and Leung to provide 30.9% of impedance bandwidth, which was possible with the strip-fed excitation method [72]. All these DRA designs provide wide bandwidth with good radiation patterns however, the bandwidth is limited to only 40%. In 2011, Ge et al. have proposed an ultra-wideband rectangular DRA design which achieved 60-110% bandwidth with an average gain of 6 dBi by employing a low permittivity dielectric insert of full-length between the DR and the ground plane [73].

2.5 Dielectric Resonator Antenna Array

In recent years, the DRA is extensively studied due to its several advantages [2, 3, 15, 16]. The size and bandwidth of DRA can easily be controlled by varying the dielectric

constant of the dielectric materials in a wide range [2]. For an antenna, high gain with high efficiency and directional radiation pattern cannot be synthesized with a single DRA of any shape. The gain, bandwidth and radiation performances of DRA can be improved by using array instead of single DRA [34,57]. For some applications, a DRA array with suitable element arrangement and feed configurations (like conformal patch connected to microstrip line feed) can be used to provide desired performances [34,74].

In case of DRA array, the DR of proper dimensions can be assembled and fed in a proper way [34, 57]. The DRA arrays find uses in terrestrial applications as well as radars. Varieties of array designs have been proposed in literature to obtain broadband multi-frequency operations. Among them EBG antenna using double-layer frequency selective surfaces [75], PCB integrated waveguide fed array antennas [76] or coplanar waveguide spiral antennas [77] are mostly exploited ones for Ku band applications.

A four-element cylindrical dielectric resonator antenna (CDR) array was proposed by Guha and Antar in 2006 [57]. The array offers the impedance bandwidth of 29% ($S_{11} \leq$ -10 dB) with monopole like radiation pattern over the entire band, with 4 dBi peak gain. Al-Zoubi et al. have proposed a linear rectangular DRA Array fed by dielectric image guide to achieve a specific power distribution with low cross polarization in 2010 [58]. In 2010, Tian et al presented a compact six-port DRA array for MIMO channel measurements and performance analysis which gives a higher degrees of freedom (DOF), than the monopole array [59]. The bandwidth of the DRA array can further be enhanced by using log periodic technique.

2.6 Log Periodic Dielectric Resonator Antenna

The promising growth in high speed data transfer at high frequencies increases the necessity of flexible satellite communication systems. In modern satellite communication systems for IEEE Radar band applications, multi resonant wide frequency operation is highly desirable, which require small and light weight antenna with less metallic losses and broadband facilities. The use of multi single frequency resonant antennas can be avoided by using a single DRA array which can support a wideband

with multi resonant frequency [78, 79]. In this case, applications requiring different frequency bands can be operated simultaneously with one radiating element. This shrinks the circuit size and leads to compact systems.

An advanced method to achieve wide bandwidth with high-efficiency, high gain and less metallic losses is possible by applying the log-periodic technique to a DRA array. The log periodic dielectric resonator array substantially extends the useful application area of dielectric resonator antennas which provides wide bandwidth systems with a versatile low profile.

Log periodic antenna design is used where a wide range of frequencies, moderate gain and directionality are desirable. In 1960, D.E. Isbell proposed a new antenna design for dipole arrays which provides unidirectional radiation patterns of constant beam width and nearly constant input impedance over any desired bandwidth [6]. Isbell introduced that broadband properties are achieved by making use of the principles of log periodic antenna design.

Various log periodic antenna designs have also been reported to achieve modest levels of gain with wide bandwidth for high frequency applications. In the 1960's, some theoretical as well as experimental works on log periodic dipole array design were carried out by Carrel, who demonstrated that log periodic antennas have a reasonable gain with broad bandwidth [13, 14]. In 1981, Pues et al. have described a new design method for a wideband array of quasi-log-periodic microstrip antenna. The array provides 22% bandwidth with reasonable power gain in the broadside direction [10]. In 1986, Hall et al. have obtained a wide bandwidth by applying a log periodic technique to the series-fed electromagnetically coupled overlaid patch array [80].

Due to the requirements of high gain, broad bandwidth, low weight, reliability, ease of manufacture and integration with widely used planar microwave circuitry, Pantoja et al. have proposed a microwave printed planar Log-Periodic Dipole Array antenna in 1987, which fulfill all the above requirements [7]. A coplanar waveguide (CPW) fed log-periodic dumb-bell slot antenna array operating as a frequency independent antenna was presented by Kim et al in 2006 [81]. In the same year, Chen et al have proposed a uniplanar log periodic slot antenna excited by CPW feeding for UWB

radio systems [82].

A number of different log periodic antennas have been investigated by different researchers. A log periodic Koch-dipole array as a miniaturized wideband antenna for 2-3 GHz impedance bandwidth was designed by Anagnostou et al. in 2008 [83].

In 2009, Baek et al. had successfully fabricated a 94 GHz log periodic planar on-chip antenna on GaAs by using MMIC process technology [84]. A single layer printed log periodic dipole array fed by substrate integrated waveguide was presented in 2010 by Zhai et al. The array provides a low profile, light weight and wideband characteristics [11]. There are some log periodic arrays of special geometry to achieve multi-frequency wideband applications.

Wu et al. have designed a single-layered log periodic array of rectangular microstrip patches to achieve ultra wideband applications in 2010 [8]. The patches in the array are proximity-coupled to the microstrip feeding line and the impedance bandwidth of this antenna is from 2.26-6.85 GHz. This antenna has stable directional radiation patterns, very low-profile and low fabrication cost, which are suitable for various broadband applications.

J. Yang has described a guide rule for designing a wideband log-periodic array with constant radiation performance in 2010 [85]. In the same year, Muruk et al. have presented antennas to operate between 1.8 and 11 GHz with rejection at 6 GHz. The authors demonstrated a band-rejection technique including the removal of resonant teeth (aperture rejection technique), an integration of a dual band filter and the combination of above two techniques. The aperture rejection technique was resulted in more than 25 dB realized gain reduction [86]. A novel reconfigurable low profile log periodic patch array is presented by inserting switches within aperture slots coupling the feed line to the patches (7-10 GHz) by Hamid et al. in 2010 [87].

Recently, in 2011 a technique has been demonstrated by Jardon-Aguilar et al. to reduce the size of the log periodic dipole array antennas, which employs inductive loads on the elements of an antenna [88]. In this case, the total area is approximately 50% smaller than the size area of the reference antenna. A printed log-periodic dipole antenna with multiple notched bands is presented by Yu et al. for UWB applications

in the same year [89].

However, it was found that all the above described dipole or planar log periodic antennas suffer from metallic or conductor losses and results in reduction of bandwidth and less radiation efficiency which limit their performance. These limitations have prompted a desire for DRs instead of metallic elements in the log periodic array that can minimize the losses up to some extent.

The broadband Log Periodic Dielectric Resonator Antenna (LPDRA) array relies on recent developments of broadband DRA array and high efficiency log periodic technique. It is an advanced method to achieve low profile, light weight antenna with conformal mounting capabilities.

The LPDRA array has various advantages over single DRA elements including directional radiation patterns, increased gain, and often wider bandwidths [9]. It has generally low cross polarization levels [10] and low metallic loss which results in high efficiency. The LPDRA will predominately find applications in point-to-point communications, point-to-multi point communications, wireless communications, satellite communications systems and dynamic RADAR systems.

2.7 Summary

In this chapter, the state-of-art of Dielectric Resonator Antenna has been presented. It is started by describing the introduction of DRA, its features, feeding techniques, advantages, limitations, and applications. The applications of DRA as a wideband antenna in a wireless communication system and satellite communication systems are illustrated. The techniques to enhance the bandwidth of DRA have also been described and followed by investigating research work related to the DRA, DRA array, bandwidth enhancement in DRA. The chapter also presents several research works related to log periodic antenna, reconfigurable antenna, circular polarized antennas and wideband linear antenna arrays. It is found that the present wireless communication systems need more compact, wideband, high gain antennas with low conductor losses.

CHAPTER 3

Branched Microstrip line fed Log Periodic Dielectric Resonator Antenna in Ku band

3.1 Introduction

Ku-band (12-18 GHz) is providing wide bandwidth with more targeted coverage range for deploying services to multiple users. Ku-band is designed for satellite communications exclusively, eliminating competition and signal interference from other communications systems. Initially, C-band was the primary spectrum for satellite communications. The C-band applications require large antennas and providing communications across large areas. The C-band achieved a commercial success, the spectrum was immersed under tremendous pressure with infringement from number of terrestrial services which enforced the satellite industry to move towards Ku-band. The Ku-band enables the use of smaller antennas and results in cost reduction of network deployment. This band is less vulnerable to rain fade and hence offers a user more flexibility. Therefore, Ku band is normally preferred as an ideal band for digital data transmission via satellites.

In recent years, various types of small antennas are developed for Ku-band applications. A low profile mobile antenna for Ku-band satellite communication is designed in a stair structure shape using 24 active phased array elements [90]. The elements of the antenna are placed in a non-periodic array distance using the genetic algorithm. A waveguide-fed low profile and light weight microstrip antenna arrays for Ku-band applications was developed using a low-cost printed circuit board waveguide (PCB-WG) technology which gives 71% efficiency with high gain [76]. A wideband highly direc-

tive EBG Antenna has been designed using double-layer frequency selective surfaces and multi feed technique to operate in the Ku-band [75]. For satellite communication, there is an inherent trade-off between conductor losses and broad bandwidth.

In this chapter, LPDRA array with branched microstrip line feeding is proposed for Ku band applications. This array design is based on the recent developments of low loss DRA array and wideband log periodic technique. The design methodology of the DRA array using log periodic technique is discussed and the detailed results of the proposed antenna are investigated in this chapter.

3.2 Log Periodic Dielectric Resonator Antenna Array with parallel feed line

A seven element log periodic DRA array is designed and fabricated. The elements of the LPDRA array are arranged in a log periodic fashion. The proposed array is excited by log periodic branched microstrip feed line which results in a better coupling of energy between the elements and the feed line. This feed line technique enables a much more precise amplitude control for high frequency applications.

3.2.1 Antenna Geometry

The physical structure of the LPDRA array antenna is repetitive, which results in repetitive behavior in its electrical characteristics. The design of a frequency independent array consists of a basic geometric pattern that repeats, except with a different size pattern. Figure 3.1 shows the geometry of the LPDRA array configuration. In this array design, seven different sized rectangular shaped resonators are arranged in a log periodic fashion. The dielectric resonator (DR) of rectangular cross-section offers a second degree of freedom making it a versatile and flexible DRA [79]. The length (L), width (W), height (H) and spacing (S) of LPDRA element increases logarithmically from one end to another.

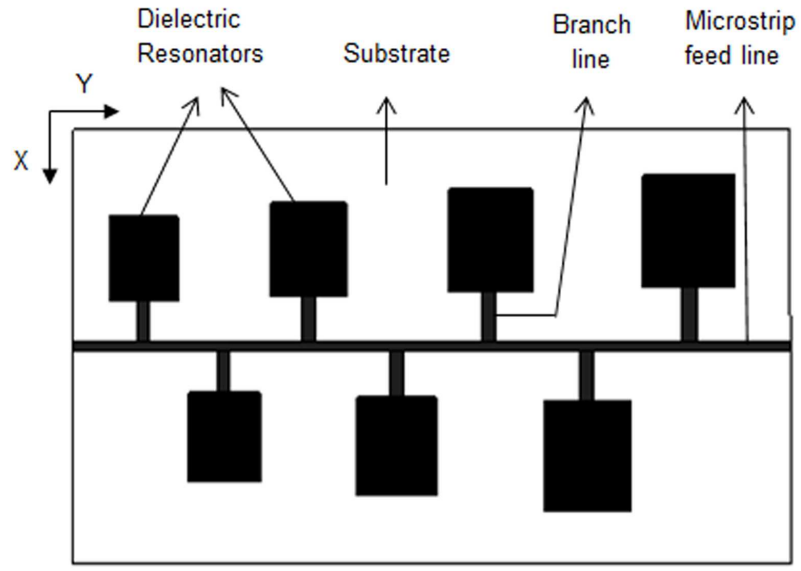

(a)

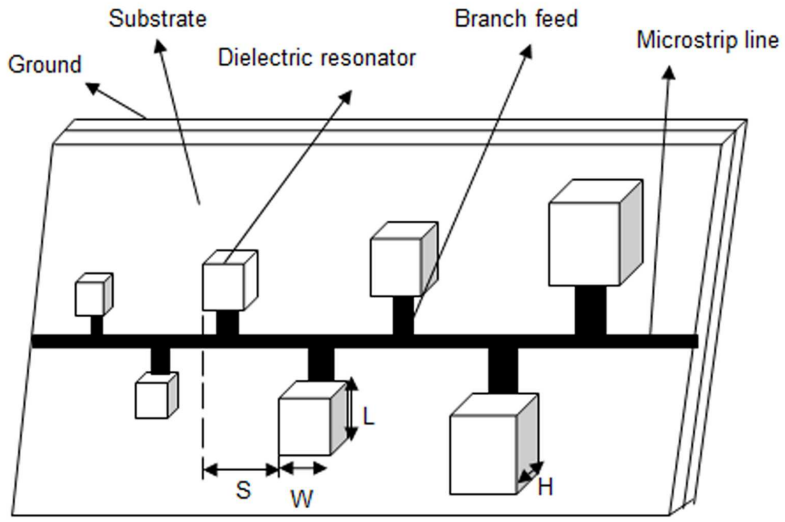

(b)

Figure 3.1: The branched microstrip line fed LPDRA array. (a)Top view, and (b) schematic view.

The schematic view of the LPDRA array is shown in Figure 3.1 (b). The array is excited by 50Ω branched microstrip line feeding which offers an advantage of easy and cost-effective fabrication of the antenna. In the resonant approach, the feed line is terminated in an open circuit, which creates a standing wave on the line where the voltage maxima or minima of each wave is located at multiples of $\lambda_g/2$ from the open-circuit location. The guided wavelength λ_g can be approximated using Equation

(3.1), where ϵ_r is the relative permittivity of the dielectric resonator and λ_0 is the free space wavelength.

$$\lambda_g = \frac{\lambda_0}{\sqrt{\varepsilon_r}} \tag{3.1}$$

For this LPDRA design, a dielectric resonator with relative permittivity $\epsilon_r = 2.1$ (Teflon) is used. Teflon based dielectric materials are best suited for DRA array design. The dielectric resonators along with the feed line are mounted on one side of inexpensive FR4 substrate measuring $\approx$ 250 mm long by 130 mm wide with a thickness (h_s) of 1.6 mm. The substrate has a relative dielectric constant (ϵ_s) of 4.4 with a loss tangent (tan δ) of 0.001 as shown in Figure 3.1 (b). A partially printed ground plane with dimensions 195 mm $\times$ 130 mm ($L_g \times W_g$) is layered on the opposite side to enhance the ensued bandwidth with full ground plane. The basic design of LPDRA array is similar to that of a normal log periodic array. The array is fed at the end of the structure, where smallest resonators are attached and the maximum radiation is obtained towards this end.

For simple log periodic antenna design the scaling factor (τ) and relative spacing (σ) values depend upon the desired gain and are chosen directly from Carrel's table [17]. The τ value of this LPDRA array design is chosen as 1.05. The value of σ can be obtained by using Equations (3.2) and (3.3), where σ_i is the ideal value of relative spacing.

$$\sigma_i = 0.258\tau - 0.066 \tag{3.2}$$

$$0.05 \leq \sigma \leq \sigma_i \tag{3.3}$$

The design parameter α_d, can be described by

$$\alpha_d = \tan^{-1}\left[\frac{1-\tau}{4\sigma}\right] \tag{3.4}$$

The desired bandwidth of the array, B_0 is the ratio of the highest (f_H) to lowest (f_L) range of frequency given by Equation (3.5).

$$B_0 = \frac{f_H}{f_L} \tag{3.5}$$

In a log periodic antenna, the designed bandwidth (B_d) should be more than the desired bandwidth (B_0). Thus the designed bandwidth is expressed as given in Equations (3.6) and (3.7).

$$B_d = B_0 B_r \tag{3.6}$$

$$B_d = B_0 \left[1.1 + 7.7\,(1-\tau)^2 \cot\alpha\right] \tag{3.7}$$

where B_r is the active region bandwidth of log periodic DRA.

The number of dielectric resonators (N_R) required to design the log periodic DRA array can be obtained as

$$N_R = 1 + \left[\frac{\ln B_d}{\ln \frac{1}{\tau}}\right] \tag{3.8}$$

Among all basic shapes (hemispherical, cylindrical, and rectangular) DRA, rectangular shaped DRA is more flexible as it is having one degree of freedom more compared to cylindrical shaped DRA and two degrees of freedom more than hemispherical DRA.

The length (L) of the dielectric resonators and their spacing (S) are graduated in such a way that certain dimensions of adjacent elements allow a constant ratio to each other. The design ratio is given by τ.

$$\tau = \frac{L_{m+1}}{L_m} = \frac{W_{m+1}}{W_m} = \frac{S_{m+1}}{S_m} \tag{3.9}$$

If the dimension of the array is multiplied by τ, it scales into itself with element m become element m+1, element m+1 become element m+2 etc. [13, 14, 91]. This self-scaling property implies that the array will have the same radiating properties at all those frequencies which are related by a factor of τ. The values of L, W and S will be scaled into log periodic elements. The dimensions of the smallest dielectric resonator element are length L_1 = 25.01 mm, width W_1= 23.82 mm and spacing S_1 = 27.34 mm, the dimensions of other dielectric resonators are scaled by τ. In this

design, length of the largest dielectric resonator has been found out by using Equation (3.10),

$$L = \frac{v}{\Delta f} \tag{3.10}$$

where speed of electromagnetic waves for the resonator,

$$v = \frac{c}{\sqrt{\varepsilon_r}}$$

$$\Delta f = f_H - f_L$$

and c is the speed of light in free space.

The width of the resonators is given below.

$$W = \frac{L}{\tau} \tag{3.11}$$

Spacing between elements should be,

$$S \geq \tau W \tag{3.12}$$

The dielectric resonator's height (H_m) in active region (region of high current excitation) of LPDRA is 3 mm. In a LPDRA array design, the whole array is divided into three regions (for short, medium, and long height resonators). Active region resonators are with medium height (H_m), whereas the other two regions, resonator's heights (H_{m-1} and H_{m+1}) are scaled by τ.

$$H_{m-1} = \frac{H_m}{\tau} \tag{3.13}$$

and

$$H_{m+1} = \tau H_m \tag{3.14}$$

The branched microstrip line feeding is used to excite the LPDRA array and the same log periodic technique is used for length and width of the branch feed line. The total length and width of the main microstrip feed line which is at the center of the array and common for the whole array is 250 mm and 3 mm respectively. For the first smallest branch feed line connected to the smallest dielectric resonator, the length

(f_L) and width (f_W) are 37.18 mm and 4 mm respectively. The length and width of other branch feed line connected with the rest of the dielectric resonators are scaled by τ.

$$\tau = \frac{f_{L_{m+1}}}{f_{L_m}} = \frac{f_{W_{m+1}}}{f_{W_m}} \tag{3.15}$$

The length and width of the whole array are 250 mm and 130 mm respectively. Since the resonant frequency and the radiation resistance depend primarily on the dielectric resonator's dimension and slightly influenced by the substrate thickness, so the height of both the substrate layer and feed line are kept constant.

3.2.2 k-β diagram and its analysis

The basic geometry of log periodic antenna having infinite periodic structure is given in Figure 3.2. The antenna consists of 'n' number of elements arranged side by side on a plane and forming a planar array.

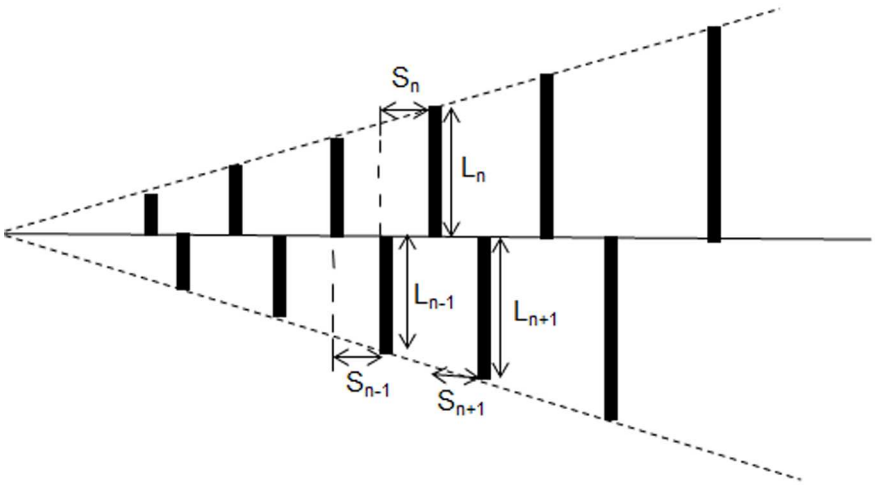

Figure 3.2: Basic Geometry of Log Periodic Antenna.

S = Spacing between two adjacent elements

Z_0 = characteristic impedance

For the given infinite log periodic structure, γ is the propagation constant, and it is described as:

$$\gamma = \alpha + j\beta \tag{3.16}$$

where α is the attenuation constant (Np/m) and β is the phase constant (rad/m). Generally,

$$\gamma = \alpha + j\beta = \sqrt{(R + j\omega L)(G + j\omega C)} \tag{3.17}$$

and

$$Z_0 = \frac{R + j\omega L}{\gamma} = \sqrt{\frac{R + j\omega L}{G + j\omega C}} \tag{3.18}$$

The equations described above are the general solutions which include some loss effects, and thus the propagation constant and characteristic impedance were found as complex.

In some practical cases, the loss in the periodic structures is very small, so it can be neglected. For a lossless case, the attenuation constant α is zero. Thus, R= G = 0 in the Equation (3.17) gives the propagation constant for α=0 as

$$\gamma = \alpha + j\beta = j\omega\sqrt{LC} \tag{3.19}$$

$$\beta = \omega\sqrt{LC} \tag{3.20}$$

The characteristic impedance in (3.18) reduces to

$$Z_0 = \sqrt{\frac{L}{C}} \tag{3.21}$$

which is a real number. Thus, the real value of propagation constant for a lossless log periodic structure can be expressed as,

$$\gamma = \beta \tag{3.22}$$

This equation is purely real. When α=0 and $\beta \neq 0$, this case corresponding to a non-attenuating, propagating wave on the periodic structure.

In Log Periodic antenna array, it is useful to plot the propagation constant, β versus the free space wave number, k to study the propagation characteristics of a

periodic structure. Such a graph is called as a k-β diagram, or Brillouin diagram [4, 80, 92].

β = the propagation constant = real

k is the free-space wavenumber,

$$k_c = \frac{2\pi f}{c} = \frac{2\pi}{\lambda} \tag{3.23}$$

For free space propagation,

$$k = \beta = \frac{2\pi}{\lambda} \tag{3.24}$$

The value of β is greater than k upto certain frequency, as the frequency increased, the wave becomes fast i.e. β becomes less than k ($\beta < k$).

$$\beta = \sqrt{k^2 - k_c^2} \tag{3.25}$$

$$k = \sqrt{\beta^2 + k_c^2} \tag{3.26}$$

where k_c is the cutoff wavenumber of the mode.

The k-β diagram can be plotted from (3.25) and (3.26) as shown in Figure 3.3.

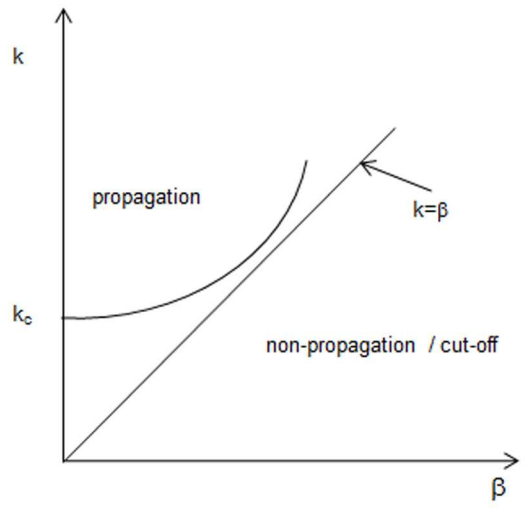

Figure 3.3: k-β diagram for an infinite periodic structure.

For values of $k < k_c$, there is no real solution for β, so the mode is non-propagating. For $k > k_c$, the mode propagates, and k approaches β.

The propagation values can be plotted for a periodic antenna at several different frequencies. The characteristics of the k-β diagram of a periodic structure vary widely depending upon the nature of the structure. The k-β diagram can be used to study the dispersion characteristics of many types of microwave components and transmission lines. The suitability of the LPDRA array can be accessed by its k-β characteristics plot.

3.2.3 Simulation Results

A branched microstrip line fed LPDRA array for Ku band has been designed and analyzed. The results of the seven element LPDRA array are discussed in terms of bandwidth response, input impedance, radiation pattern, gain and propagation characteristics. The simulation studies for the proposed LPDRA array have been carried out by using CST Microwave Studio suite 2012.

The impedance bandwidth of LPDRA from 11.4 - 18 GHz is the desired frequency range for Ku band applications. As discussed in the previous chapter, the gain, bandwidth, and radiation performances of DRA can be modified by using a log periodic array instead of basic shaped DRA.

A seven element LPDRA array compared to five elements and three elements LPDRA array results in a wide impedance bandwidth. A comparison in performance of the array in terms of bandwidth and gain based on the number of resonators is given in Table 3.1.

Table 3.1: Comparison of the performance (bandwidth and gain) of LPDRA based on the number of resonators in the array.

Number of Resonators	**Bandwidth (%)**	**Gain (dBi)**
3	9	8.3
5	35	10.6
7	46	11.4

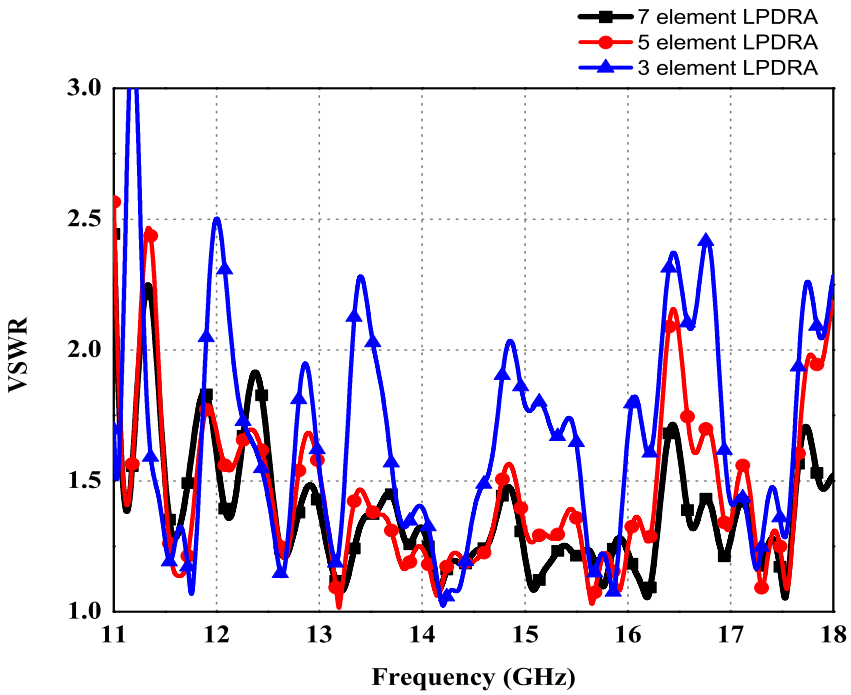

Figure 3.4: VSWR curves of the branched microstrip line fed LPDRA array with different number of dielectric resonator elements.

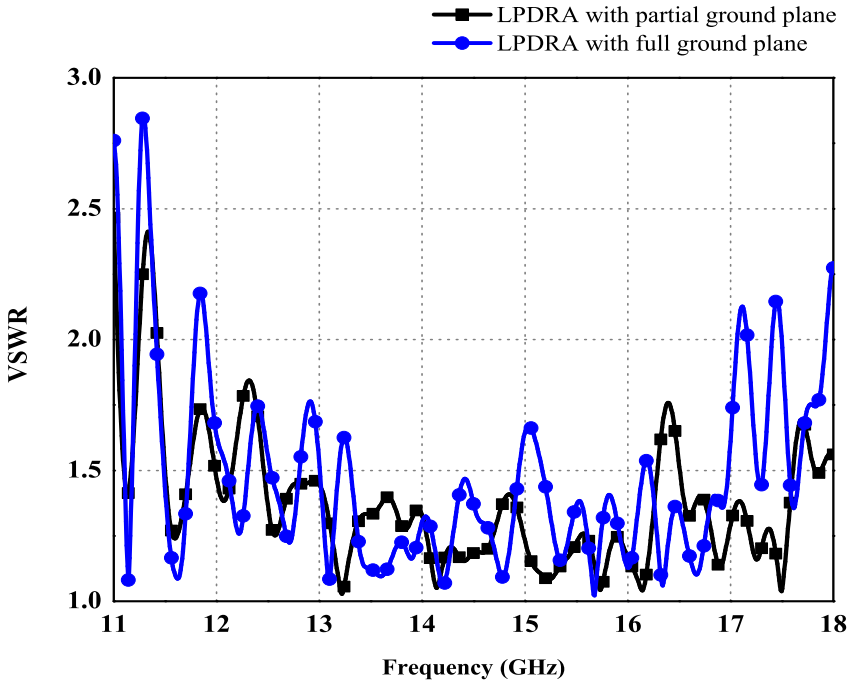

Figure 3.5: VSWR curves of the branched microstrip line fed LPDRA array with full ground plane and partial ground plane.

The array with seven elements is providing 46% of impedance bandwidth covering the frequency range 11.4 - 18 GHz with 11.4 dBi of gain. The VSWR vs frequency characteristic of LPDRA array for different number of elements (three, five and seven) is shown in Figure 3.4.

This LPDRA array is designed with a partial ground plane to achieve enhanced bandwidth. A parametric study for LPDRA array with full ground plane and with a partial ground plane has been shown in Figure 3.5. For LPDRA array with full ground plane, the impedance bandwidth ranges up to 17 GHz (39.4%) whereas for partial ground plane, the desired bandwidth is up to 18 GHz (46% for VSWR ≤ 2).

The gain of the LPDRA array depends on the value of scaling factor (τ). Any variation in τ value affects the gain of the array. Table 3.2 gives a comparison in performance of the array based on the values of scaling factor τ. The proposed LPDRA array is providing 11.4 dBi of gain for scaling factor 1.05.

Table 3.2: Comparison of the performance (bandwidth and gain) of LPDRA based on the value of scaling factor.

Scaling factor (τ)	**Bandwidth (%)**	**Gain (dBi)**
0.9	35	8.89
0.95	35	9.42
1	27	10.05
1.05	46	11.4
1.1	34	8.96

Table 3.3: Comparison of the performance (bandwidth and gain) of LPDRA based on the relative permittivity of dielectric material.

Relative permittivity (ϵ_r)	**Bandwidth (%)**	**Gain (dBi)**
2.1	46	11.4
6	48	10.7
9.8	47	10.04
10	47	11.2
10.2	47	11.06

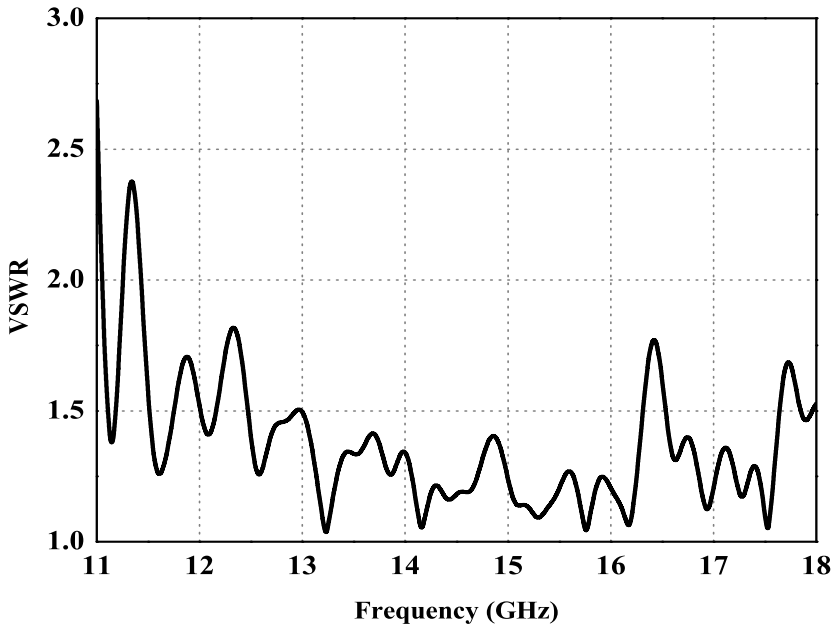

Figure 3.6: Simulated VSWR curve of the branched microstrip line fed LPDRA array.

The bandwidth and gain of the LPDRA array are also affected by the change in the dielectric constant of the resonating material. Table 3.3 illustrates a comparison in performance of the array in terms of bandwidth and gain based on the relative permittivity of the dielectric material. There is a small variation in bandwidth and gain of the array with different types of dielectric material. The LPDRA array with Teflon (ϵ_r =2.1) is providing 11.4 dBi of high gain.

In Figure 3.4, it has been perceived that the bandwidth of the DRA directly influenced by the number of elements used in the array. Compared with the bandwidth of 3 and 5 elements, 7 elements LPDRA array is giving desired bandwidth. Finally, the simulated VSWR curve of the 7 element LPDRA with scaling factor 1.05 is shown in Figure 3.6. The resulted bandwidth is found as 46%.

The real and imaginary parts of input impedance curves and the smith chart of the LPDRA array have been presented in Figure 3.7 (a) and (b). From the figures, it has been observed that the average input impedance for the array is 52.77 ohm which is approximately equal to 50 ohm.

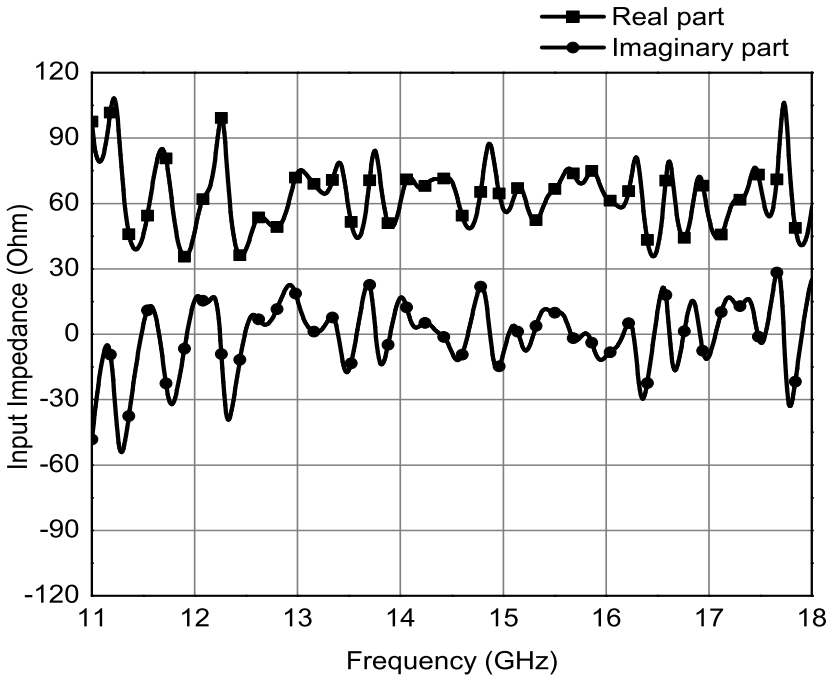

(a)

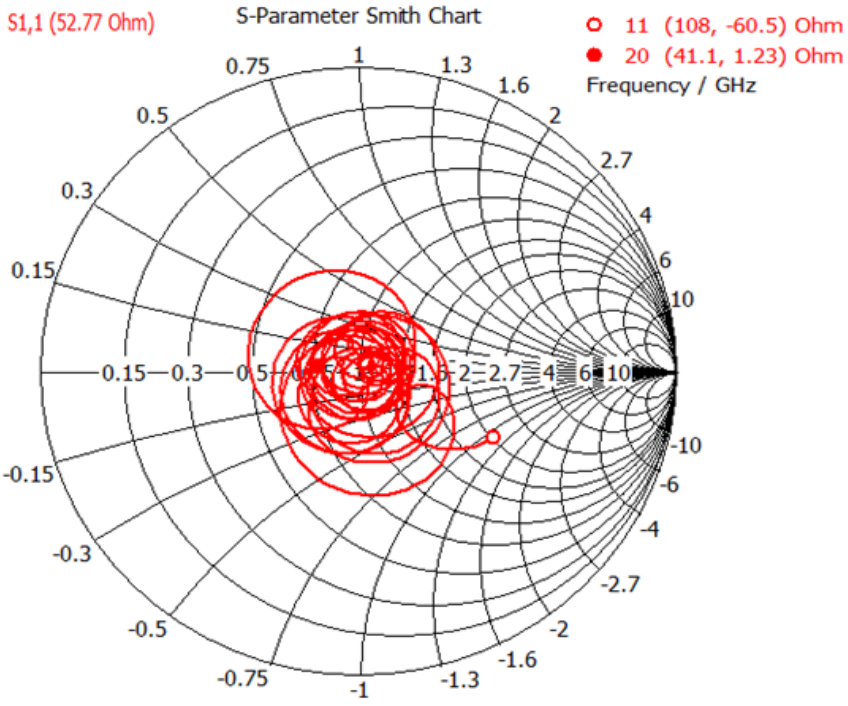

(b)

Figure 3.7: Simulated Input Impedance curves of the branched microstrip line fed LPDRA array: (a)real and imaginary part and (b) smith chart.

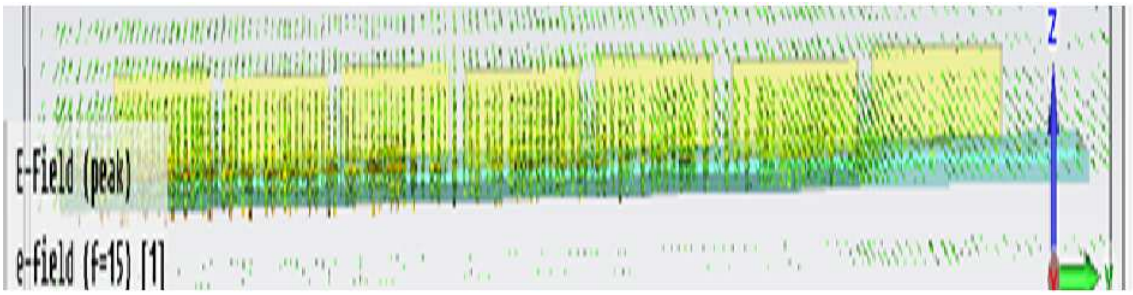

(a)

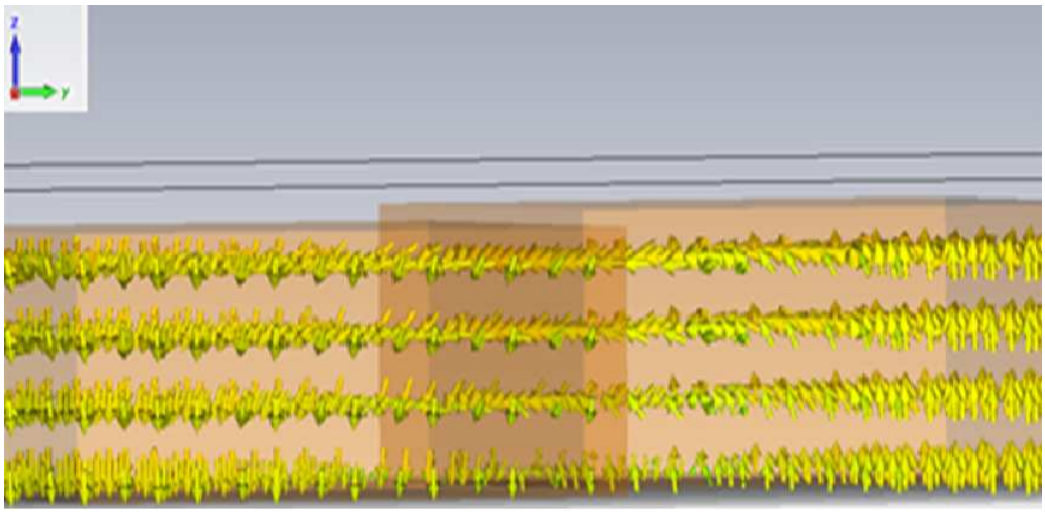

(b)

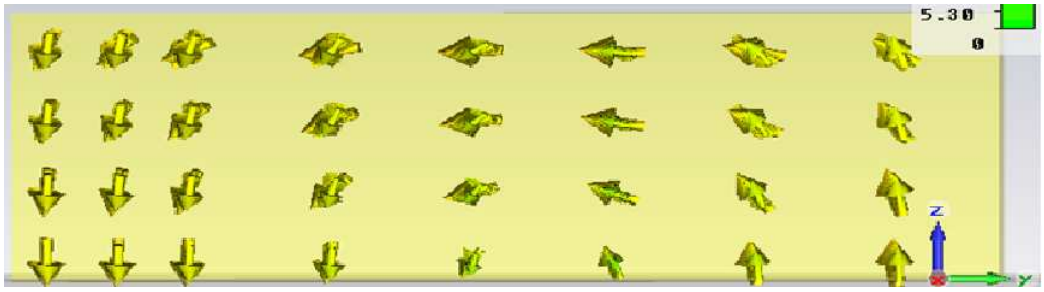

(c)

Figure 3.8: Simulated electric field distributions of branched microstrip line fed LPDRA array at 15 GHz in: (a) seven elements LPDRA array, (b) two consecutive resonators and (c) single resonator.

The electric field distributions of LPDRA array have been monitored to verify the resonant mode in the dielectric resonators as described in Chapter 2. The simulated results for electric-field distribution at 15 GHz are shown in Figure 3.8. The field distributions represent $TE_{\delta 11}\,(0 < \delta \leq 1)$ mode in the resonators of the array, which is the lowest modes of rectangular DRA [21].

Figure 3.9 displays the simulated co-polar and cross polar radiation patterns for both E and H-planes at 14 GHz and 16 GHz. The H-plane radiation patterns are almost omnidirectional and the E-plane radiation patterns are in the broadside direction against frequency. The cross polar rejection is below -20 dB.

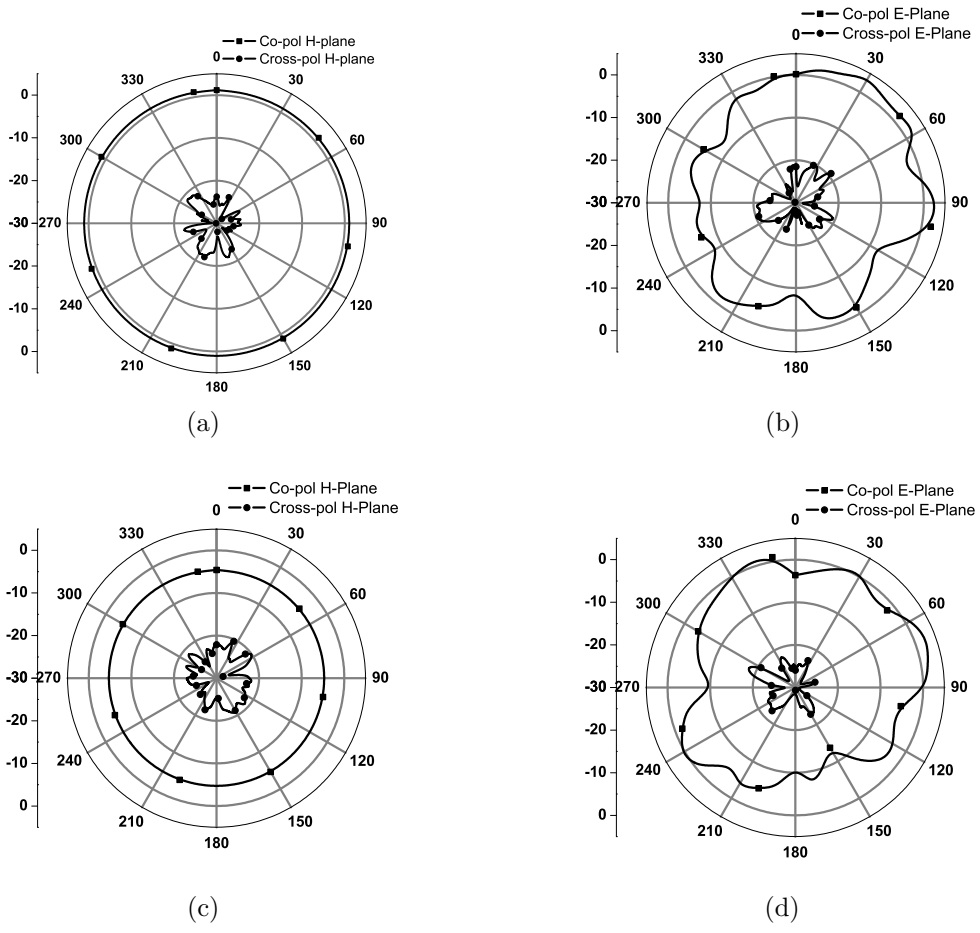

Figure 3.9: Simulated co-polar and cross-polar radiation patterns of LPDRA array. (a)H-plane at 14 GHz, (b) E-plane at 14 GHz, (c)H-plane at 16 GHz and (d) E-plane at 16 GHz.

Dielectric resonator antenna can be superior to microstrip antenna in some cases as it has negligible metallic loss and high efficiency at microwave frequencies. Due to low loss of the dielectric materials, DRAs offer a high radiation efficiency as well as high gain in contradiction of microstrip antenna.

Figure 3.10 presents the gain versus frequency plot of the log periodic antenna with dielectric resonators and without dielectric resonators which confirms that within the

desired band the gain of DRA is better than the gain of microstrip antenna. In case of log periodic microstrip patch antenna (LPMPA), a wide band with less radiation efficiency and low gain can be achieved due to more conductor losses in comparison to LPDRA array.

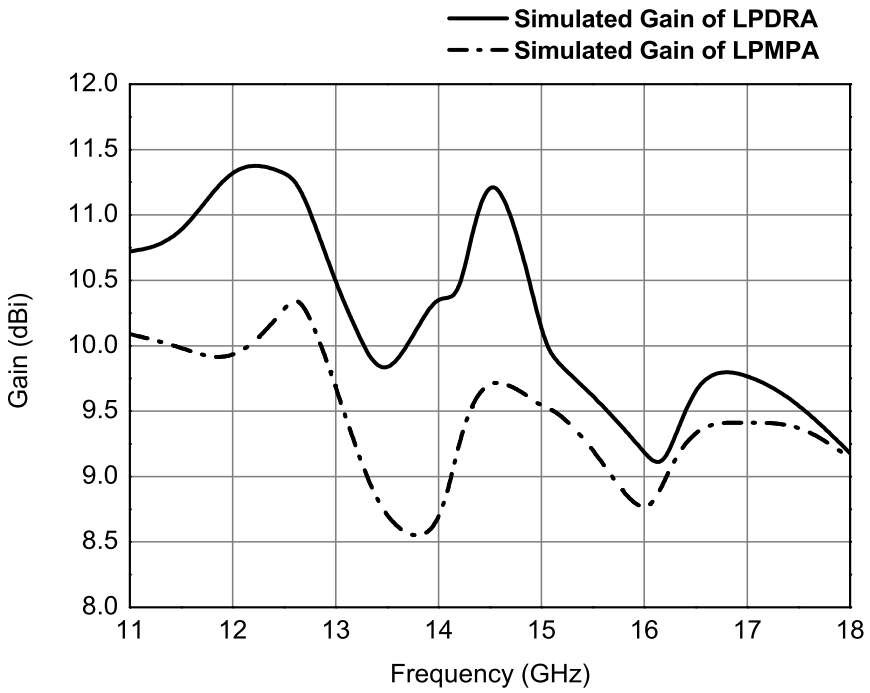

Figure 3.10: Simulated Gain of Log Periodic antenna with dielectric resonator and without dielectric resonator.

The gain characteristics of LPDRA array vary nearly log periodically in the range of 9.2-11.4 dB with 96% of simulated antenna efficiency whereas in log periodic antenna without dielectric resonators (LPMPA), gain varies from 8.5-10.25 dB with less radiation efficiency.

k-β Analysis

The Propagation characteristic of LPDRA array can be derived from the Equation (3.25) and (3.26). The k-β diagram for the branched microstrip line fed LPDRA array is given in Figure 3.11. The resonance in LPDRA array starts at $k_c \approx 0.24$. It can be seen from the figure that the log periodic array is resonating beyond this point with less attenuation.

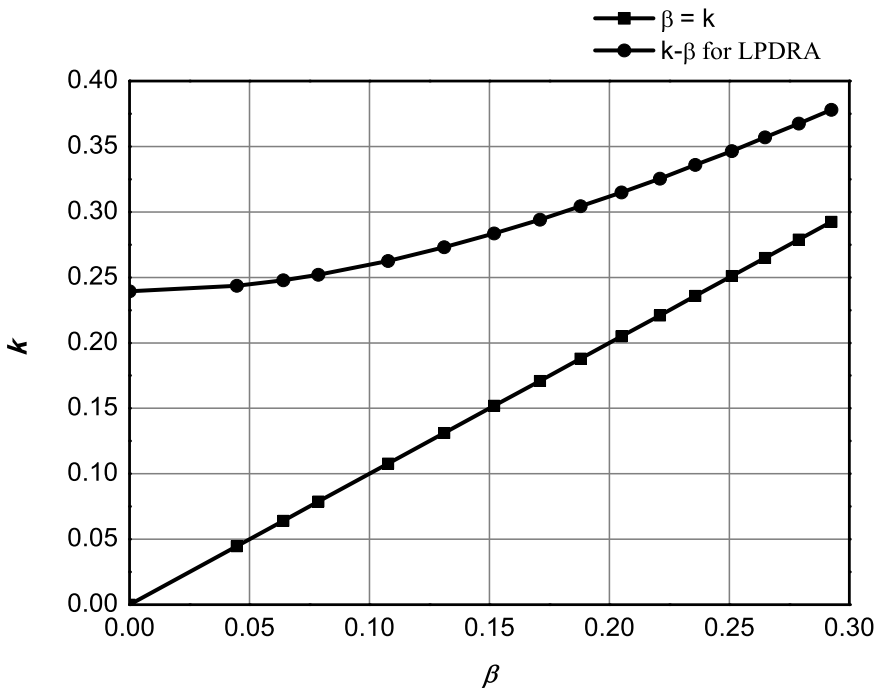

Figure 3.11: k-β diagram of LPDRA array.

3.2.4 Experimental Verifications

The designed LPDRA array is fabricated with Teflon on a dielectric substrate FR4 ($\epsilon_r = 4.4$, $\tan\,\delta = 0.0024$, h =1.6 mm) and experimentally studied.

The VSWR measurement of the fabricated LPDRA array is performed by using an Agilent 8720B network analyser and the radiation performance has been measured in the anechoic chamber at Advanced Microwave Laboratory, I.I.T., Roorkee.

The photograph of fabricated LPDRA array is shown in Figure 3.12. From the figure, an airgap can be observed between the largest DR element and the ground. The introduction of air gap between the DR elements and the ground plane can increase the impedance bandwidth of the antenna (as described in chapter 2). Further increase in introduction of air gap can results in an enhancement of bandwidth with some back lobes. In this proposed LPDRA array with seven DR elements, the airgap has been introduced only in between the largest DR element and the ground plane to enhance the bandwidth with less back radiation.

Figure 3.13 shows the simulated and measured VSWR curves. Any changes in the

dimension will affect the resonant frequency of the antenna. It provides a wideband with 46% of impedance bandwidth covering the frequency range of 11.4-18 GHz with VSWR ≤ 2.

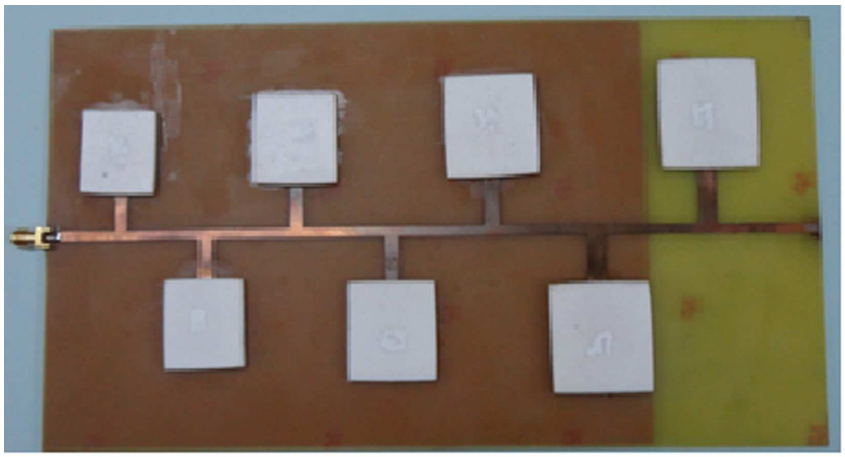

(a)

(b)

Figure 3.12: The prototype of the fabricated branched microstrip line fed LPDRA array. (a)Front view, and (b) Rear view.

The simulated and measured VSWR results of the proposed LPDRA array shows a good matching with slight discrepancies at some frequencies which may be mainly due to errors in the fabrication process or it may be due to the mismatching between the connector and the antenna feeder. The fabricated LPDRA array in the anechoic chamber has been shown in Figure 3.14.

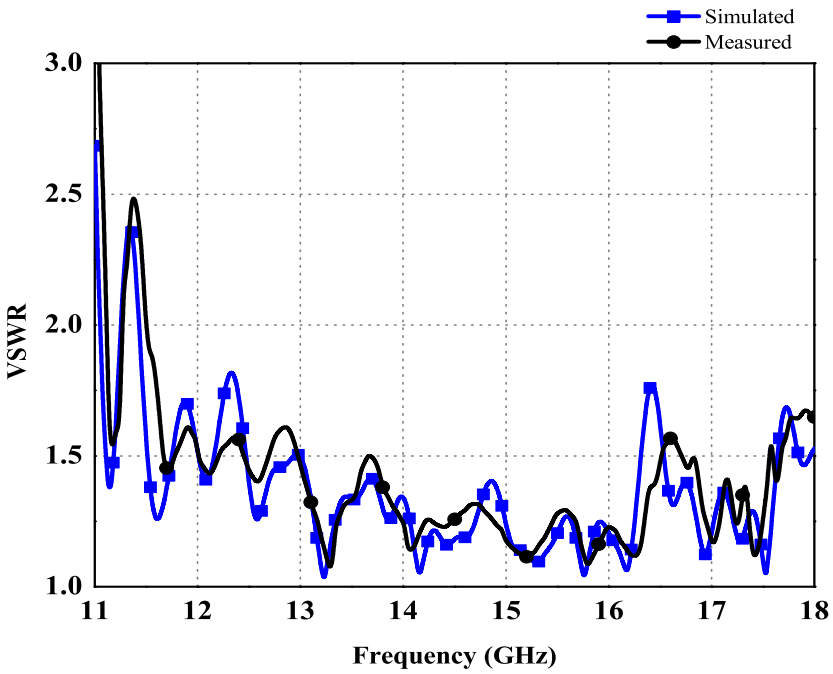

Figure 3.13: Simulated and measured VSWR curves of branched microstrip line fed LPDRA array.

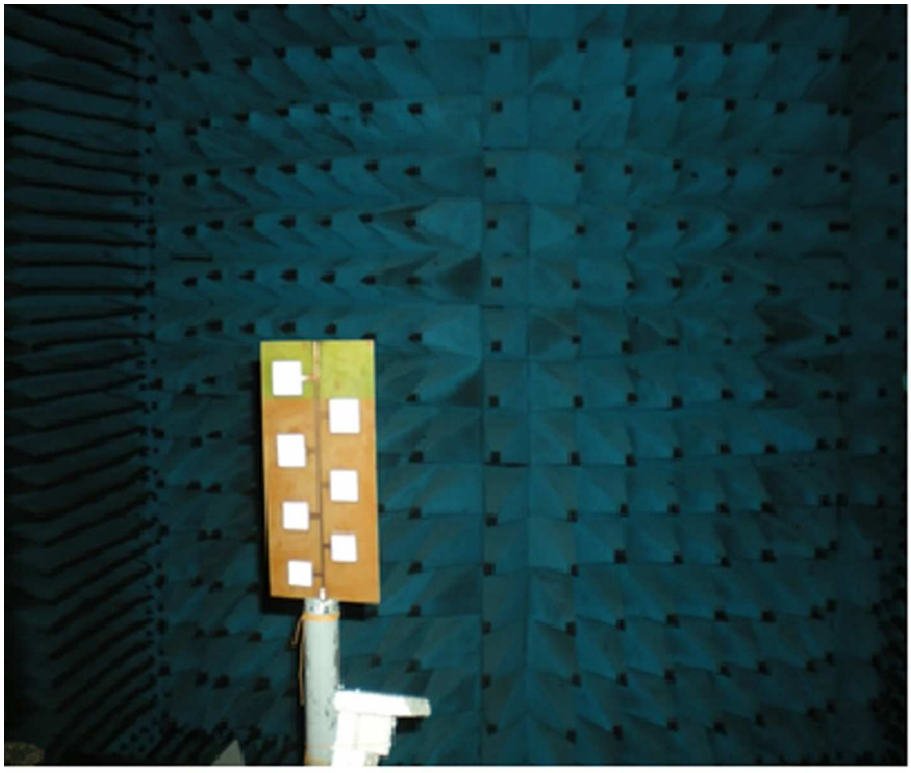

Figure 3.14: Far field measurement of branched microstrip line fed LPDRA array in anechoic chamber.

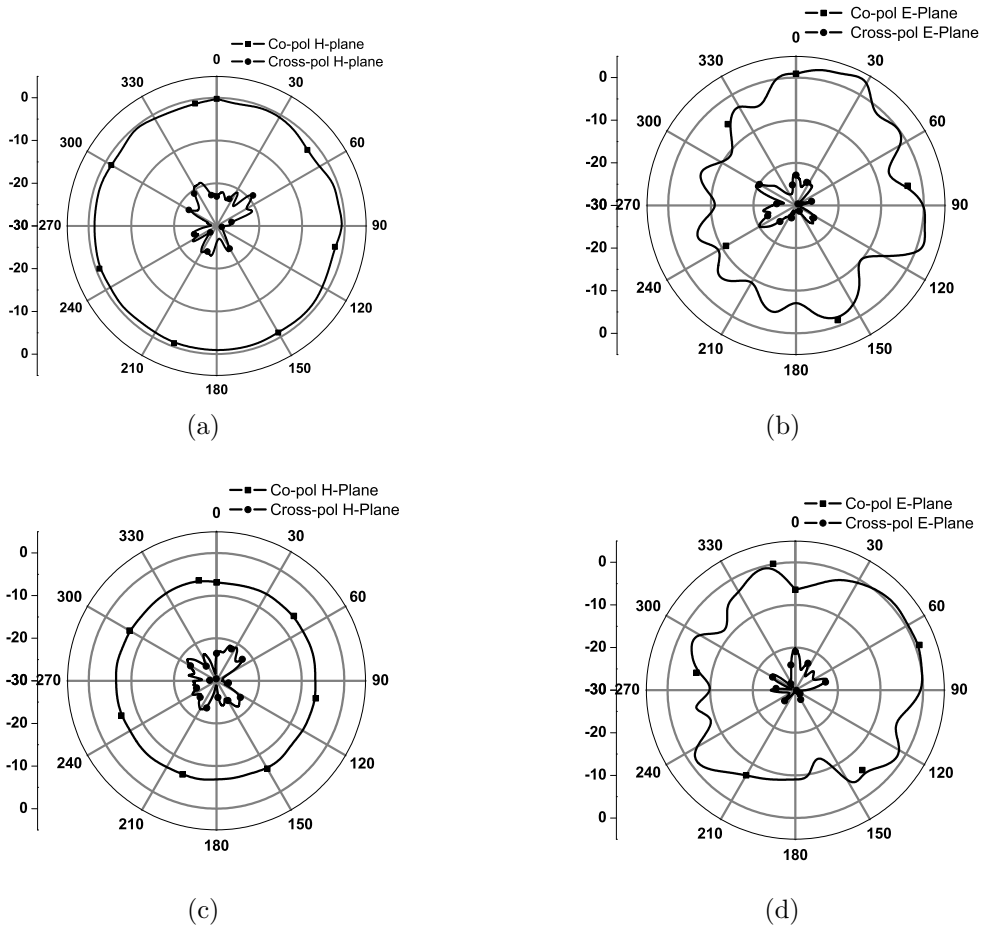

Figure 3.15: Measured co-polar and cross-polar radiation patterns of LPDRA array. (a)H-plane at 14 GHz, (b) E-plane at 14 GHz, (c)H-plane at 16 GHz and (d) E-plane at 16 GHz.

Figure 3.15 presents the measured far-field radiation patterns of the proposed antenna in H-plane and E-plane (both co-polar and cross polar) at the operating frequency bands of 14 GHz, and 16 GHz. The presence of nearly omnidirectional radiation in the H-plane and broadside radiation in the E-plane can be observed in the results. The measured far field H-plane radiation patterns of the LPDRA array are almost same for all frequencies. The measured cross polar rejection is below -20 dB.

The measured radiation patterns in Figure 3.15, are normalized for setting the maxima at 0 dB. Good agreement has been found between the simulated and measured values of radiation patterns at two distinct operating frequencies which validate the proposed design. Some difference between the simulated and measured field patterns

may be attributed due to the alignment error and possible presence of interference and noise.

The measured gain curve of the array is presented in Figure 3.16. The proposed array offers measured peak gain of 11.2 dBi at 12.8 GHz.

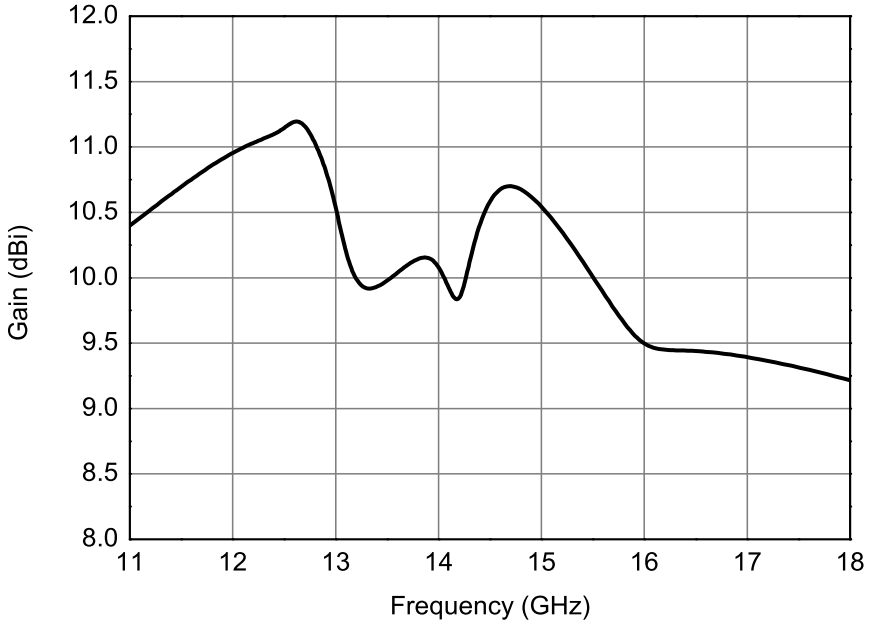

Figure 3.16: Measured Gain of branched microstrip line fed LPDRA array.

From the RF power generator 15 dBm of power is given to the transmitter horn antenna. The distance between the transmitter and receiver is kept at 1.5 meter. The gain of the LPDRA array is calculated by using the substitution method (as explained in Appendix A) with the help of the standard calibrated gain horn antennas (reference antenna) working in the 8-12 GHz and 12-18 GHz. About 0.5 dB of difference is observed between the simulated and measured gains which could be attributed from fabrication and measurement errors. Connectors and other devices such as cables also cause some signal losses. Also the spurious radiation at the connector/antenna junction can affect the radiation pattern and gain of the antenna.

3.3 Summary

A wideband seven element branched microstrip line fed LPDRA array with high radiation efficiency has been designed in this chapter. The LPDRA array has been introduced to achieve significant wide bandwidth with low conductive losses. The array design encompasses a low cost dielectric material (Teflon) with permittivity (ϵ_r) of 2.1 for ease in the fabrication of arrays. A good agreement between simulated and measured results has been found. The VSWR matching is better than 2:1 in the working bandwidth. With both input match and radiation efficiency consideration, the bandwidth of this antenna is 46% with VSWR less than 2. This array design is used to resonate over a wide range of frequency 11.4-18 GHz with high gain nearly 10-11 dB. The maximum efficiency of the proposed antenna is 96%. This LPDRA array can be used in satellite communication systems for Ku band applications.

CHAPTER 4

Capacitive Coupled Log Periodic Dielectric Resonator Antenna in X-Band

4.1 Introduction

Now-a-days, the communication systems operating in X-band are becoming more prevalent. Satellite communication requires small and light weight antenna with less metallic losses and broadband facilities. The frequency range of X-band has covered approximately 7.0-11.2 GHz for communication engineering applications.

Varieties of antenna arrays are designed by a number of researchers for X-band applications. A phased array antennas based on Substrate-Integrated Waveguide (SIW) structure for X-band satellite communication is investigated for Right-Handed Circular Polarization (RHCP) with multi-layered fabrication [93]. A dual-frequency, dual-polarization array antenna is developed for S-Band and X-Band airborne applications, where a multilayer structure is adopted for dual-band operation [94]. The antenna arrays for the two frequencies are separated on different layers and the X-band array used a series-fed configuration to save the space of the feeding-line network. However, these antennas can be seldom used because of the complex circuitry structure. With the increase in demand of compactness and low metallic losses, it is appropriate to implement a simple and compact DRA array design to offer an improved performance. Therefore, efforts were made to devise alternative LPDRA array design which could provide acceptable wideband with enhanced performances.

In the previous chapter, a branched microstrip line fed LPDRA array is presented for Ku-band applications. In some applications, the concept of achieving wide band-

width by utilizing an LPDRA array with branch feeding leads to excitation difficulties and the feed line can introduce some losses. However, if a series feed is used, these problems can be overcome. The dielectric resonators can in principle be etched on the same substrate as the feed line and the resonators are capacitive (directly) coupled to the feed line [4].

An LPDRA array excited by a series fed microstrip line is designed in this chapter. The designed LPDRA is fabricated and measured to verify the simulated results. The resultant bandwidth covers the desired frequency range for X-band applications. The measured VSWR, gain and radiation patterns at different frequencies are presented. The antenna design and detail results of the proposed LPDRA array are discussed in the following sections.

4.2 Log Periodic Dielectric Resonator Antenna Array with microstrip series feed line

An LPDRA array with microstrip series feed line is designed, simulated, fabricated and practically tested. The elements of the array are directly coupled to the feed line which results in more compact and low loss DRA array. The volume and weight of the array can also be reduced by using this series microstrip line feeding. This array is developed to achieve wide bandwidth with low conductor loss for X-band applications.

4.2.1 Antenna Geometry

This section elaborates the design of the seven elements LPDRA array. Figure 4.1 shows the antenna configurations of the proposed LPDRA array. The LPDRA array consists of seven Dielectric Resonators (DRs) of rectangular cross-section arranged in a log periodic fashion. The DRs are made up of Teflon (ϵ_r= 2.1), a dielectric material with low relative permittivity.

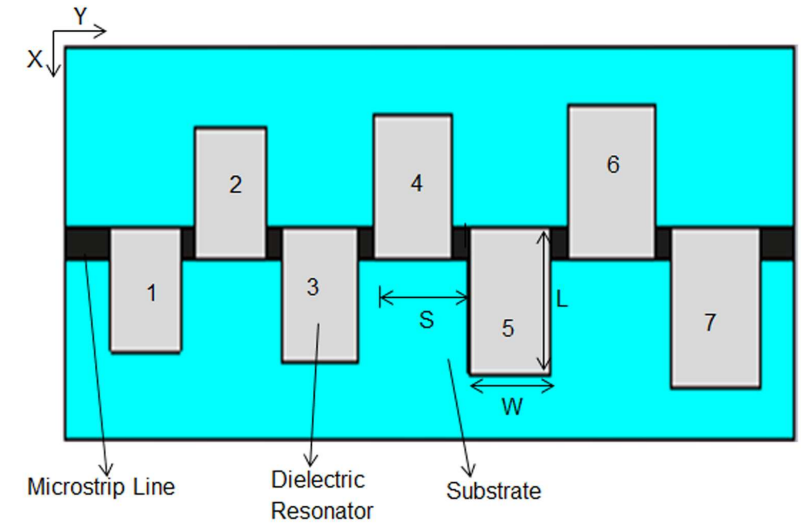

(a)

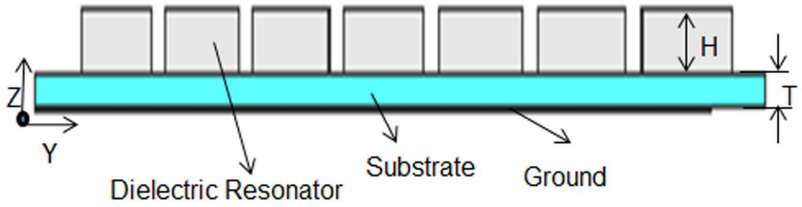

(b)

Figure 4.1: The Geometry of Seven element LPDRA with microstrip series feed line. (a)Front view, and (b) Side view.

The proposed array is excited by capacitive coupled microstrip line feeding. The DRs are directly coupled to the microstrip feed line, dimensioned as 80×2.5 mm^2. All the resonators along with the feed line are etched on the same FR4 substrate measuring ≈ 80 mm long by 30 mm wide with a relative permittivity of 4.4 and a thickness (T) of 1.6 mm. The array is fed at the end of the structure having smallest resonators and the maximum radiation is towards this end. The far end of the feed line is terminated with an open circuit. On the rear side of the substrate, a finite ground plane with dimension 74 × 30 mm^2 is partially printed. The resulting air gap between the resonator and the ground plane helps to reduce the Q-factor of LPDRA.

The basic design of the array is similar to that of a normal log periodic array.

The resonators of the array are arranged at 180^0 phase shift from one another. The resonators with Length (L), Width (W), Height (H) and Spacing (S) between resonating elements along the array are varied by scaling factor (τ) [83,95]. Usually, the value of τ and relative spacing (σ) depends upon the gain of the desired applications which can be directly chosen from Carrel's table [17, 18]. The preferred τ value for this design is 0.96.

The elements of a typical log periodic antenna are arranged in ascending order starting from the feeding end towards the far end of the antenna which lies within an angle $2\alpha_d$ as shown in Figure 4.2.

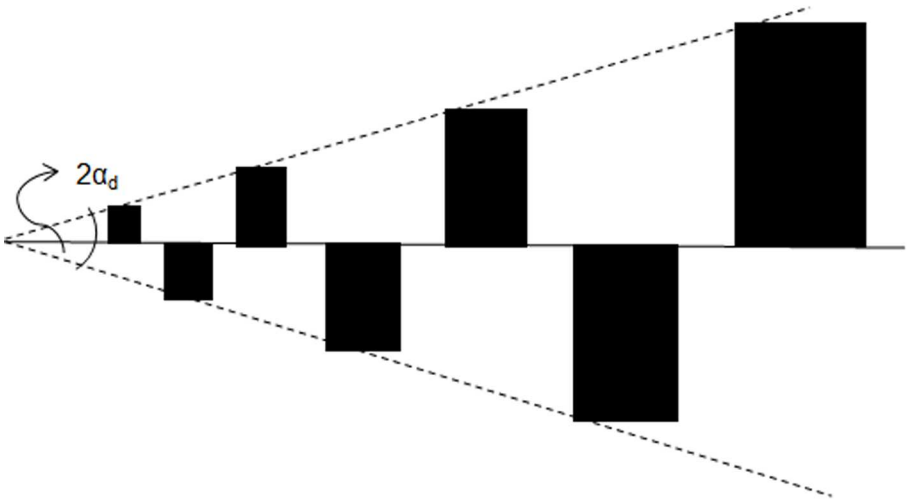

Figure 4.2: Typical Log Periodic Antenna configuration.

The design parameter α_d is expressed by Equation (3.4). Generally, $10^0 \leq \alpha_d \leq 45^0$. The value of τ starts to decrease with the increase of α_d. The designed bandwidth can be expressed in terms of B_0 (desired bandwidth) and B_r (active region bandwidth) using Equations (3.5) to (3.7).

The dimensions of each DR elements are varying log periodically from one end to another. When the dimensions of larger resonators (L, W, H and S) are multiplied by τ, it scales into itself where the larger resonator m+1 becomes m, resonator m becomes m-1, which implies that the array will have the same electrical characteristics at all frequencies that are related by τ.

In this LPDRA array with series fed microstrip line, the dimensions of largest resonators are always related to lowest frequency and can be found out by using Equations (4.1) to (4.3) where the smallest resonator's dimensions are associated with the highest frequency of the band.

$$L = \frac{\lambda_{\max}}{4} \tag{4.1}$$

$$\lambda_{\max} = \frac{c}{f_{\min}\sqrt{\varepsilon_r}} \tag{4.2}$$

where λ_{max} is the wavelength of the lowest frequency (f_{min}), c is the speed of light in free space and ϵ_r is the relative permittivity of the dielectric resonator.

$$W = 0.8 \times L \tag{4.3}$$

$$W < S \leq \tau.L \tag{4.4}$$

Equation (4.4) can be used to find the spacing between the adjacent resonators. As the τ value for this design is 0.96 (<1), so the dimensions of the other dielectric elements can be calculated by using Equation (4.5).

$$\tau = \frac{L_m}{L_{m+1}} = \frac{W_m}{W_{m+1}} = \frac{H_m}{H_{m+1}} = \frac{S_m}{S_{m+1}} \tag{4.5}$$

Table 4.1: Dimensions of the LPDRA elements.

Dielectric Resonators (Largest to Smallest)	**L (mm)**	**W (mm)**
DR_7	12.3	9.8
DR_6	11.81	9.41
DR_5	11.33	9.03
DR_4	10.88	8.67
DR_3	10.45	8.32
DR_2	10.03	7.99
DR_1	9.63	7.67

In the proposed LPDRA, the dimensions of the largest element is 12.3 mm length,

9.8 mm width and 3 mm height with center to center spacing (S) between two resonators being 11.3 mm. The dimensions of other DR elements are scaled by τ as depicted in Table 4.1. The overall dimension of the array is 80 $\times$ 30 mm^2. This antenna design can be used to achieve wide bandwidth with high gain and broadside radiation patterns.

4.2.2 Simulation Results

A capacitive coupled LPDRA array for X-band applications has been designed and simulated using CST Microwave Studio suite 2012. The simulated results of the array in terms of bandwidth, VSWR, input impedance, radiation pattern, gain and propagation characteristics are studied and analysed.

The VSWR characteristics of LPDRA for different number of array elements (five, six and seven) have been shown in Figure 4.3. It has been observed that among all arrays, the array with seven dielectric resonators cover wide impedance bandwidth. So, for further investigations of LPDRA characteristics, LPDRA with seven dielectric resonator is selected.

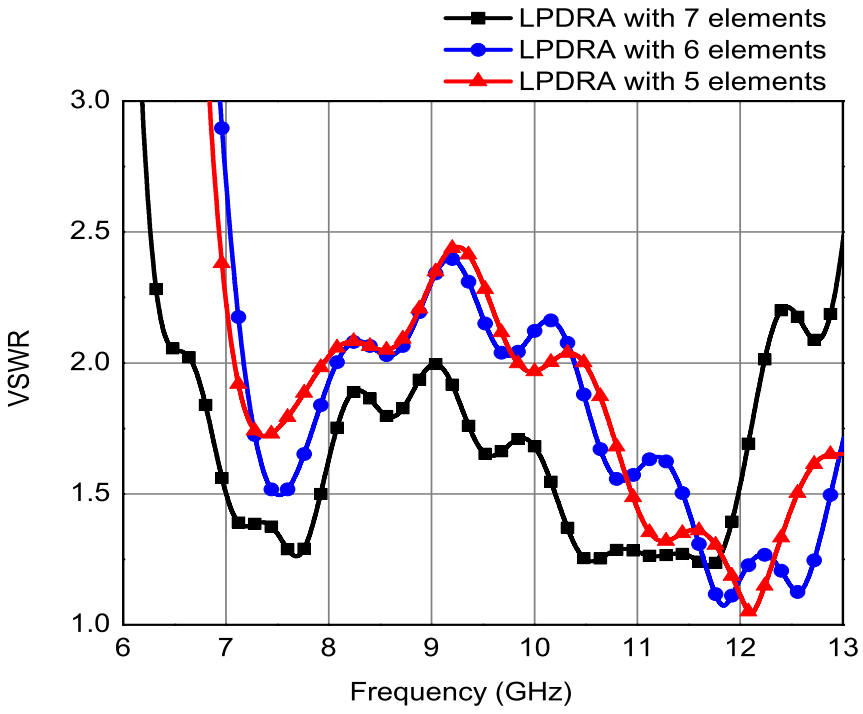

Figure 4.3: VSWR curves of capacitive coupled LPDRA for variation in number of dielectric resonators of array.

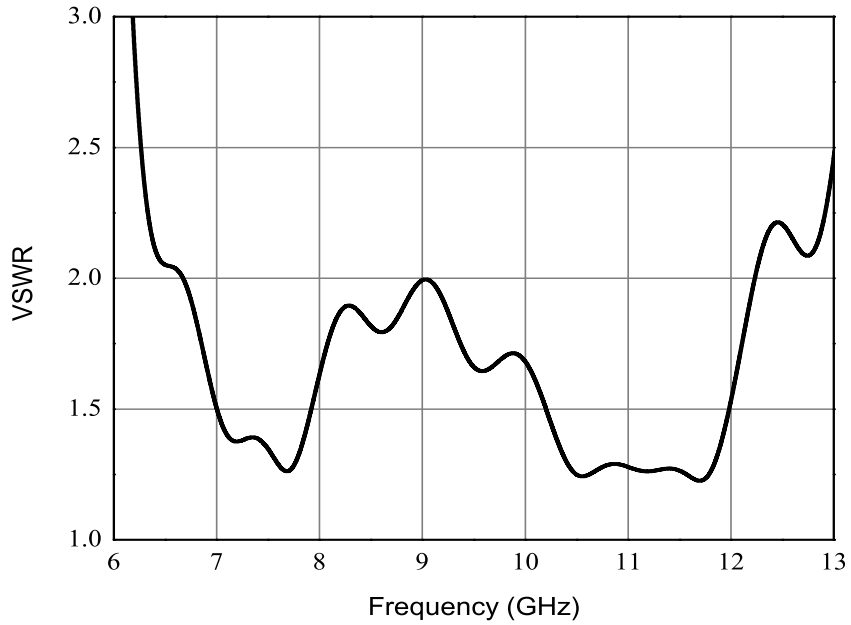

Figure 4.4: Simulated VSWR curve of capacitive coupled LPDRA.

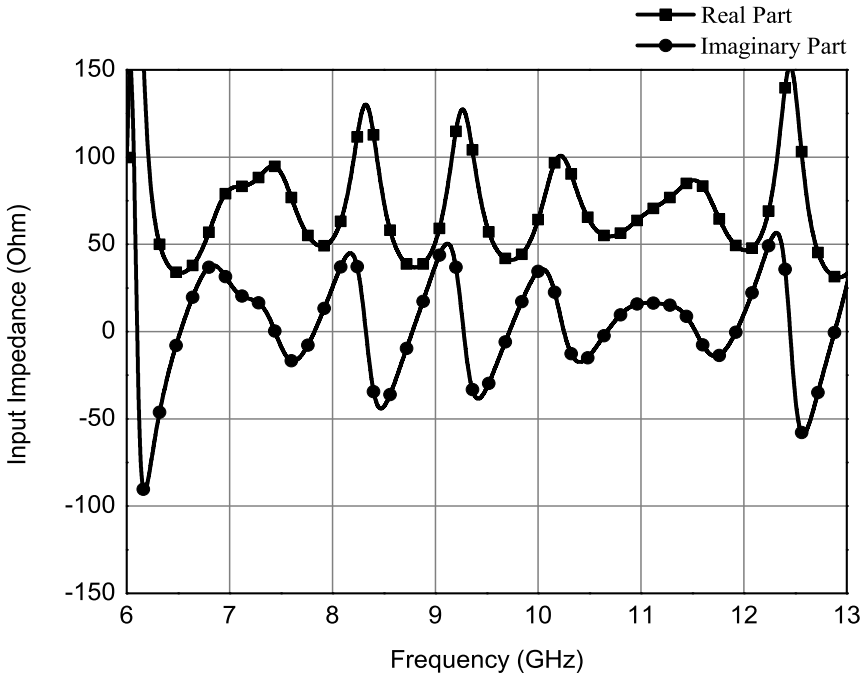

Figure 4.5: Input Impedance curve of capacitive coupled LPDRA.

The simulated VSWR curves of LPDRA array with seven elements are shown

in Figure 4.4. The bandwidth of the array covers the desired frequency range of 6.2 to 12.2 GHz for X-band applications. The proposed array offers an impedance bandwidth of 65.2% for VSWR ≤ 2.

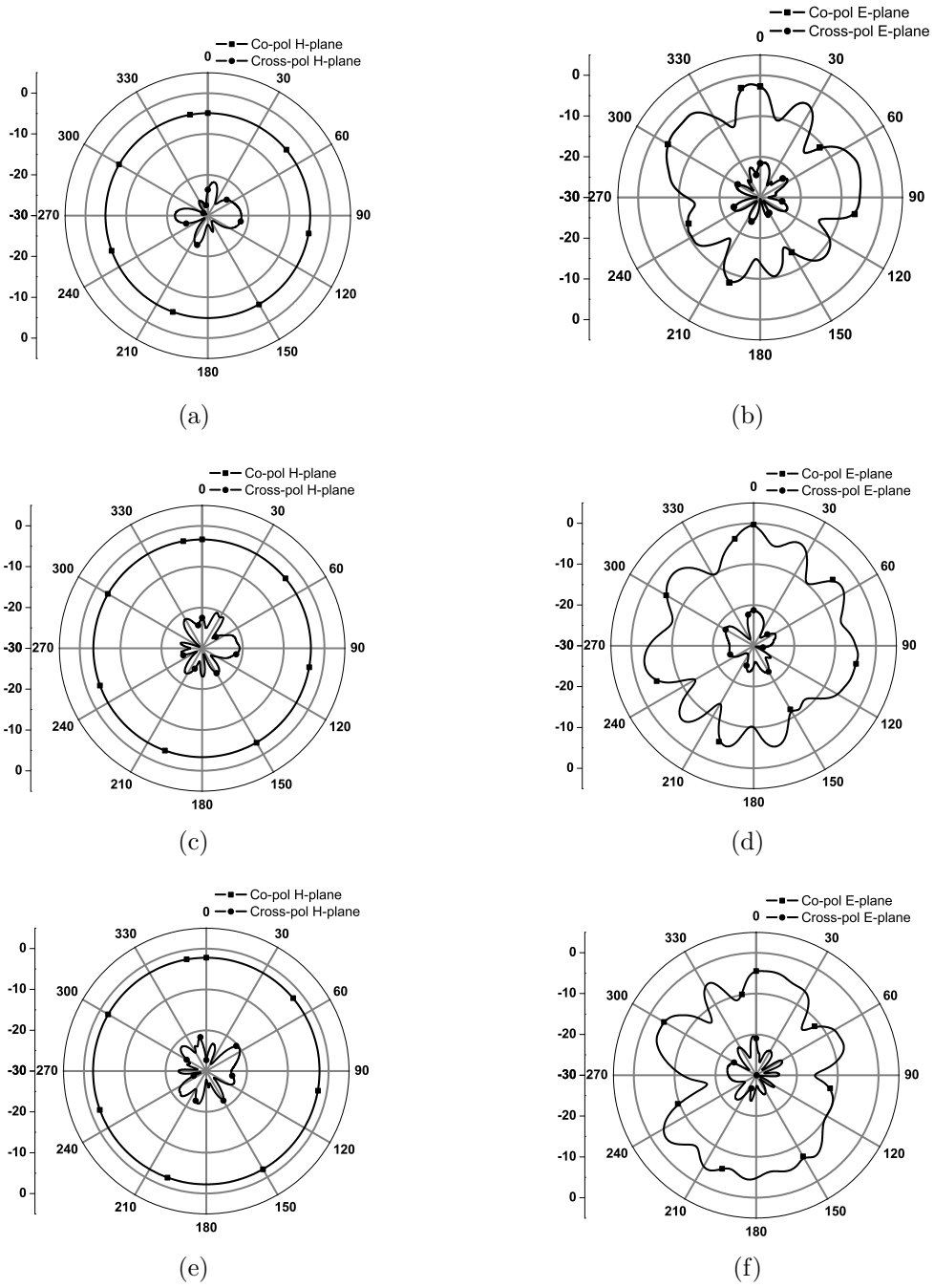

Figure 4.6: Simulated Radiation Patterns of capacitive coupled LPDRA. (a) H-plane at 7 GHz, (b) E-plane at 7 GHz, (c) H-plane at 8 GHz, (d) E-plane at 8 GHz, (e) H-plane at 10.5 GHz and (f) E-plane at 10.5 GHz.

The input impedance curve of the LPDRA array has been presented in Figure 4.5. The real part of the input impedance at the resonant frequencies of the LPDRA is found to be nearly 50Ω providing very good impedance matching to 50Ω microstrip feed line whereas the imaginary part of input impedance is almost zero at resonant frequencies.

The far field radiation patterns of the proposed LPDRA array are varying strongly with frequency. Figure 4.6 illustrates the simulated H-plane and E-plane (co-pol and cross-pol) radiation patterns at 7 GHz, 8 GHz and 10.5 GHz. The H-plane patterns are almost omni directional whereas the E-plane radiation patterns are altered with the change in frequency. The cross-pol level is below -20 dB.

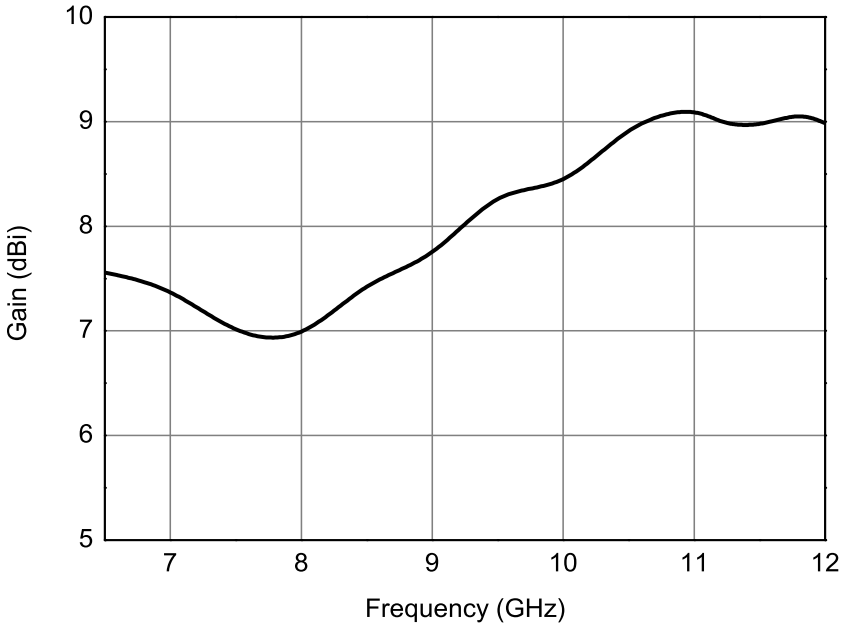

Figure 4.7: Simulated Gain curve of capacitive coupled LPDRA.

The gain of the proposed LPDRA is investigated. Figure 4.7 shows the simulated gain of LPDRA array against frequency. The proposed array offers an average gain better than 7 dBi over the entire frequency band. The simulated antenna efficiency of the array is found as 94.8%.

k-β Analysis

The k-β diagram for the LPDRA array is plotted in the Figure 4.8. The capacitive coupled LPDRA array gives a good log-periodic action. This log periodic DRA array is resonating beyond k $\approx$ 0.13.

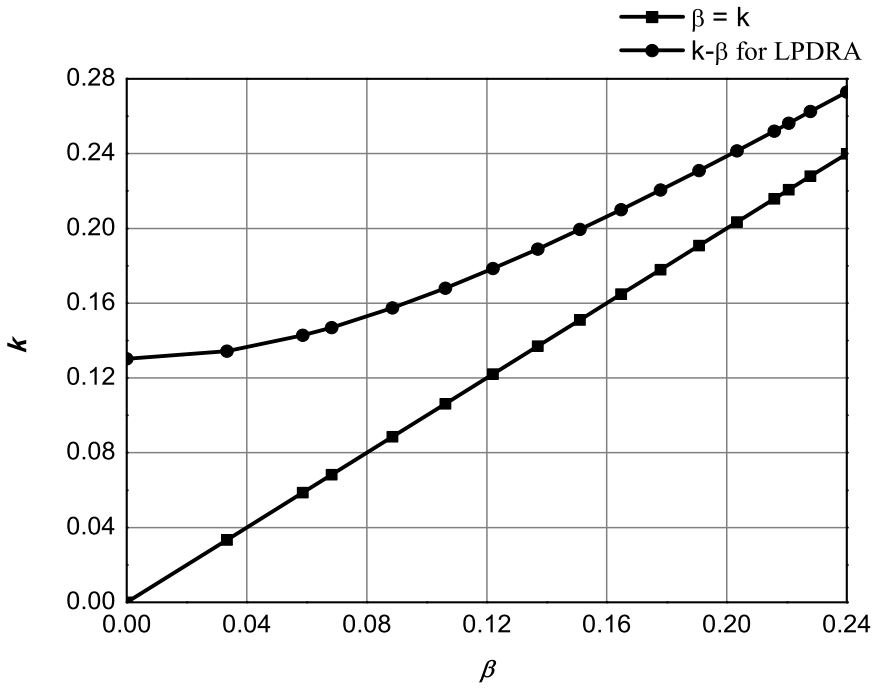

Figure 4.8: k-β diagram of capacitive coupled LPDRA.

4.2.3 Experimental Verifications

The photographs of the prototype LPDRA array are shown in Figure 4.9. The VSWR curves are plotted in Figure 4.10. The simulated VSWR result is compared favourably with the physically measured values. It shows a good agreement between simulated and measured results. The -10 dB measured impedance bandwidth is 6.2-12.2 GHz. The proposed array covers the X-band for communication applications. The VSWR measurement of LPDRA is taken by using an 8720B Agilent Network Analyser. The gain and radiation pattern measurements are taken in an anechoic chamber. The fabricated LPDRA array in anechoic chamber is shown in Figure 4.11.

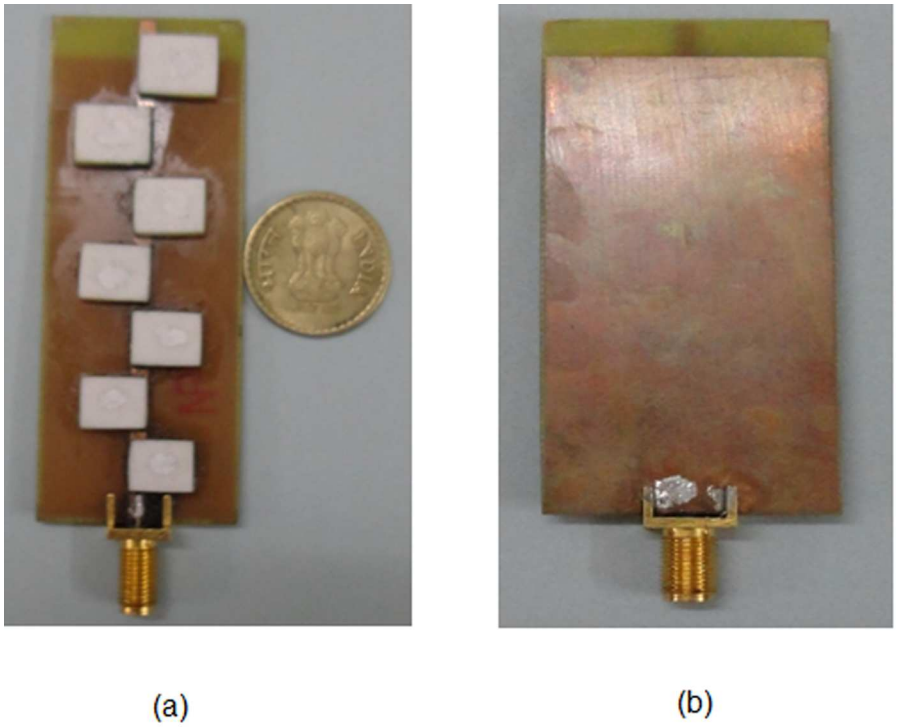

Figure 4.9: The Photographs of Fabricated capacitive coupled LPDRA. (a)Front view, and (b) Rear view.

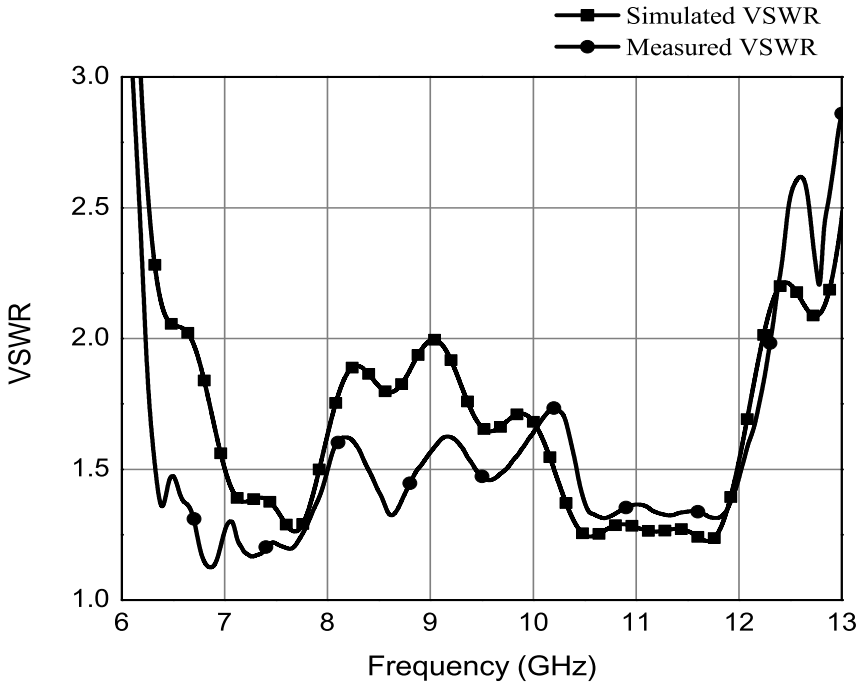

Figure 4.10: Simulated and measured VSWR curves of capacitive coupled LPDRA.

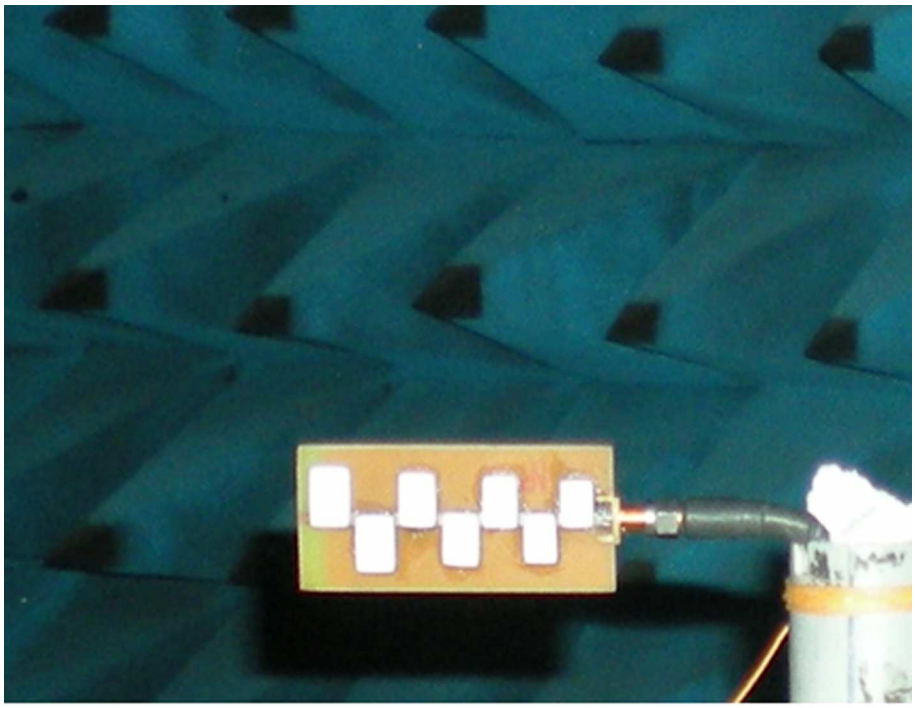

Figure 4.11: Capacitive coupled LPDRA in anechoic chamber.

The measured E-plane and H-plane (co-pol and cross-pol) radiation patterns at 7 GHz, 8 GHz and 10.5 GHz are shown in Figure 4.12. The radiation patterns for the array are normalized by setting the maxima at 0 dB. The measured H-plane patterns are almost omni directional at low frequencies but at 10.5 GHz it has some inconsistencies. The measured E-plane radiation patterns are nearly broadside direction. The measured cross-polar rejection is found below -20 dB.

Figure 4.13 displays the measured gain of the array for the entire band. The measured peak gain is 9.2 dBi. There are some discrepancies in measured results in compared to simulated results. This may be due to the manual placements of dielectric resonators over the substrate or the connector losses. Overall, the result exhibits a reasonable agreement.

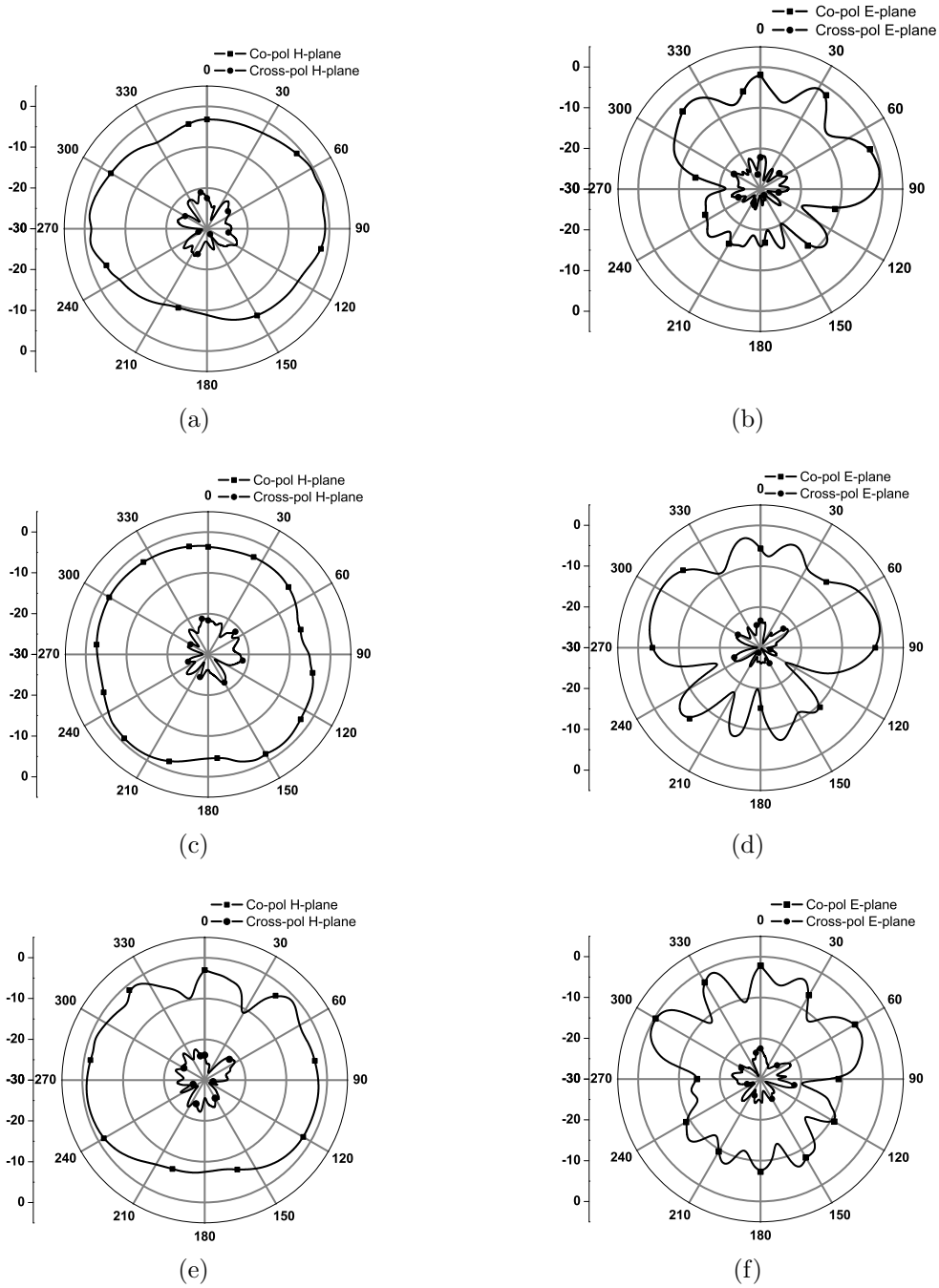

Figure 4.12: Measured Radiation Patterns of capacitive coupled LPDRA. (a) H-plane at 7 GHz, (b) E-plane at 7 GHz, (c) H-plane at 8 GHz, (d) E-plane at 8 GHz, (e) H-plane at 10.5 GHz and (f) E-plane at 10.5 GHz.

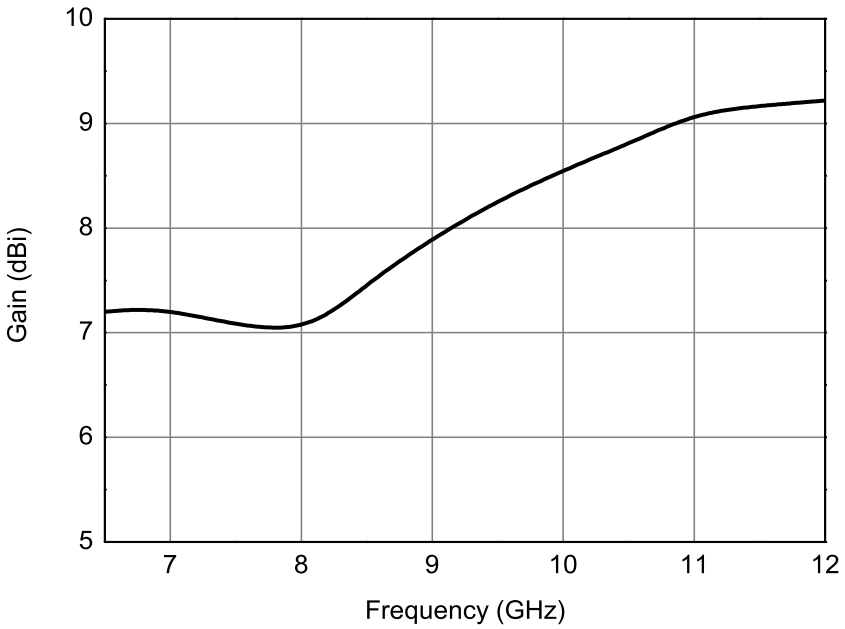

Figure 4.13: Measured Gain curve of capacitive coupled LPDRA.

4.3 Summary

In this chapter, a wideband log periodic LPDRA array has been investigated. This LPDRA array is excited by series fed microstrip line and the resonators are directly coupled to the feed line which reduces the further losses in the array. The parametric studies have been performed to observe the effect of a number of elements in the array. The simulated and measured VSWR result of the LPDRA array shows a good approximation. The impedance bandwidth of the proposed antenna is found to be 65.2% (6.2 to 12.2 GHz) for 2:1 VSWR. Experimental as well as the simulated results confirm the wideband property of the proposed array with nearly stable omnidirectional radiation patterns over the entire frequency band of interest. The obtained measured E-plane radiation characteristics at different frequencies are in broadside direction. The LPDRA has a peak gain about 9.2 dBi. The simulated antenna efficiency of the array is 94.8%. For further understanding the propagation characteristics of the proposed antenna, a k-β diagram is presented. These features make this LPDRA array attractive for X-band satellite communication systems and RADAR applications.

CHAPTER 5

Electromagnetically Coupled Log Periodic Dielectric Resonator Antenna for Wideband Applications

5.1 Introduction

The strong reliability, high data-rate and robustness are favourable features of wireless and satellite communication systems. However for these applications, there is a severe necessity of small sized antenna arrays with light-weight, low loss and low power handling capacity, while simultaneously requiring the multi resonant wideband radiation functions using the same antenna. Many progresses on wideband compact antennas have already been achieved. A dual-polarized wideband Short Backfire Antenna (SBA) excited by a hybrid configuration of waveguide and ortho-mode transducer is designed for mobile satellite communications and Wireless Local Area Network (WLAN) applications [96]. A compact wideband balanced mobile handset antenna is presented which covers Digital Communication System (DCS), Personal Communication System (PCS), Universal Mobile Telecommunication System (UMTS) and WLAN applications [97]. Moreover, the necessity for wideband antenna is continuing importance in the field of wireless communication, radar and satellite communication systems. Due to the advantages such as compactness, high efficiency and high integration ability, LPDRA arrays can be used for wideband applications.

In this chapter, a wideband LPDRA array design with yet another type of feed is considered. The proposed electromagnetically coupled LPDRA array design consists of seven dielectric resonators of rectangular shape with multilayer substrate. The

elements of the array can be directly coupled to the microstrip line without using another layer of substrate but in that case, the LPDRA array design (with a single layer of substrate) has to face improper matching due to the higher inductive effect. One additional layer of substrate compensates the inductive effect. This will exhibit better flexibility of coupling as well as proper matching of the DRA elements with feeding [91]. The LPDRA array design, simulation studies of the array and the experimental verifications of the results are elaborated in the following sections.

5.2 Log Periodic Dielectric Resonator Antenna Array with Overlaid Microstrip Feed Line

The main objective of this LPDRA array design is to achieve wide bandwidth by using electromagnetically coupled overlaid DRAs. This feeding method is provides greater flexibility of the coupling and significantly simplifies the array design. The LPDRA array with overlaid resonators has multilayer configuration, where the DRAs and microstrip feed line are in different layers. This feeding circuit provides sufficient isolation between the DRs and the feed circuit, which reduces the surface wave losses.

5.2.1 Antenna Geometry

This LPDRA array design consists of dual layers of substrate with the same width, same height but different length. The DRAs of different widths and lengths are mounted on the top of the upper substrate and a partial ground plane is fabricated on the rear side of the lower substrate. A microstrip feed line is printed on the lower substrate as shown in Figure 5.1 (a). The coupling between the DRAs and the microstrip feed line is controlled by the width 'd' as shown in Figure 5.1 (b).

All the resonators are electro-magnetically coupled, which makes the LPDRA array design simpler [9]. In this design, the DRs are the radiating portion of the array which have low loss and moderate gain with good efficiency for high frequency applications. In a log periodic DRA array, the resonator's length, width, height and spacing between resonating elements along the array vary by a scaling factor (τ).

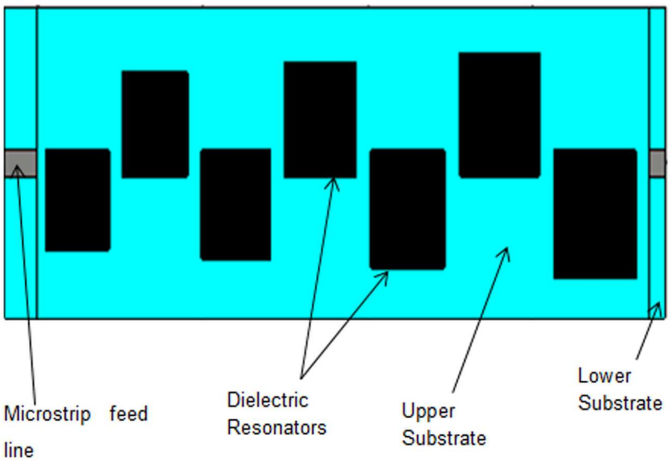

(a)

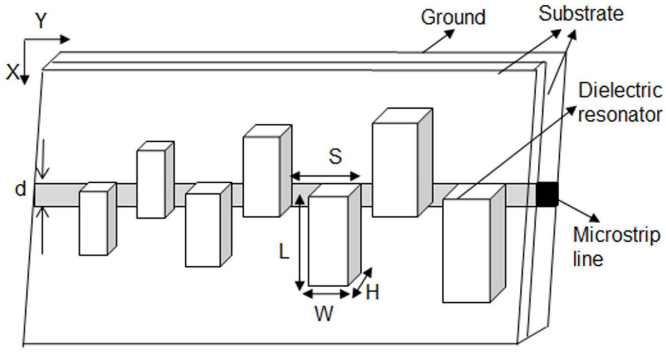

(b)

Figure 5.1: Electromagnetically Coupled LPDRA. (a) Top view and (b) Schematic view.

An analytical study has been carried out on seven element LPDRA array design. The design of the proposed antenna initializes with the τ and σ (relative spacing) values depending upon our desired gain, which has been chosen from Carrel's table [91]. For the proposed antenna, the value of τ is chosen as 0.96 and the related σ value can be obtained by using Equations (3.2) and (3.3) [91].

The length, width, height and spacing of the array elements are graduated logarithmically from one end to the other in such a way that certain dimensions of adjacent elements allow a constant ratio to each other. As the design ratio τ for this LPDRA is 0.96 which is less than 1, so the length (L), width (W), height (H) and spacing (S) between the DRA elements are given by Equation (4.5) [83, 91]. The designed band-

width can be expressed in terms of B_0 (desired bandwidth) and B_r (active region bandwidth) using Equations (3.5) to (3.7).

According to Equation (4.5), the dimensions (L, W, H and S) of each dielectric resonator vary log periodically from one end to another. The dimensions of the largest element are always associated with the lowest frequency whereas the smallest element dimensions are related to the highest frequency. If L_{m+1} is the length of largest element (m+1) and λ_{max} is the maximum wavelength with the lowest frequency (f_{min}), then L_{m+1} can be realized by

$$L_{m+1} = \frac{\lambda_{\max}}{4} \tag{5.1}$$

where

$$\lambda_{\max} = \frac{c}{f_{\min}\sqrt{\varepsilon_r}}$$

c = speed of light in free space.

ϵ_r = Relative permittivity of dielectric resonator.

After resolving the value of length, the other dimensions associated with the largest element such as width (W_{m+1}), height (H_{m+1}) and spacing between elements m+1 and m ($S_{m+1\leftrightarrow m}$) can be achieved as shown below,

$$W_{m+1} = 0.8 \times L_{m+1} \tag{5.2}$$

$$S_{m+1\leftrightarrow m} = \tau \times L_{m+1} \tag{5.3}$$

The elements of the log periodic DRA array are made up of Teflon dielectric material with relative permittivity $\epsilon_r = 2.1$. In this proposed array design, the DRs are supported by double layers of inexpensive FR4 substrate with relative permittivity (ϵ_s) 4.4 where, the thickness of each substrate layer is 1.6 mm. The upper substrate of the array is of 74 mm length (L_{us}) and 30 mm width (W_{us}) while the lower substrate has the same height and width with 80 mm length. The rear side of the lower substrate is having a partially printed ground plane dimensioned as 74 mm × 30 mm. The array

is excited by an overlaid microstrip line feeding with a center aligned feed line of length (L_f) 80 mm and width (W_f) 2.5 mm. The largest dielectric resonator is of length (L) 12.3 mm, width (W) 9.84 mm and height (H) 3 mm with 11.8 mm of center to center spacing (S) between the two elements. The dimensions of the other dielectric resonators are scaled by τ as shown in Figure 5.1 (a) and (b). Since the resonant frequency and the radiation resistance depend primarily on the dielectric resonator's dimension and slightly influenced by the substrate thickness, the height of both the substrate layer and feed line are kept constant. The overall dimension of the array is 80 mm $\times$ 30 mm.

5.2.2 Simulation Results

In this chapter, a seven element LPDRA array with 0.96 scaling factor has been designed and analyzed using CST microwave studio suite 2012. Different characteristics such as S-parameter, input impedance, far field radiation patterns, gain and propagation characteristics of the proposed array are presented.

A parametric study on LPDRA array with different number of dielectric resonators (five, six and seven) has been given in Figure 5.2. Among the VSWR curves for different number of elements, the curve with seven elements is covering wide bandwidth compared to the VSWR curves for five and six dielectric elements.

In figure 5.2, the LPDRA array with seven resonators achieves 54% of impedance bandwidth, the array with six elements are providing 52% impedance bandwidth whereas 50% of impedance bandwidth is resulted by LPDRA with five elements. The proposed log periodic array with seven resonators provides a wide bandwidth from 6.5 GHz to 11.3 GHz. The simulated VSWR plot for LPDRA array with seven dielectric resonators is shown in Figure 5.3. The LPDRA array is providing a multi resonant wideband.

The results of the log periodic DRA array also presenting a very good input impedance values over the entire frequency range. The input impedance curves of the proposed array are presented in Figure 5.4.

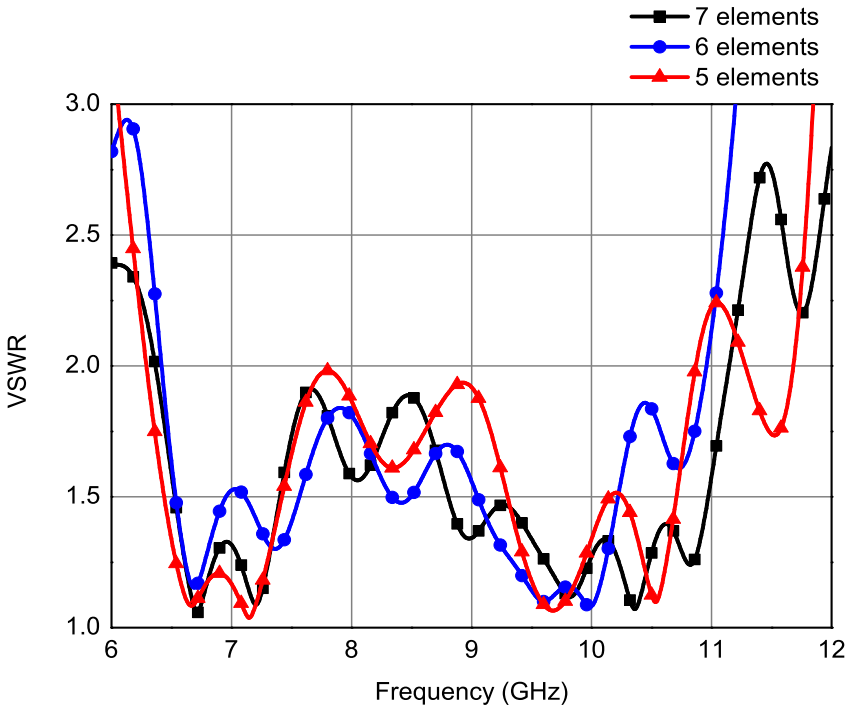

Figure 5.2: VSWR curves of electromagnetically coupled LPDRA with different number of dielectric resonators.

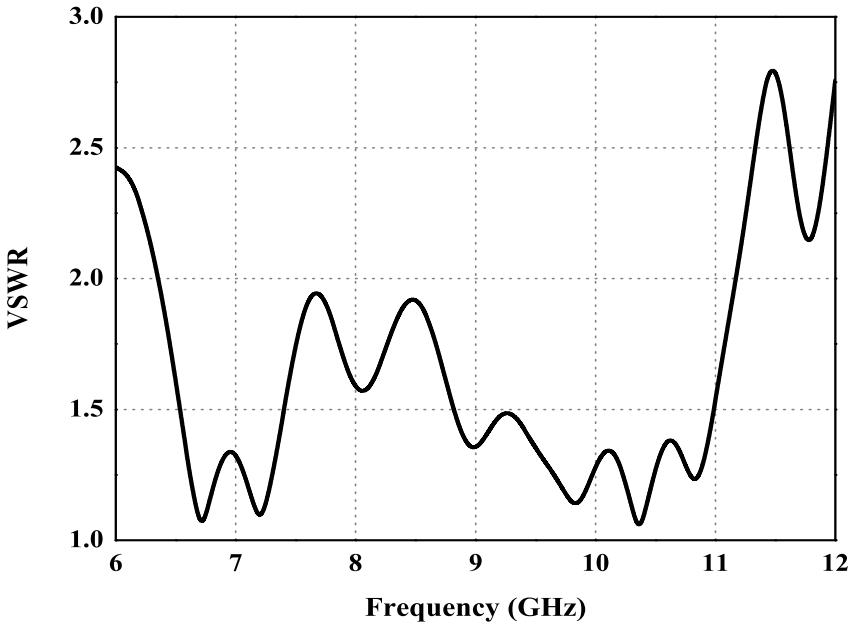

Figure 5.3: Simulated VSWR curve of electromagnetically coupled LPDRA.

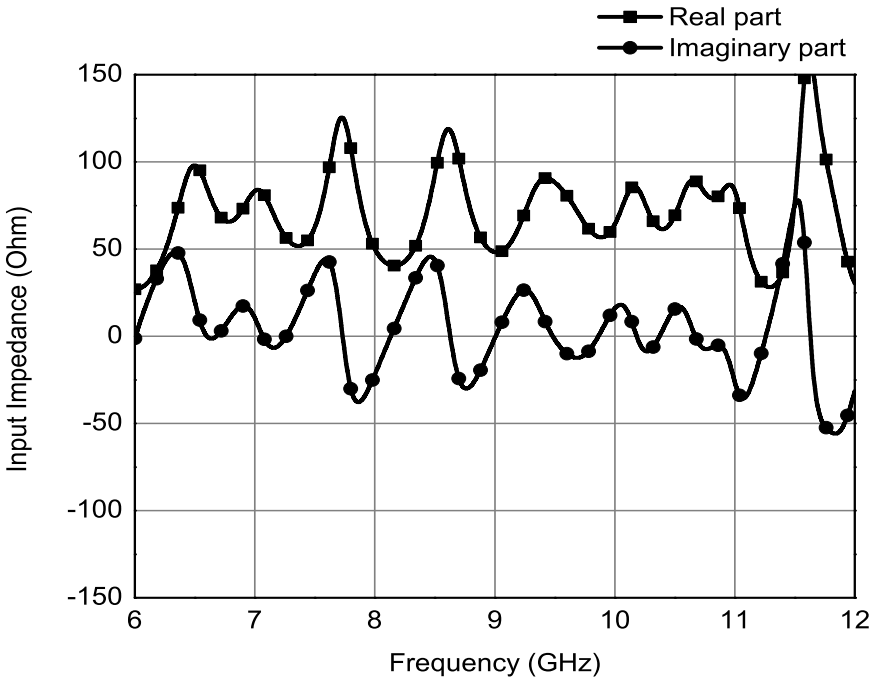

Figure 5.4: Input Impedance curves of electromagnetically coupled LPDRA.

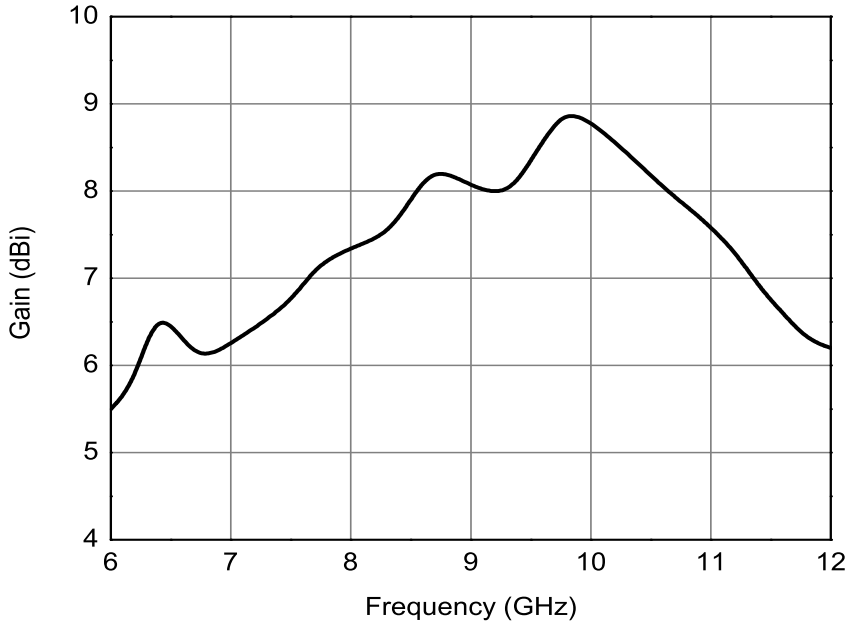

Figure 5.5: Simulated Gain curve of electromagnetically coupled LPDRA.

The simulated gain plot of the LPDRA array is given in the Figure 5.5. Initially, the simulated gain is increasing from the low frequency range towards high frequency. At 9.9 GHz, the peak gain of the array is 8.8 dBi and then the gain value starts to reduce. The overall gain of the array is better than 6 dBi within the operating band.

Figure 5.6 shows the simulated radiation patterns of LPDRA array. The E-plane as well as H-plane patterns at different frequencies (7.5 GHz and 10.5 GHz) have been studied. The H-plane co-pol radiation patterns are almost omnidirectional, whereas the E-plane co-pol radiation patterns are in the broadside direction for high frequencies. The simulated cross polar rejection for electromagnetically coupled LPDRA array is below -30 dB. From the far field simulation, the simulated antenna efficiency is found to be better than 83% within the overall band.

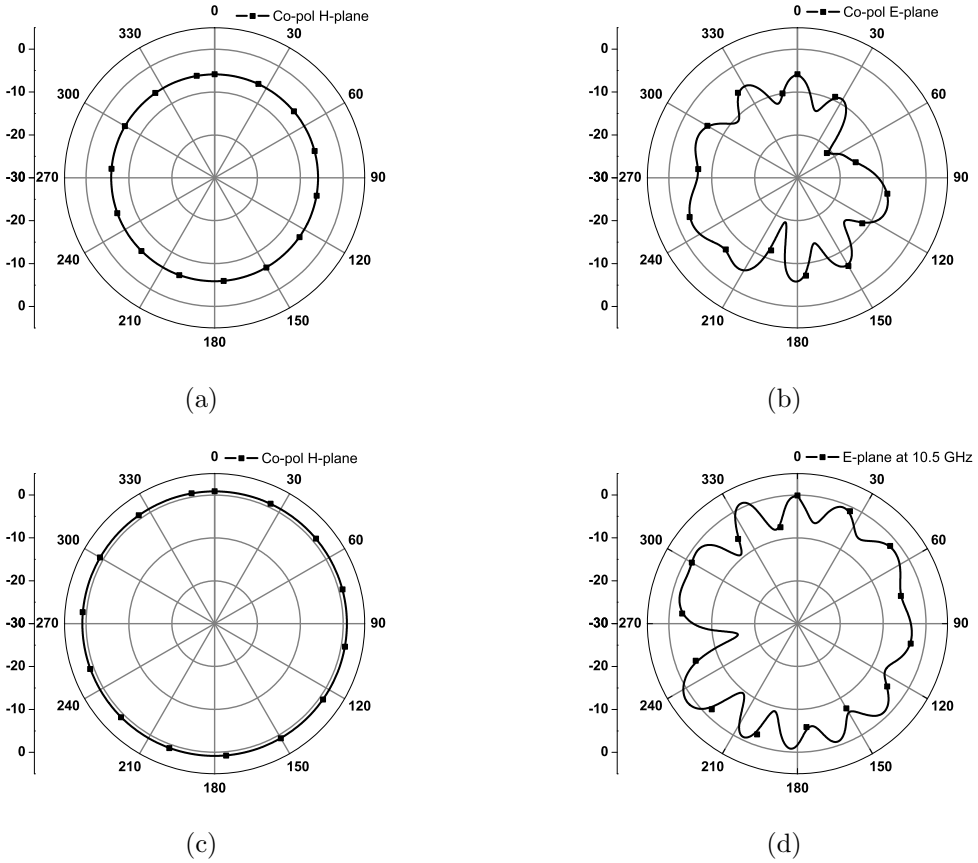

(a) (b)

(c) (d)

Figure 5.6: Simulated co-polar and cross-polar radiation patterns of electromagnetically coupled LPDRA. (a)H-plane at 7.5 GHz, (b) E-plane at 7.5 GHz, (c)H-plane at 10.5 GHz and (d) E-plane at 10.5 GHz.

k-β Analysis

The propagation characteristic of LPDRA array is illustrated in Figure 5.7. The LPDRA array achieves a good log-periodic action. At $k \approx 0.14$, the array starts to resonate and beyond this value of k, the array is radiating log periodically.

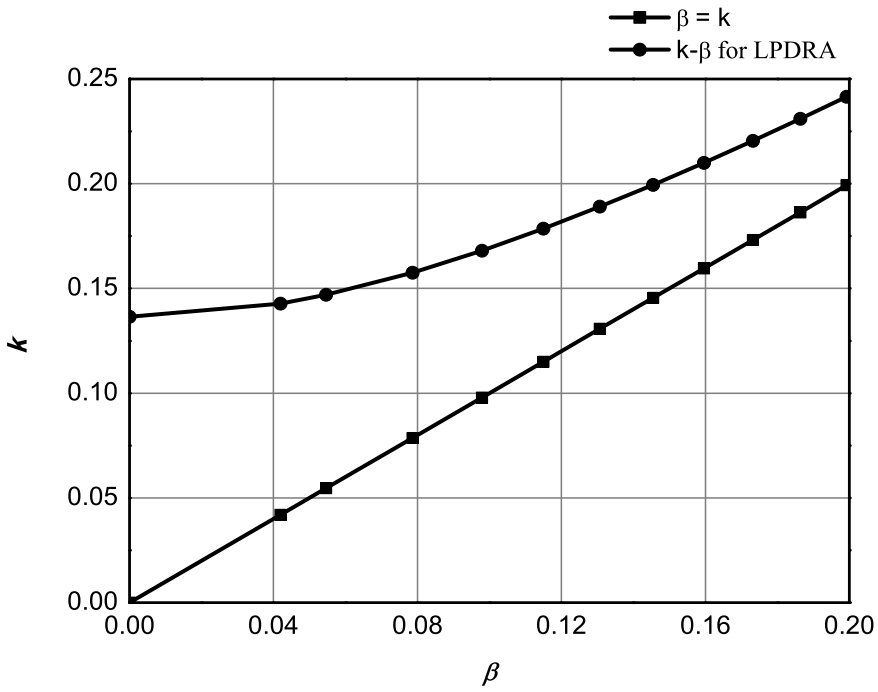

Figure 5.7: k-β diagram of electromagnetically coupled LPDRA.

5.2.3 Experimental Verification

The photographs of the fabricated LPDRA array are shown in Figure 5.8. The VSWR measurement of the fabricated LPDRA array has been carried out by using an 8720B Agilent Network Analyzer. The gain and radiation pattern are measured in an anechoic chamber at Advanced Microwave Laboratory, IIT Roorkee.

The simulated as well as measured VSWR curves of the seven element frequency independent LPDRA array with scaling factor 0.96 are plotted against frequency in Figure 5.9. The simulated VSWR curve well approaches the measured curve. The measured impedance bandwidth of the LPDRA array is 54% (6.5-11.3 GHz).

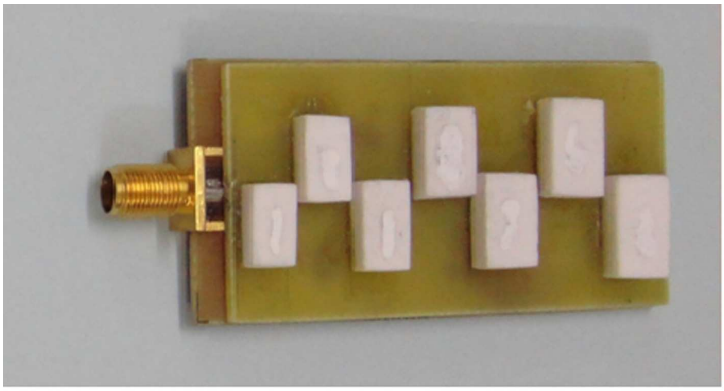

(a)

(b)

Figure 5.8: Electromagnetically Coupled fabricated LPDRA. (a) Front view and (b) Rear view.

The radiation patterns and gain measurement of the LPDRA array in an anechoic chamber is shown in Figure 5.10.

The measured co-polar along with the cross-polar radiation patterns of the proposed log periodic DRA array are given in Figure 5.11. The E-plane as well as H-plane patterns at different frequencies (7.5 GHz and 10.5 GHz) have been studied.

The H-plane radiation patterns are almost omnidirectional, whereas the E-plane radiation patterns are in the broadside direction for high frequencies. The simulated cross polar rejection is below -30 dB whereas the measured cross polar rejection is below -20 dB. The variation in the simulated and experimental results may be due to some losses during the fabrication or the manual alignment of the dielectric resonators over the substrate.

The fabricated prototype exhibits a minimum measured gain of 6 dBi (or better)

over wideband frequency from 6.5 GHz to 11.3 GHz. The measured gain of the antenna is shown in Figure 5.12. The measured peak gain of the array is 8.5 dBi at 9.8 GHz.

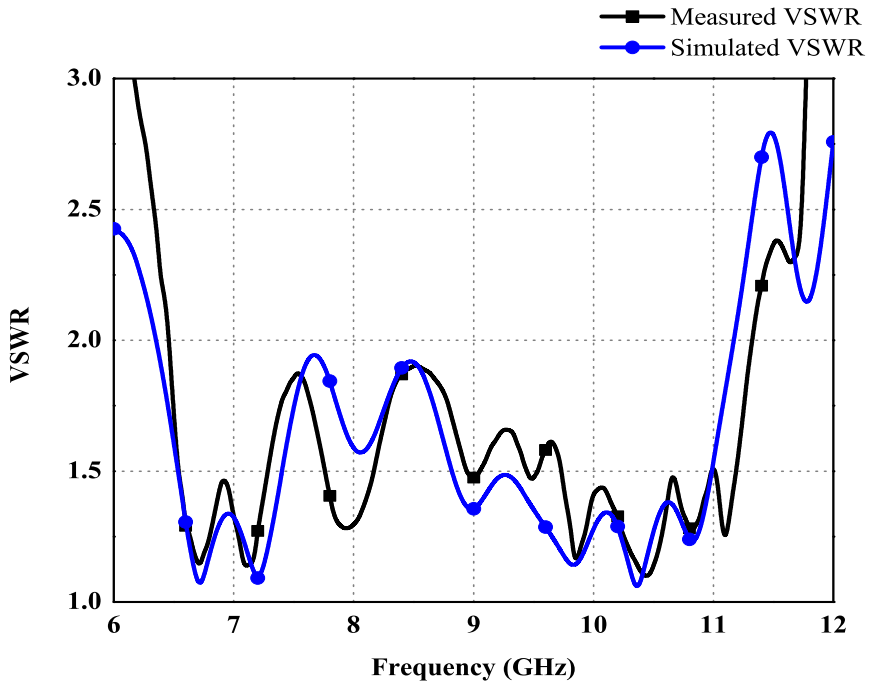

Figure 5.9: VSWR curves of electromagnetically coupled LPDRA.

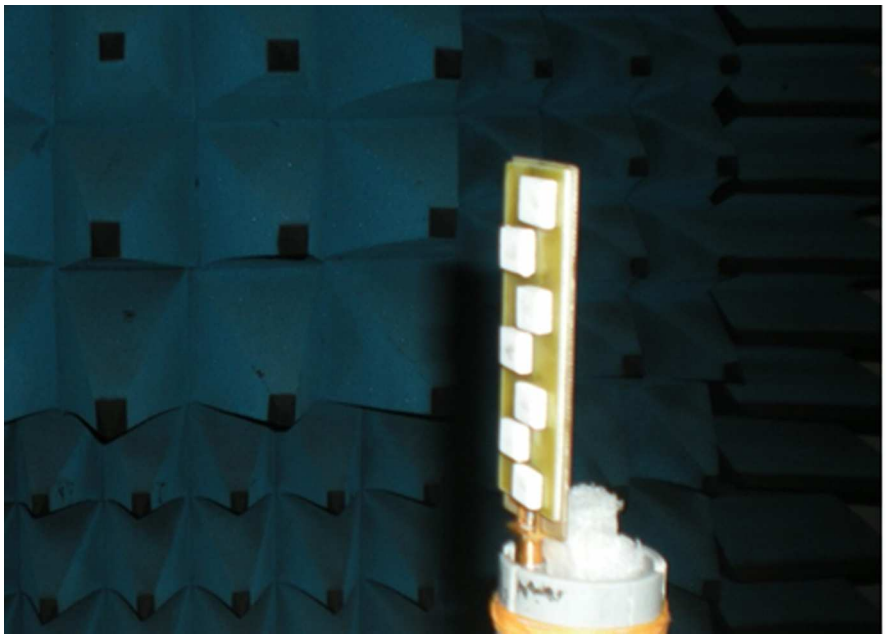

Figure 5.10: Gain and radiation pattern measurement of electromagnetically coupled LPDRA in anechoic chamber.

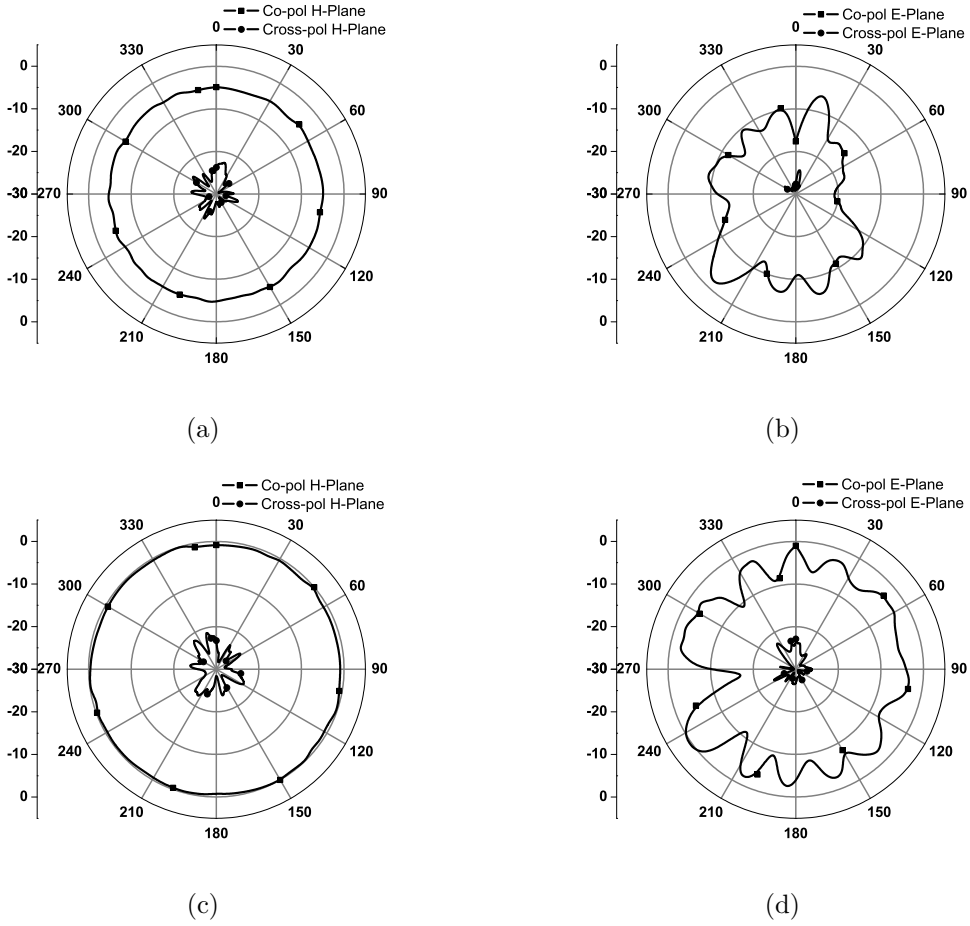

(a) (b)

(c) (d)

Figure 5.11: Measured co-polar and cross-polar radiation patterns of electromagnetically coupled LPDRA. (a)H-plane at 7.5 GHz, (b) E-plane at 7.5 GHz, (c)H-plane at 10.5 GHz and (d) E-plane at 10.5 GHz.

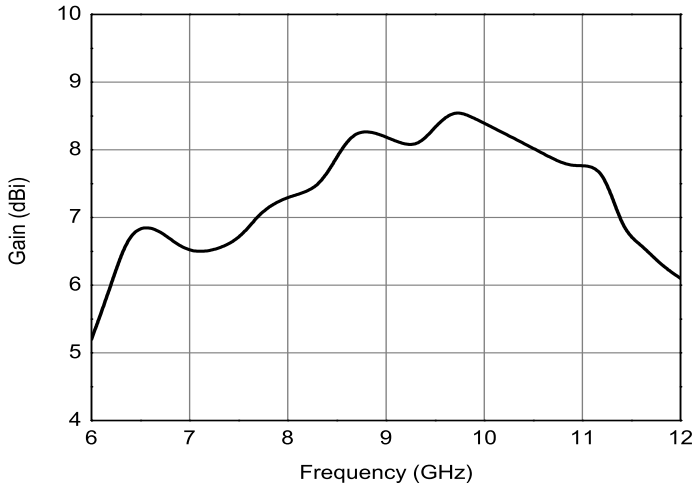

Figure 5.12: Measured gain of electromagnetically coupled LPDRA.

5.3 Summary

In this chapter, a wideband LPDRA array has been studied. The proposed antenna is based on recent developments of high efficiency DRA arrays and wideband log periodic techniques. Seven rectangular shaped resonators of different dimensions are integrated in a log periodic fashion. The dimensions of the adjacent resonators maintain a constant design ratio (τ) with each other. The value of τ for the proposed array is 0.96. An overlaid microstrip feed line is used to excite the log periodic array. The dielectric resonators are electro magnetically coupled to feed line by using an additional layer of substrate in between the microstrip line and resonators. This additional layer of substrate helps in reducing the inductive effect which results in proper matching of elements with feed line. The prototype of the designed antenna has been fabricated as well as measured. The VSWR, input impedance, gain and radiation patterns for the array have been reported. The log periodic array offers 54% bandwidth (6.5-11.3 GHz). It provides a peak gain of 8.5 dBi at 9.8 GHz. The antenna efficiency of the array is better than 83%. The radiation characteristics at different frequencies are in the broadside direction with an omnidirectional radiation in the H-plane of the antenna. There is a good agreement between the simulated and experimental results. This LPDRA array can be used in satellite communication system for X- band applications.

CHAPTER 6

Nine Element Log Periodic Dielectric Resonator Antenna

6.1 Introduction

The goal of this chapter is to explore the performance of Log Periodic Dielectric Resonator Antenna array with different types of dielectric material suitable for wideband high frequency applications. The design and analysis of nine element LPDRA arrays with overlaid microstrip line feeding are investigated. In this chapter, nine element rectangular shaped dielectric resonators are arranged in a log periodic fashion to attain electrical characteristics which will vary insignificantly with frequency over the entire desired bandwidth.

The important design considerations throughout this chapter is investigating the LPDRA array design by varying the dielectric material with different relative permittivity values as well as studying the characteristics of the array for different values of scaling factor 'τ' to obtain wide impedance bandwidth.

Nine element LPDRA array designs using two different dielectric materials for high frequency wideband applications are presented here. The first design describes an analysis on LPDRA with dielectric resonators made up of ceramic materials having a high relative permittivity value ($\epsilon_{r1} = 12$). This LPDRA array has been designed for K (18-26.5 GHz) and Ka-band (26.5-40 GHz), jointly known as NATO-K band. The NATO-K band provides an increased spectrum compared to C-band and Ku-band, enabling greater volumes of traffic to be transmitted. Another LPDRA array with Teflon based dielectric material (relative permittivity, $\epsilon_{r2} = 2.1$) is designed and

investigated for X-band applications. The signals for systems working in the lower range of frequencies (X-band) suffer less from attenuation compared to the communication systems operating in higher bands. Therefore, these arrays are providing improved range and better coverage. The design methodology of the LPDRA arrays has been discussed and their results are presented in the following sections.

6.2 LPDRA Array with Dielectric Resonators of high relative permittivity

The proposed DRA array is a nine-element log periodic array for NATO-K band applications. The LPDRA array is excited by overlaid microstrip line feeding. The NATO-K band is a frequency band ranging from 18 to 40 GHz for Ultra High Frequency (UHF) applications. This band is well suited to support the communication applications require large amounts of high-throughput capacity which cannot be obtained using C and Ku band frequency allocations alone.

6.2.1 Antenna Geometry

The LPDRA array including its excitation feed line is shown in Figure 6.1. The length, width and spacing between the adjacent elements of a log periodic antenna increase logarithmically from one end to the other. The schematic view of the Log Periodic DRA array is shown in Figure 6.2. In the resonant approach, the microstrip line is terminated in an open circuit, which creates a standing wave on the line where the voltage maxima/minima of each wave are located at multiples of $\lambda_g/2$ from the open-circuit location. The guided wavelength, λ_g can be approximated by using Equation (3.1).

The proposed LPDRA array consists of nine elements of different length, width and spacing. The radiators are excited by an inductive coupled overlaid microstrip feed line to reduce the surface wave losses.

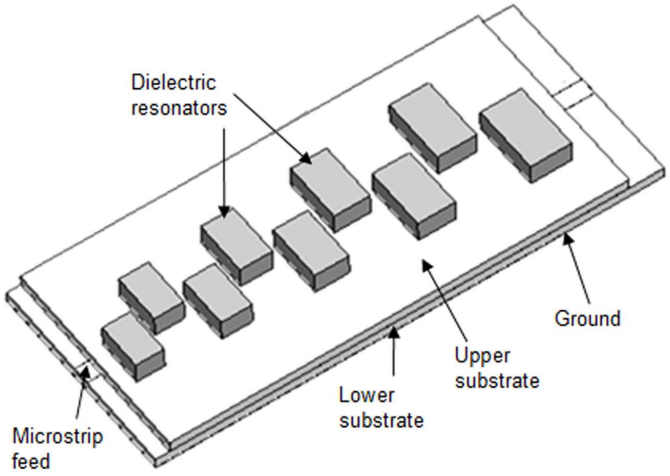

(a)

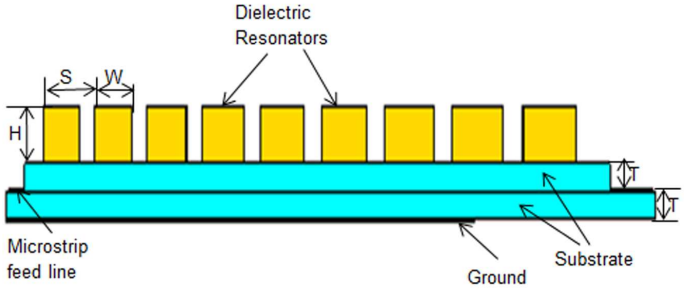

(b)

Figure 6.1: The Log Periodic Dielectric Resonator Antenna with dielectric resonators of high relative permittivity. (a) Top view and (b) Side view.

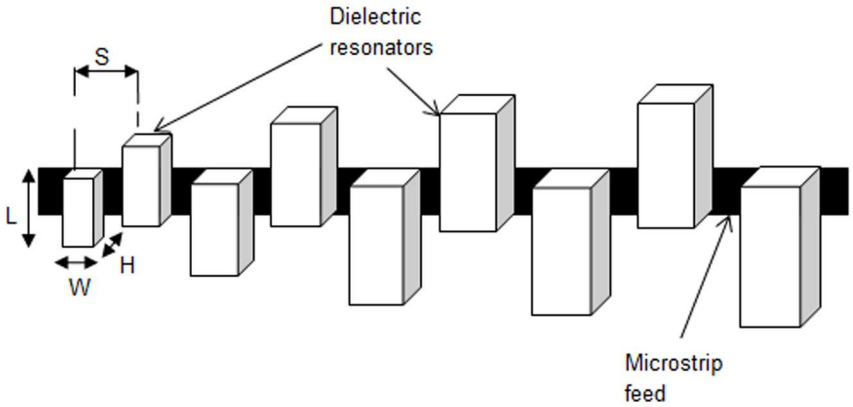

Figure 6.2: Schematic view of LPDRA with dielectric resonators of high relative permittivity.

The array is fed at the end of the structure having smallest resonators. The length (L), width (W) of the dielectric resonators and the spacing (S) between the two adjacent elements are graduated in such a way that certain dimension of adjacent element sustains a constant ratio with each other. The length (L), width (W) and spacing (S) between the DRA elements has been expressed by the Equation (3.9). The value of L, W and S for all the elements are scaled log periodically. For the design of the proposed LPDRA array, τ value is chosen as 1.05 and the value of σ is obtained by using Equations (3.2) and (3.3).

As illustrated in Figure 6.1, the LPDRA array has been designed with nine dielectric resonators of dielectric constant (ϵ_{r1}) 12 and height (H) of 3.2 mm with double layered FR4 substrate (relative permittivity (ϵ_s)=4.4. The elements are arranged in a log-periodic manner. All the resonators are placed on upper substrate. The dimensions of upper substrate are 65 mm length (L_{us}), 30 mm width (W_{us}) and 1.6 mm thickness (T) whereas the lower substrate is having the same width and thickness with 72 mm length. A partial ground plane dimensioned as 52 mm $\times$ 30 mm is printed on the back side of the lower substrate.

Table 6.1: Dimensions of the elements of LPDRA array with dielectric resonators of high relative permittivity.

Dielectric Resonators (Smallest to Largest)	**L (mm)**	**W (mm)**	**S (mm)**
DR_1	6.8	4.0	5.6
DR_2	7.14	4.2	5.88
DR_3	7.5	4.41	6.17
DR_4	7.87	4.63	6.48
DR_5	8.26	4.86	6.81
DR_6	8.68	5.12	7.15
DR_7	9.11	5.36	7.5
DR_8	9.57	5.63	7.88
DR_9	10.01	5.91	-

The smallest dielectric resonator of the array is dimensioned as length L = 6.8 mm, width W= 4 mm and spacing S = 5.6 mm. All the other dielectric resonator's dimensions are scaled by τ [91]. The dimensions (L, W and S) of LPDRA elements

are given in Table 6.1. The displacement of the radiators from the center of feed line is same for the whole array and equal to 1.25 mm. The overall length and width of the array are 72 mm and 30 mm respectively.

The microstrip feed line offers an advantage of easy and cost-effective fabrication of the DRA array. The proposed LPDRA array is excited by the overlaid microstrip line feeding of length 72 mm and width 2.5 mm. The feed line is etched on the lower substrate as shown in Figure 6.1. This antenna design can be used in radar and satellite communication systems for NATO-K band applications.

6.2.2 Simulation Results

A LPDRA array for 18-40 GHz bandwidth has been designed and analyzed using CST Microwave studio suite 2012. The results of the nine element array are discussed in terms of bandwidth response, input impedance, radiation patterns, gain and propagation characteristic. Parametric studies of the antenna with simulation based design data are presented here. It has been found that the LPDRA array offers continuous operation from 18 to 40 GHz bandwidth.

In case of LPDRA array, bandwidth variation can be realised by altering the scaling factor τ. A parametric study has been carried out by varying the scaling factor of LPDRA to achieve optimum antenna performance. Figure 6.3 shows the VSWR plots with different values of scaling factor τ such as 0.95, 1.0 and 1.05. In case of $\tau = 1.05$, a wide bandwidth with VSWR ≤ 2 is observed.

The VSWR characteristics of LPDRA for different number of array elements (3, 5, 7 and 9) are shown in Figure 6.4. From the figure, it has been observed that among all arrays, only the nine elements LPDRA array covers the desired impedance bandwidth from 18-40 GHz for NATO-K band applications.

VSWR curves of the antenna array are shown in Figure 6.3 and 6.4. From Figure 6.3, it has been perceived that the array is not showing good performance with 0.95 scaling factor compared to scaling factor 1 and 1.05. The bandwidth of the LPDRA array is also influenced by the number of elements used in the array design.

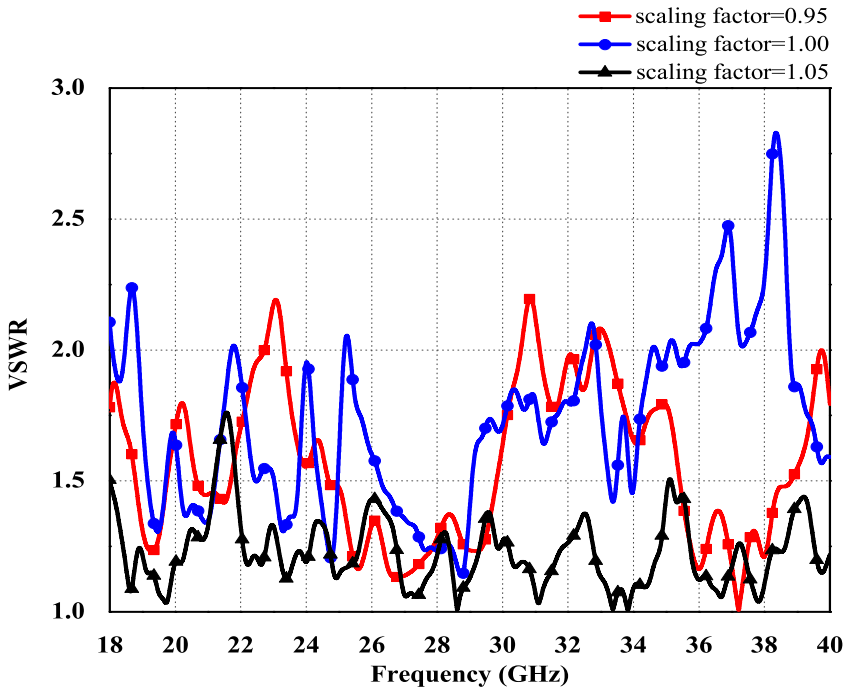

Figure 6.3: Simulated VSWR curves of LPDRA for different values of scaling factors.

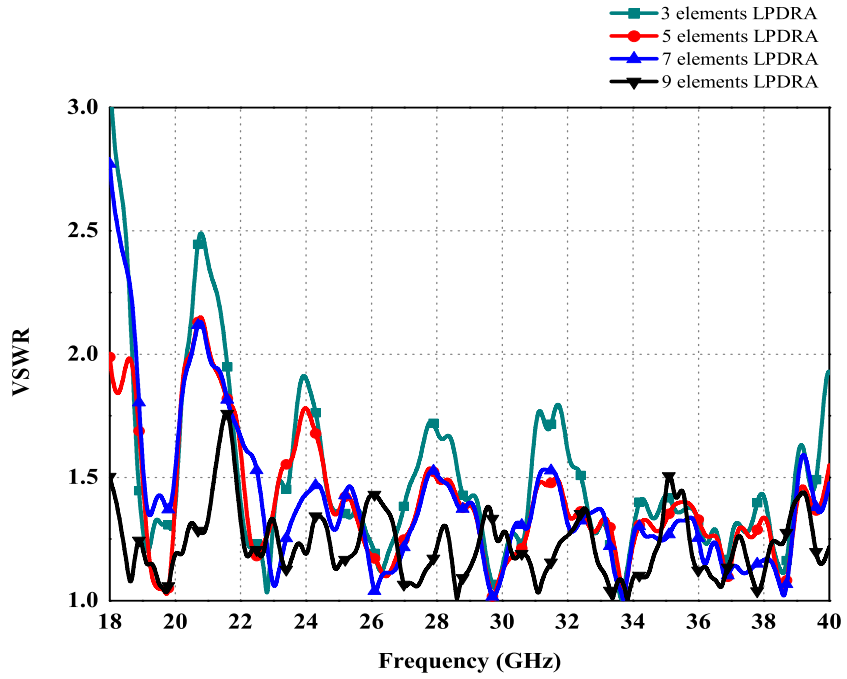

Figure 6.4: Simulated VSWR curves of LPDRA for variation in number of elements of the array.

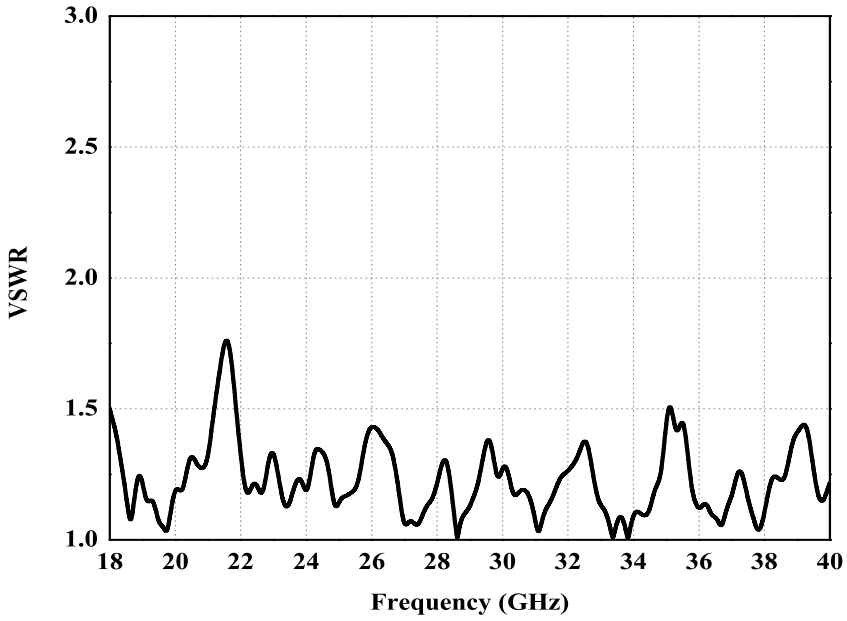

Figure 6.5: Simulated VSWR curve of LPDRA with nine dielectric resonators of high relative permittivity.

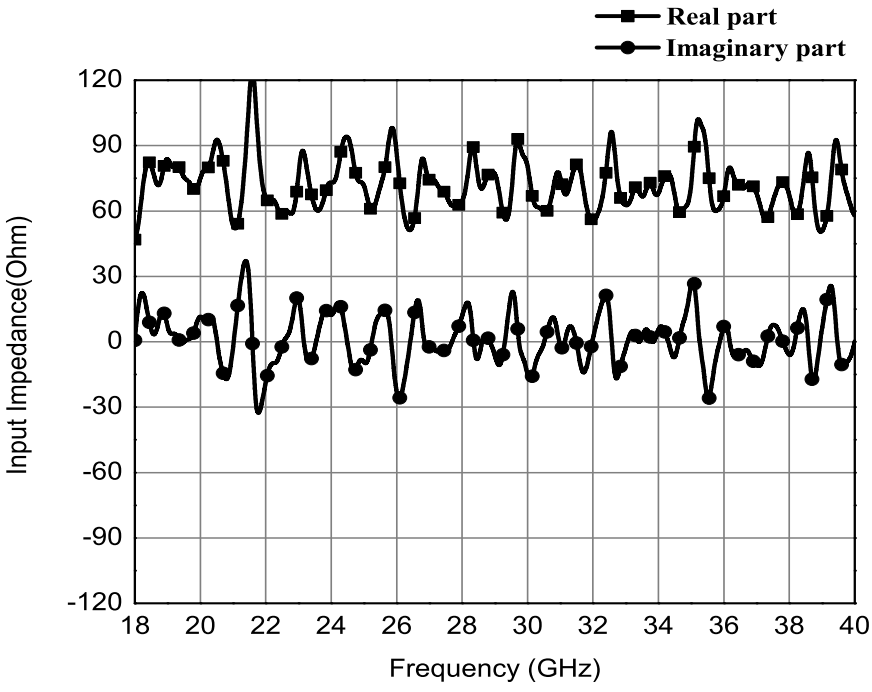

Figure 6.6: Input impedance curve of LPDRA with nine dielectric resonators of high relative permittivity.

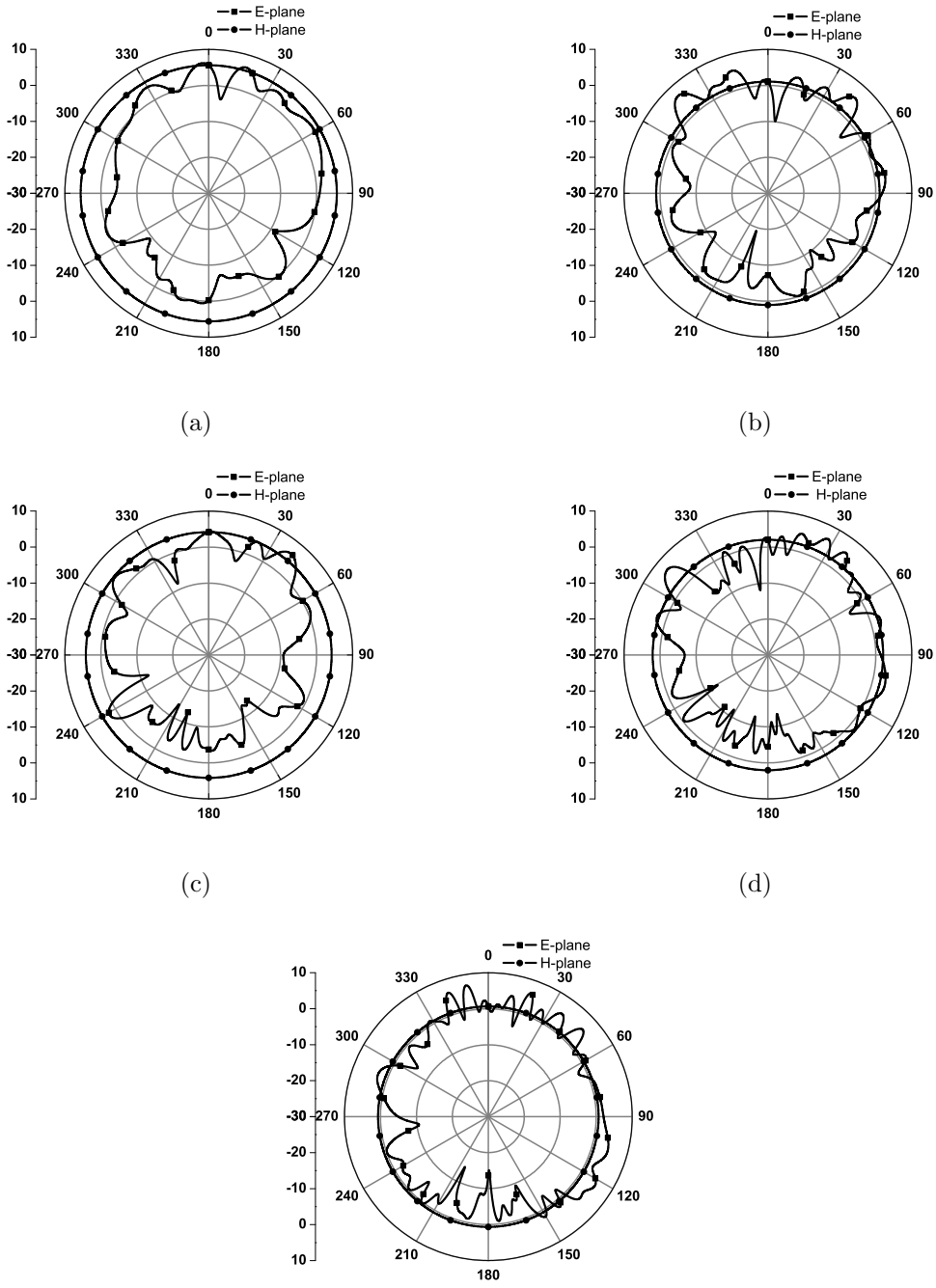

(a) (b)

(c) (d)

(e)

Figure 6.7: Simulated E-plane and H-plane radiation patterns of LPDRA with dielectric resonators of high relative permittivity. (a)18 GHz, (b) 24 GHz, (c)28.6 GHz, (d)37.8 GHz and (e) 40 GHz.

Finally, a VSWR curve of the nine-element LPDRA array with scaling factor 1.05 is shown in Figure 6.5. The resulted impedance bandwidth of the array is 76% (18-40 GHz). Any further change in the dimension can affect the resonance frequency of the

antenna.

The overall VSWR covers the frequency range of 18-40 GHz (VSWR ≤ 2) which is showing 76% of wider impedance bandwidth with low conductor loss. The simulated antenna efficiency of the LPDRA array is greater than 95% throughout the entire band.

The input impedance curves of the proposed antenna have been presented in Figure 6.6. The input impedance (resistance) at resonant frequencies of the LPDRA array is providing very good impedance matching to 50 Ω microstrip feed line.

The far field radiation patterns of the proposed DRA array are varying strongly with frequency. Figure 6.7 plots the radiation patterns at different frequencies (18 GHz, 24 GHz, 28.6 GHz, 37.8 GHz and 40 GHz). The E-plane radiation patterns are in the broadside direction against frequency whereas the H-plane radiation patterns are almost omnidirectional. The simulated cross-pol level is below -30 dB.

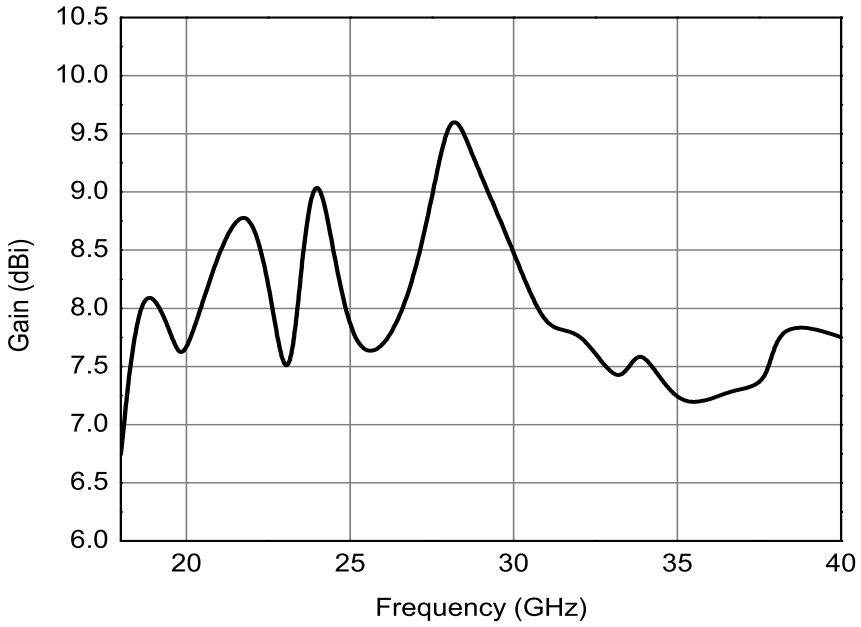

Figure 6.8: Simulated gain of LPDRA with nine dielectric resonators of high relative permittivity.

Figure 6.8 presents the gain versus frequency curve for the proposed LPDRA array. The gain characteristics of LPDRA array vary log periodically between 6.97 dBi to 9.9

dBi with a maximum at resonant frequencies and minimum in between the adjacent resonant frequencies. The LPDRA array results in peak gain of 9.9 dBi at centre frequency 28 GHz.

The value of peak directivity varies from 7.01-10 dB within the overall band. At any frequency, the number of array elements contributing to the radiation is dependent on the bandwidth of the individual radiators, and the scaling factor used in constructing the array. Therefore, adding more elements does not increase the peak gain. Instead, a reduction in peak gain is obtained, probably because the efficiency is degraded when more elements are added.

k-β Analysis

Figure 6.9, displays the k-β diagram for the nine element LPDRA array with high dielectric constant resonators. The inductive coupled LPDRA array with overlaid resonators is well propagating beyond $k \approx 0.38$. The array is showing good log-periodic behavior.

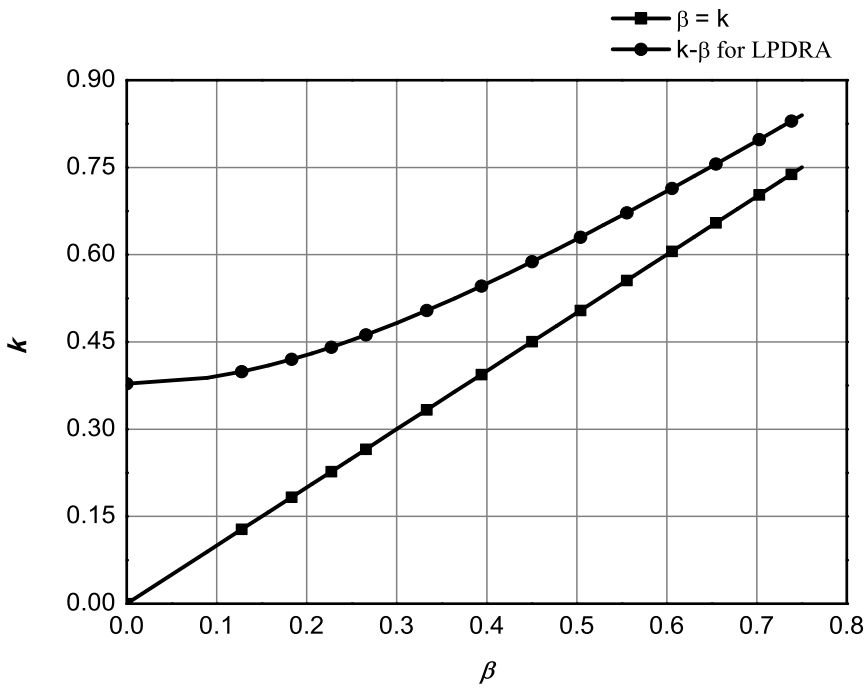

Figure 6.9: k-β diagram of LPDRA with dielectric resonators of high relative permittivity.

6.3 LPDRA Array with Dielectric Resonators of low relative permittivity

In this section, a nine-element log periodic DRA array has been designed and investigated for X-band applications. There is a considerable risk to machine a ceramic material into a number of small pieces. For ease of fabrication point of view, low cost Teflon based dielectric resonators with low relative permittivity ($\epsilon_{r2} = 2.1$) is used.

6.3.1 Antenna Geometry

The geometry of the proposed LPDRA array is shown in Figure 6.10. The proposed DRA Array consists of nine dielectric resonators having different dimensions. The structure of the array and its feeding techniques are same as that of the nine elements LPDRA array for NATO-K band applications as described in the previous section. The scaling factor 'τ' used for this LPDRA array design is 1.05. The length, width and spacing between the DRA elements are calculated by using Equation (3.9).

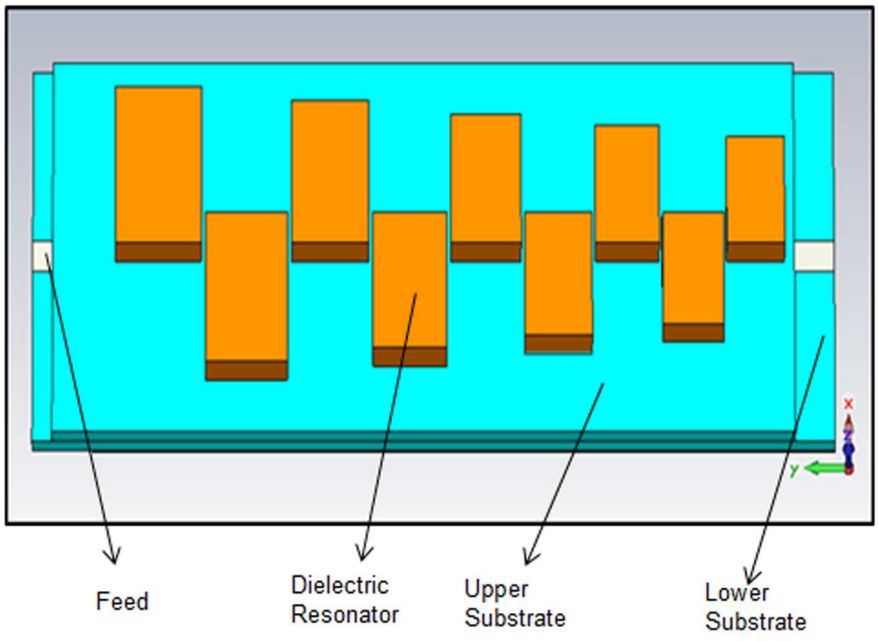

Figure 6.10: Basic Geometry of the proposed LPDRA with dielectric resonators of low relative permittivity.

The height (H) of dielectric resonators is 3 mm. This array is supported by a

double layered FR4 substrate with dielectric constant ((ϵ_s) of 4.4 with height (T) of each sheet is 1.6 mm. The proposed antenna is an electromagnetically coupled array which is excited by overlaid microstrip line feeding of length 80 mm and width 2.5 mm. The feed line is etched on lower substrate and all the resonators are located on the upper substrate as shown in Figure 6.10. The upper substrate is dimensioned as 74 mm length ((L_{us})) and 30 mm width ((W_{us})) whereas the lower substrate is having the same height, width and length of 80 mm. A partial ground plane of dimension as 74 mm $\times$ 30 mm is printed on the rear side of the lower substrate.

Table 6.2: Dimensions of the elements of LPDRA array with dielectric resonators of low relative permittivity.

Dielectric Resonators (Smallest to Largest)	**L (mm)**	**W (mm)**	**S (mm)**
DR_1	8.63	5.8	6.1
DR_2	9.06	6.09	6.4
DR_3	9.51	6.4	6.714
DR_4	9.99	6.71	7.05
DR_5	10.48	7.05	7.4
DR_6	11.01	7.4	7.77
DR_7	11.56	7.77	8.16
DR_8	12.14	8.16	8.57
DR_9	12.74	8.57	-

The smallest dielectric resonator element is having length L= 8.6 mm, width W= 5.8 mm and spacing S=6.1 mm, whereas the dimension of other dielectric resonators is scaled by τ. The dimensions of all the DR elements of LPDRA array are given in Table 6.2. The distance of the radiators from the center of feed line is 1.25 mm. The array is fed at the end with smallest resonators and the far end of the array is terminated with an open circuit, which is shown in Figure 6.10. The overall length and width of the array are 80 mm and 30 mm respectively.

6.3.2 Simulation Results

A frequency independent LPDRA for 6.3-11.2 GHz bandwidth has been designed and simulated. The simulation studies for the proposed LPDRA array have been carried

out by CST Microwave Studio suite 2012. The results of the nine element array are discussed in terms of VSWR, radiation patterns, gain and propagation characteristics.

At any frequency, the number of array elements contributing to the radiation is dependent on the bandwidth of the individual radiators and the scaling factor used in constructing the array. Therefore, a parametric study is carried out by altering the scaling factor of LPDRA to achieve optimum performance of the array. The simulated VSWR with different values of scaling factor (such as 1.05, 1 and 0.95) is shown in Figure 6.11.

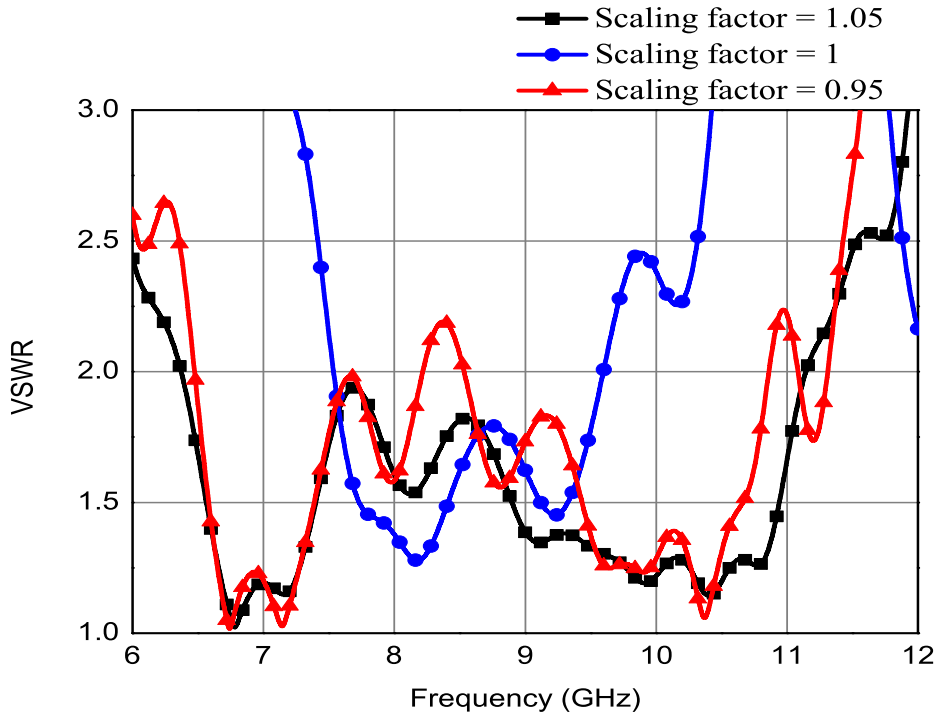

Figure 6.11: Simulated VSWR curves of LPDRA with dielectric resonators of low relative permittivity for different values of scaling factors.

For $\tau = 1.05$, a wide bandwidth (for VSWR ≤ 2) is observed which has been shown in Figure 6.12. The simulated antenna efficiency of the array is 86% . The input impedance curve of LPDRA array with dielectric resonators of low relative permittiity is given in Figure 6.13.

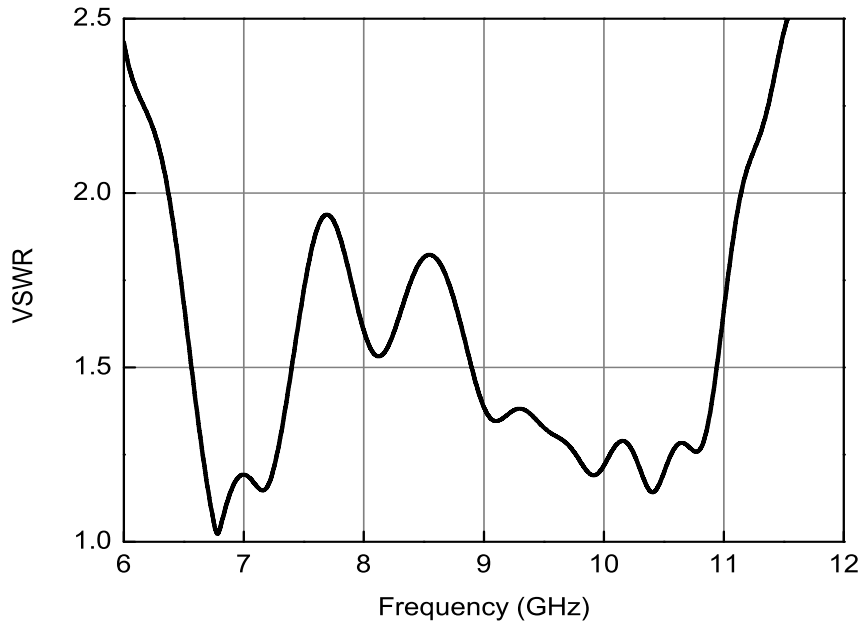

Figure 6.12: Simulated VSWR curve of LPDRA with dielectric resonators of low relative permittivity.

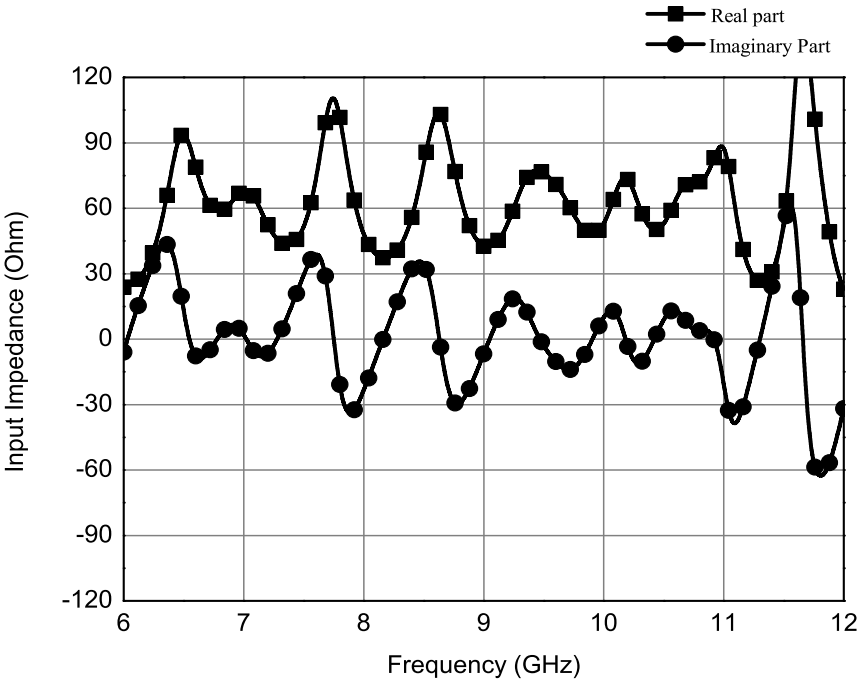

Figure 6.13: Input impedance curve of LPDRA with dielectric resonators of low relative permittivity.

k-β Analysis

Figure 6.14, shows the k-β diagram for the nine element LPDRA array with dielectric material of low relative permittivity. The propagation characteristic of inductive coupled LPDRA array is smoothly rising from $k \approx 0.135$ and beyond this point the array starts to propagate.

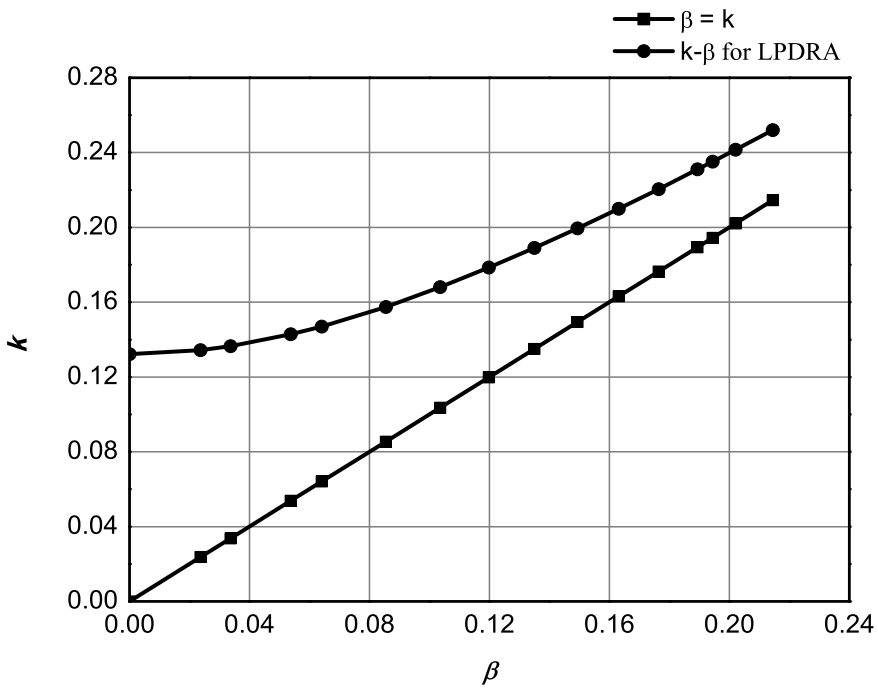

Figure 6.14: k-β diagram of LPDRA with dielectric resonators of low relative permittivity.

6.3.3 Experimental Verifications

The designed LPDRA array has been fabricated and measured for X-band applications. The VSWR measurement of the array is performed by using an 8720B Agilent Network Analyser whereas the gain and radiation pattern measurements have been carried out in an anechoic chamber. The fabricated LPDRA array has been shown in Figure 6.15.

Figure 6.16 shows the simulated and measured VSWR plot of the nine element frequency independent LPDRA with scaling factor (τ) 1.05 against frequency. The proposed LPDRA array offers 56% wider impedance bandwidth for VSWR ≤ 2. The

bandwidth covers a frequency range of 6.3-11.2 GHz for X-band applications in communication engineering.

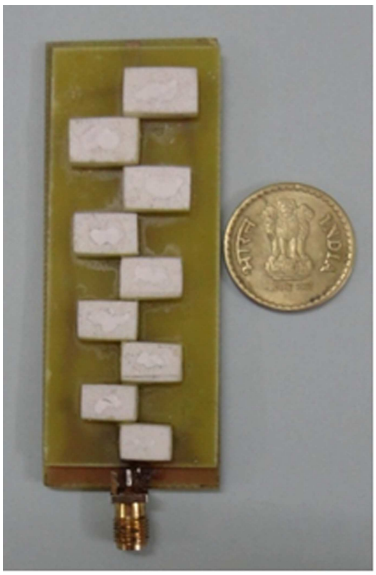

Figure 6.15: The prototype of the fabricated LPDRA with dielectric resonators of low relative permittivity.

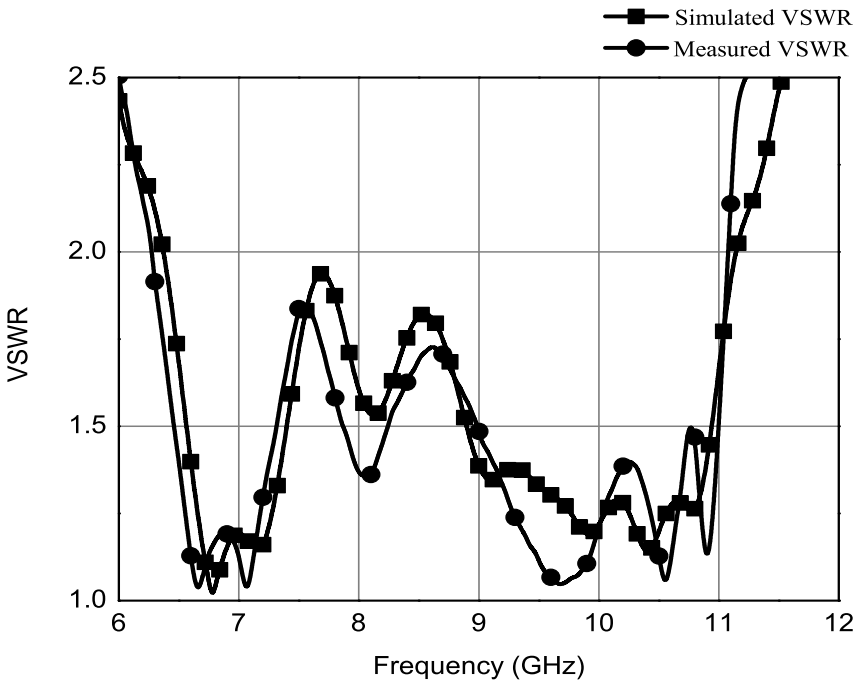

Figure 6.16: Simulated and measured VSWR curves of LPDRA with dielectric resonators of low relative permittivity.

These VSWR results exhibit reasonable agreement although there is a frequency shift that can be attributed to reflection from SMA connector and some uncertainty in the electrical properties of the substrate and dielectric resonators.

The measured impedance bandwidth of the LPDRA array is 56% covering the X-band (6.3-11.2 GHz) which gives a good approximation. Figure 6.17 presents the photograph of fabricated DRA inside an anechoic chamber. The measured results of the proposed LPDRA array are showing a very good gain and radiation patterns curves.

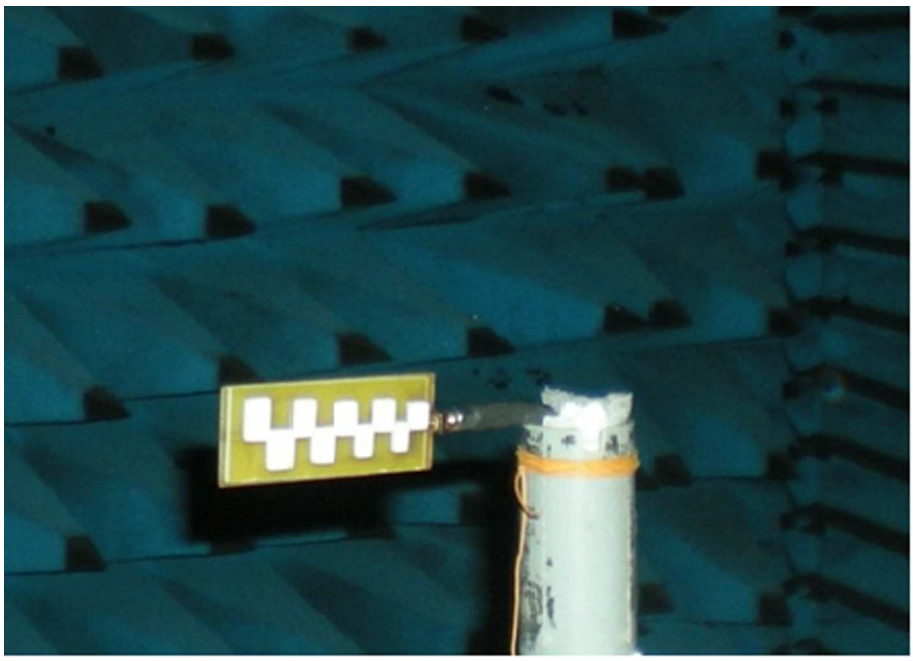

Figure 6.17: Measurement of LPDRA with dielectric resonators of low relative permittivity: Fabricated LPDRA in anechoic chamber

Figure 6.18 plots the measured radiation patterns for E and H-planes at different frequencies, 8.5 GHz and 10.5 GHz. The measured H plane radiation pattern at low frequency is more omnidirectional in compared to high frequency. The E-plane radiation patterns are in the broadside direction against frequency. The measured cross-polar rejection is below -30 dB.

The gain curve for the proposed LPDRA array is shown in Figure 6.19. The gain characteristics of LPDRA array are varying nearly log periodically between 6 to 8.3 dBi with a peak gain of 8.295 dBi at 9.75 GHz frequency.

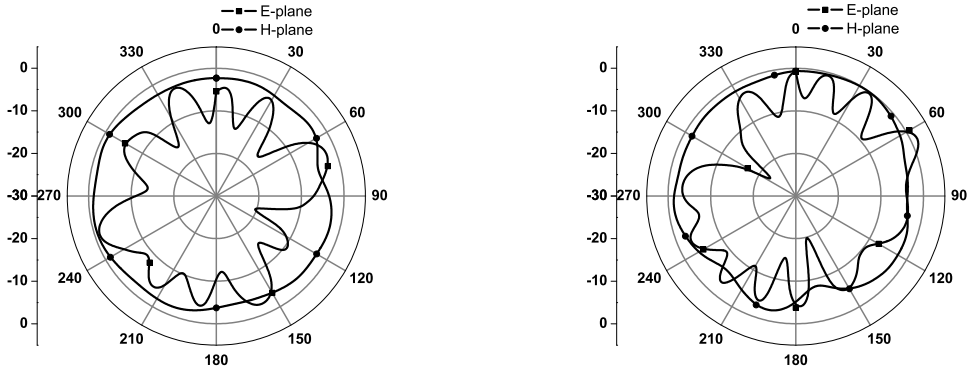

(a) (b)

Figure 6.18: measured E-plane and H-plane radiation patterns of LPDRA with dielectric resonators of low relative permittivity (measured cross polar rejection is below -30 dB). (a)8.5 GHz, and (b) 10.5 GHz.

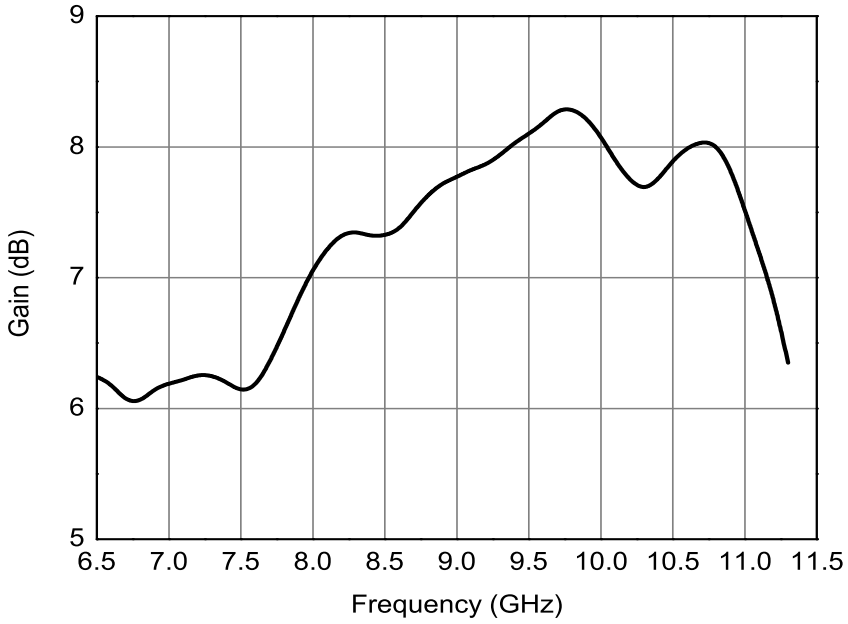

Figure 6.19: Measured Gain curve of LPDRA with dielectric resonators of low relative permittivity.

6.4 Summary

In this chapter, two new wideband LPDRA arrays are investigated. The nine elements LPDRA array with different types of dielectric material are designed to explore its

suitability for wideband high frequency applications.

A wideband LPDRA array is designed for NATO-K band (18- 40 GHz) applications. This array is designed with dielectric resonators of high relative permittivity (ϵ_r = 12). The significant achievements of this LPDRA array design are multi resonant wideband at high frequency. This array provides high efficiency with less metallic losses. With both input match and radiation efficiency consideration, the bandwidth of the LPDRA array with resonators of high relative permittivity is 76% (18 - 40 GHz). The array is providing 95% of simulated antenna efficiency with peak gain of 9.9 dBi.

This array design with high dielectric constant material is suffering from some fabrication limitations. In this case, a ceramic material is used as a dielectric resonator. For the fabrication of the DRA array, the dielectric resonators have to machine into some desired shapes. As the ceramic materials have a tendency to chip or fracture, it can be a risk to machine the ceramic DRs into small sizes.

For ease of fabrication, a wideband nine element LPDRA array with dielectric resonators of low relative permittivity is designed by using low cost, easily available Teflon based dielectric material (ϵ_r = 2.1). Since Teflon based materials are not prone to chipping so it is easy to machine the dielectric resonators into small pieces. The simulated LPDRA is fabricated and experimentally investigated. The measured performances of LPDRA array are in good agreement with the simulated results. This array is providing impedance bandwidth of 56% (6.3 - 11.2 GHz). The maximum gain of this LPDRA array is 8.3 dBi. The simulated antenna efficiency of the array is better than 86%. The proposed LPDRA array covers the X-band for satellite and communication engineering applications.

Both the nine elements LPDRA array designs can be used for wideband high frequency satellite and RADAR applications.

CHAPTER 7

Conclusions and Future Work

The overall contributions of the thesis are briefly discussed in this chapter. Future research problems are also outlined for further investigation on the same or related topics. Some LPDRA array with different types of feeding techniques have been designed, fabricated and experimentally verified to achieve better desired applications. LPDRA arrays designed with the same feeding technique but using different dielectric materials are also analyzed to explore the effect of dielectric material on this array.

7.1 Conclusions

In this thesis, investigation has been done on designing the log periodic dielectric resonator antenna arrays for wideband high frequency applications with reduced amount of conductor losses. The effects of variation in feeding technique on the performance of the log periodic DRA array such as bandwidth, radiation patterns and gain have been studied. The performance of the LPDRA array with alteration in the number of elements, dielectric materials, scaling factor are also verified.

The **FIRST** chapter of the thesis explains the motivation for carrying out this work. The problem statements of the research work and the organization of the thesis are also outlined in this chapter.

In the **SECOND** chapter some techniques to enhance the bandwidth of Dielectric Resonator antenna have been discussed. One of the techniques to improve the bandwidth is using a DRA array instead of single element DRA. The performances of the DRA array such as bandwidth, radiation pattern, gain, efficiency can be further improved by applying the log Periodic technique to DRA arrays. The Log periodic DRA

array has received advantages over single DRAs such as wideband with low metallic loss, high efficiency etc. They also have low cross polarization levels, sufficient gain and bandwidth for practical applications. Compared to microstrip antenna arrays, LPDRA arrays have the flexibility in the feed design. Log Periodic DRA arrays have their applications at microwave and millimeter wave communication and radar systems. Considering these advantages of the log periodic DRA array, efforts have been given to investigate the behavior of log periodic dielectric resonator antennas with a variation in different parameters.

In this thesis, the design of three LPDRA arrays with different feeding techniques have been presented.

In the **THIRD** chapter, a LPDRA array excited by log periodic branched microstrip feed line is developed. This feeding technique results in better coupling of energy in between the dielectric resonator and the feed line. The branched line fed LPDRA array is providing 46% (11.4-18 GHz) of impedance bandwidth. The array offers measured peak gain of 11.2 dBi. The maximum simulated radiation efficiency of the LPDRA is 96%. The designed LPDRA array is suitable for Ku band applications.

A capacitive coupled log periodic dielectric resonator antenna array has been presented in chapter **FOUR**. The LPDRA array is excited by the series microstrip line feeding to avoid the excitation difficulties and to reduce the losses due to branched line feeding. In a capacitive coupled DRA array, all the dielectric resonators along with the feed line are etched on the same substrate and the resonators are capacitively or directly coupled to the feed line. The capacitive coupled LPDRA array offers 65.2% (6.2-12.2 GHz) of impedance bandwidth. The measured gain of the array is 9.2 dBi whereas the simulated radiation efficiency of the array is 94.8%. The proposed LPDRA can be used for X-band applications.

A wideband electromagnetically coupled LPDRA array has been proposed and illustrated in chapter **FIVE**. The LPDRA array is designed with overlaid microstrip feed line. The LPDRA array has multilayer configuration where the dielectric resonators and feed line are etched on different layers of substrate. There is a sufficient isolation between the dielectric resonators and the feed line which reduces the sur-

face wave losses and hence offers a greater flexibility of coupling in the array. The electromagnetically coupled LPDRA array gives 54% (6.5-11.3 GHz) of impedance bandwidth with a measured peak gain of 8.6 dBi. The simulated antenna efficiency of the array is 83% within the desired band.

The propagation characteristics of the above mentioned three LPDRA arrays with different feeding techniques (branched feed line, capacitive coupled feeding and electromagnetically coupled feeding) have been verified by using $k - \beta$ diagram. It has been found that all the LPDRA arrays achieve a good log-periodic action. These LPDRA arrays have been designed with seven dielectric resonators of low relative permittivity (ϵ_r= 2.1). Since the electromagnetically coupled LPDRA array provides greater flexibility of coupling and low surface wave losses, this feeding technique has been selected for further study of the behaviour of log periodic array.

In chapter **SIX**, two nine element LPDRA arrays with overlaid microstrip feed line have been designed. One of the LPDRA arrays is designed for NATO-K band (18-40 GHz) applications using dielectric resonators of high relative permittivity (ϵ_r= 12) and another LPDRA array has been designed for X-band application using dielectric resonators of low relative permittivity (ϵ_r= 2.1).

The impedance bandwidth of the LPDRA array with resonators of high relative permittivity is 76% (18 - 40 GHz). The array is providing 95% of maximum antenna efficiency. The peak gain of the array is 9.9 dBi. On the other hand, the LPDRA array with low relative permittivity material is providing impedance bandwidth of 56% (6.3 - 11.2 GHz) with a peak gain of 8.3 dBi. The array provides the simulated antenna efficiency of better than 86%.

The LPDRA array with high dielectric constant ceramic material is found to perform well for high frequency applications. It has some fabrication limitations as the ceramic material has a tendency to fracture and so it can be risky to machine a dielectric material into a number of small pieces with different dimensions. Both the array designs are verified for variation in number of dielectric resonators and scaling factor values.

In case of array design, the antenna performance depends on the number of ele-

ments. In third, fourth and fifth chapters, the S-parameter or VSWR of all the seven elements LPDRA array have compared with the array having less number of elements (three or five or six) and it has been found that the seven element array is providing better impedance bandwidth. In the sixth chapter, LPDRA arrays with nine elements have been chosen to study the performance of the LPDRA for variation in the number of elements of the array. The nine elements LPDRA provides wideband for high frequency application with low cross-polarization where the cross pol level is less than -30 dB.

In log periodic antenna design, the scaling factor (τ) is the major design factor. The characteristics of the array also depend upon the scaling factor. Thus a parametric study for LPDRA array has been performed for different values of scaling factor. For all the designed antennas, measurement of antenna efficiency could not be possible due to lack of sophisticated equipment. This research work has investigated the usefulness of the log periodic dielectric resonator antenna array as well as their applications for satellite and wireless communications.

7.2 Scope for Future Work

The research work on Log periodic dielectric resonator antenna array presented in the thesis can be further extended in following ways.

In case of aperture-coupled feeding method, the dielectric resonators are directly placed on the ground plane and hence there is no source of surface wave which contributes to losses. Thus, the LPDRA array can be designed with an aperture-coupled feeding method to provide sufficient isolation between the dielectric resonator and the feed circuits which can provide better performance in the wideband frequency range.

There are various techniques for optimizing the performance indices of antenna arrays. The performance of the Log Periodic DRA array may be optimized by implementing suitable optimization techniques. The admittance matrix approach for LPDRA array can be studied as well as the mutual impedance between the elements of LPDRA array may be studied and analyzed.

Recently, reconfigurable antennas are in demand for compact size, cost efficiency,

light weight and small dimension. In case of frequency reconfigurable antenna, similar radiation pattern and gain can be achieved for all designed frequency bands as well as it can reduce the adverse effects of co-site interference and jamming. Reconfiguration of antenna can be achieved by changing the frequency without varying the whole dimension and structure of the antenna. Frequency Reconfigurable Antenna has the ability to reconfigure the resonant frequency by changing the structure, while the radiation patterns and polarization remain unchanged. Thus, a frequency reconfigurable LPDRA array can be possible to design in future for wideband applications. The polarization reconfigurable Log Periodic DRA array may be investigated through the change in the structure of the array.

APPENDIX A

Design Methodology

A.1 Introduction

The techniques used for design, fabrication and measurement of the proposed LPDRA arrays are discussed in the following sections. The design and simulations of the array are carried out using the CST Microwave Studio suite 2012. The simulated antennas after detailed parametric analysis are fabricated using photolithographic method. Network Analyzer is used to measure the S-parameter/VSWR characteristics of the antenna. The gain and radiation patterns of the antennas are measured in anechoic chamber.

A.2 Numerical and Analytical approaches

The following methods are commonly used in electromagnetic (EM) theory.

A.2.1 Analytical method (exact solution)

1. Separation of variables
2. Series expansion
3. Conformal mapping
4. Integral solution, e.g. Laplace and Fourier transformation
5. Perturbation methods

A.2.2 Numerical methods (approximate solutions)

1. Finite difference method
2. Moment method
3. Finite element method
4. Transmission-line modeling

The principles of EM fields and waves are very important for the design and development of antennas as key elements of any wireless communication system. The need for numerical solutions of electromagnetic problems is the best expressed by Paris and Hurd [98]; Most problems that can be solved formally (analytically) have been solved. Until 1940s, the most EM problems were solved using well known Maxwell's equations. These equations describe all electromagnetic phenomena of different structures and configurations. They can be expressed in their either differential or integral forms as given in equations (A.1 to A.8) [4].

A.2.3 Differential form

$$\nabla.\vec{D} = \rho_v \tag{A.1}$$

$$\nabla.\vec{B} = 0 \tag{A.2}$$

$$\nabla \times \vec{E} = -\frac{\partial \vec{B}}{\partial \vec{t}} - \vec{M} \tag{A.3}$$

$$\nabla \times \vec{H} = \vec{J} + \frac{\partial \vec{D}}{\partial t} \tag{A.4}$$

A.2.4 Integral form

$$\oiint \vec{D}.d\vec{s} = Q_{enc} \tag{A.5}$$

$$\oiint \vec{B}.d\vec{s} = 0 \tag{A.6}$$

$$\oint \vec{E}.d\vec{l} = -\frac{\partial \phi_B}{\partial t} \tag{A.7}$$

$$\oint \vec{H}.d\vec{l} = i_{enc} + \epsilon \frac{\partial \phi_E}{\partial t} \tag{A.8}$$

where the vectors $\vec{E}$ and $\vec{H}$ are the electric and magnetic field intensities and are measured in units of [V/m] and [A/m], respectively. The vectors quantities $\vec{D}$ and $\vec{B}$ are the electric and magnetic flux densities and are in units of [C/m^2] and [Wb/m^2]. The scalar quantities $\phi_E = \iint \vec{D}.d\vec{S}$ and $\phi_B = \iint \vec{B}.d\vec{S}$ are the electric and magnetic fluxes and are in units of [C] and [Wb], respectively.

When the EM field problem is complex, an exact solution in a closed form may be difficult to obtain and hence we should solve them by applying numerical techniques. In this thesis, all proposed antenna structures are complex. Hence they can be modeled using commercial simulation software programs which enable us to design, simulate, tune and optimize structure's physical parameters to reach the best design before fabricating prototypes. Currently, there are several numerical techniques that can be used to solve the EM problems, such as the Finite Element (FE) method [99], the Method of Moments (MoM) [100], the Finite Difference Time Domain (FDTD) [101] and the Finite Integration Technique (FIT) [102] etc. The first two methods solve the EM problems in the frequency domain while the other two methods use the time domain.

A.3 Simulation using Finite Integration Technique

The simulation models of the proposed LPDRA arrays are developed using Computer Simulation Technologies Microwave Studio (CST MWS) suite 2012 simulation software [103]. CST MWS is a tool for fast and accurate 3D electromagnetic simulation of high frequency designs. CST MWS is based on the Finite Integration Technique (FIT) [104] which is equivalent to FDTD. FIT is a time-domain numerical technique

for solving Maxwell's equations. Using the function of parametric study in CST MWS simulation programs, the structure physical parameters can be tune and optimize to obtain the best design before going to the fabrication process. CST MWS has different kind of solvers not only a transient solver but also a frequency domain solver, an eigen mode solver and an integral equation solver.

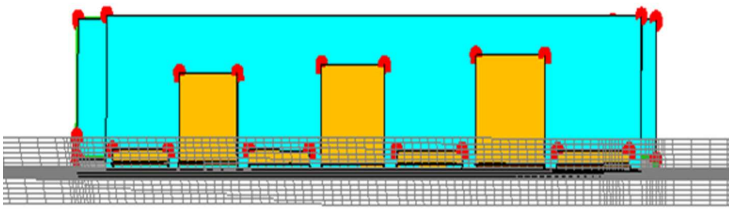

Figure A.1: Meshing of an antenna structure in CST MW studio.

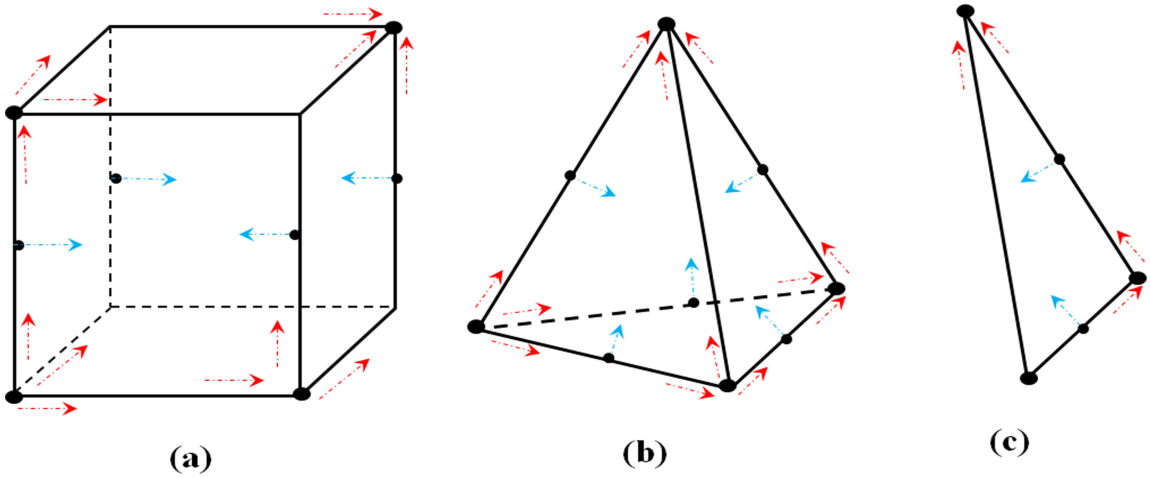

Figure A.2: A single (a) hexahedral, (b) tetrahedral and (c) surface mesh element used in CST MW Studio

In a transient or time-domain solver, the value of the vector electric $\vec{E}$ or magnetic $\vec{H}$ field quantities are computed through time at discrete spatial locations and at discrete time samples. The maximum time step Δt used in the simulation program depends on the minimum mesh step size which can be determined by the density of the mesh used in the meshing process of the whole structure. Therefore the program takes more time to run simulation if the mesh is dense. Once the spatial mesh or discretization is performed by the CST program, the finite integration method is employed. CST has two different mesh types available, i.e. hexahedral and tetrahedral

meshes. Another type of mesh used by the Integral Equation (IE) solver is called surface mesh. Figure A.1 shows a single hexahedral tetrahedral and surface mesh element used in CST program. For complex structures, CST uses a hexahedral mesh in meshing or discretization because it is considered to be very robust. Other solvers use a tetrahedral or surface mesh method. Figure A.2 shows the meshing based on hexahedral shapes of an antenna structure in CST.

The finite integration technique converts the well-known Maxwell equations in their integral form into set of discrete matrix equations called Maxwell grid equations (MGE) as follows [104]:

Integral form ⇒ Matrix form

$$\oiint \vec{D}.d\vec{A} = \iiint_{v} \rho_v d\vec{V} \Longrightarrow [\tilde{S}] = q \tag{A.9}$$

$$\oiint \vec{B}.d\vec{A} = 0 \Longrightarrow [S]b = 0 \tag{A.10}$$

$$\oint \vec{E}.d\vec{l} = -\iiint_{A} \frac{\partial \vec{B}}{\partial t} d\vec{A} \Longrightarrow [C]e = -\frac{d}{dt}b \tag{A.11}$$

$$\oint \vec{H}.d\vec{l} = -\iint_{A} \left[\frac{\partial \vec{A}}{\partial t} + J\right] d\vec{A} \Longrightarrow [\tilde{C}]h = -\frac{d}{dt}d + j \tag{A.12}$$

where $[\tilde{S}]$,[S],[C] and $[\tilde{C}]$ are square matrices represent the discrete curl and divergence operators, respectively and their sizes depend on the problem geometry. 'e' and 'h' represent the electric and magnetic grid voltages and they are related to the electric and magnetic fields according to $e = \int_{\partial A} \vec{E}.d\vec{l}$ and $h = \int_{\partial \tilde{C}} \vec{H}.d\vec{l}$ d and b are the electric and magnetic facet flux vectors over the mesh cell.

The antenna geometry is obtained in CST by specifying the coordinates for each point of the structure along with appropriate material specifications. The metallizations are specified as copper to precisely account for the losses. A finite metal with a thickness of 0.05 mm is assigned in all the simulations. The substrates and dielectric resonators can be assigned from either the in-built material data base or user-defined.

For all the investigated designs FR4 (ϵ_s=4.4) as a dielectric substrate and Teflon (ϵ_r =2.1) as a dielectric resonator are selected. The frequency sweep is then defined to get solutions for all wanted frequencies and a waveguide port is assigned to excite the antennas.

CST gives the user an option to choose from its pre-defined templates like, in this case, the planar antenna template which automatically assigns the boundary conditions, mesh type, mesh size etc. or it can as well be user-defined. From the simulated results, the antenna parameters like S-parameter/ VSWR and the input impedances are plotted as a function of frequency. The antenna geometry can then be appropriately optimized for the desired S-parameter/VSWR. The gain and radiation patterns of the array are also determined at the specified frequencies.

A.4 Antenna Fabrication and Measurements

All the antennas investigated in the thesis are fabricated using the photolithographic technique and milling machine techniques. The photo lithographic technique is a chemical etching process by which the unwanted metal regions of the metallic layer are removed so that the intended design is obtained. The milling machine technique refers to the removal of metal from the substrate using a tool which has several cutting points and is rotating about its axis. The pieces of dielectric resonators (DRs) are fixed at the appropriate position on the substrate using a permanent adhesive (epoxy). The selection of a proper substrate and dielectric resonator is the essential part in DRA design. The antennas are excited by using different types of feeding methods with 50 ohm feed line. The setup for design methodology of LPDRAs is shown in Figure A.3

A.4.1 S-Parameter/VSWR Measurement

The HP 872OB network analyser (NA) having range 130 MHz to 20 GHz is used for S-parameter/VSWR measurement of all the LPDRAs. The specific port of the analyzer should be calibrated prior to the measurement in the frequency range of interest using the standard open, short and matched load. The antenna under test

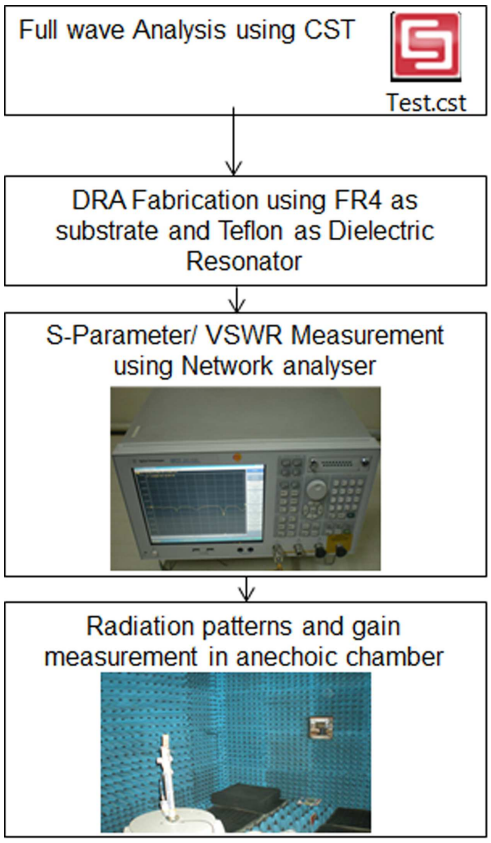

Figure A.3: Setup for design methodology of LPDRA.

(AUT) is connected to any one of the port of the NA. The bandwidth can be directly obtained from the S-parameter data by noting the range of frequencies over which the S-parameter is less than or equal to -10 dB. The range of frequency between the 2:1 voltage standing wave ratio (VSWR) points is the alternate way to obtain the bandwidth of the antenna.

The frequency bandwidth of an antenna can be expressed in terms of either the absolute bandwidth (ABW) or the fractional bandwidth (FBW). Assuming that the antenna bandwidth has a lower edge frequency of f_L, an upper edge frequency of f_H and a center frequency of f_c. The ABW is defined as the difference between the upper and the lower edge frequencies of operation while the FBW can be defined as the percentage of the ratio between the absolute bandwidth and the center frequency.

$$ABW = f_H - f_L \tag{A.13}$$

$$FBW = ABW/f_c = (f_H - f_L)/f_c \tag{A.14}$$

where the center frequency f_c=(f_H+f_L)/2.

The band width of the antenna, usually expressed as the percentage of bandwidth which is given as.

$$\%BW = 2\left[\frac{f_H - f_L}{f_H + f_L}\right] \times 100\% \tag{A.15}$$

A.4.2 Anechoic Chamber

The measurement of a test antenna should be taken in a free space environment to avoid the interference. In a normal laboratory environment, the power reflected from the walls and the various instruments of the laboratory may interfere with the power radiated by the test antenna which results in performance degradation of the AUT. The free space can be artificially created by an anechoic chamber. The anechoic chamber is an acoustic free room to minimize the spurious signals during pattern measurements. The chamber is constructed by covering the entire interior surface of a room with microwave absorbers having good coefficient of absorption in the frequency range of interest. The microwave absorbers are made up of pyramidal or wedge shaped high quality polyurethane foam to avoid the EM reflections and results in a good impedance matching for the radiation pattern measurement of AUT.

A.4.3 Radiation pattern Measurement

The antenna is kept inside the anechoic chamber for radiation pattern measurement. The AUT and the standard transmitting antenna are connected to the ports of the network analyzer. A wideband horn is used as a transmitter. The system automatically undergoes through calibration prior to the measurement. The radiation patterns of the antenna at multiple frequency points have been measured in a single rotation of the test antenna. The entire measured data are stored in ASCII format and used for further processing like analysis and plotting. The co-polar and cross-polar radiation patterns in E-Plane and H-plane of the test antenna are obtained after the analysis

of the stored patterns.

A.4.4 Antenna Gain Measurement

The gain transfer method using a standard gain antenna is employed to determine the absolute gain of the AUT. The setup for the measurement of gain is the same as that used for radiation pattern measurement. The AUT is kept inside the chamber and connected to one of the Port of the Network Analyzer and the other port is connected to the transmitting horn antenna. The relative power level is obtained from the analyzer and this provides the gain with respect to the reference antenna. The gain of the reference antenna is added to the relative gain to obtain the gain of the AUT. The gain measurement method is based on Friis transmission formula as given by equation (A.17) [91].

$$(G_t + G_r)_{dB} = 20\log_{10}\left(\frac{4\pi R}{\lambda}\right) + 10\log_{10}\left(\frac{P_r}{P_t}\right) \tag{A.16}$$

where,

$(G_t)_{dB}$= gain of the transmitting antenna (dB)

$(G_r)_{dB}$= gain of the receiving antenna (dB)

P_r= received power (W)

P_t= transmitted power (W)

R= antenna separation (m)

λ= operating wavelength (m)

From the measured value of R, λ and P_r/P_t, the gain of the antenna has been calculated.

Bibliography

[1] T. S. Rappaport, *Wireless Communications*. Principles and Practice. Prentice Hall, 1996.

[2] A. Petosa, *Dielectric Resonator Antenna Handbook*. Artech House Publishers, Norwood, USA, 2007.

[3] K. M. Luk and K. W. Leung, *Dielectric Resonator Antennas*. Herttordshire, U.K.: Research Studies Press Ltd, 2002.

[4] D. Pozar, *Microwave Engineering*. New York: Wiley, 3rd ed., 2005.

[5] S. Y. Liao, *Microwave devices and circuits*. Prentice-Hall, 3rd ed., 1996.

[6] D. E. Isbell, "Log periodic dipole arrays," *IRE Trans. Antennas Propag.*, vol. 8, no. 3, pp. 260–267, 1960.

[7] R. Pantoja, A. Sapienza, and F. M. Filho, "A microwave printed planar log-periodic dipole array antenna," *IEEE Transactions on antennas and propagation*, vol. AP35, pp. 1176–1178, Oct. 1987.

[8] Q.Wu, R.Jin, and J.Geng, "A single-layer ultra wideband microstrip antenna," *IEEE Transactions on Antennas and Propagation*, vol. 58, pp. 211–214, Jan. 2010.

[9] P. Hall, "New wideband microstrip antenna using log-periodic technique," *Electron. Lett.*, vol. 16, pp. 127–128, Feb. 1980.

[10] H. Pues, J. Bogaers, R. Pieck, and A. V. Capelle, "Wideband quasilog-periodic microstrip antenna," *IEE Proc. H, Microwaves, Opt. & Antennas*, vol. 128, no. 3, pp. 159–163, 1981.

[11] G. H. Zhai, W. Hong, K. Wu, and Z. Q. Kuai, "Wideband substrate integrated printed log-periodic dipole array antenna," *IET Microw. Antennas Propag.*, vol. 4, no. 7, pp. 899–905, 2010.

[12] J. Yang and K. Per-Simon, "Optimization of reflection coefficient of large log-periodic array by computing only a small part of it," *IEEE Transactions on Antennas and Propagation*, vol. 59, pp. 1790–1797, Jun. 2011.

[13] R. Carrel, "The design of the log-periodic dipole antenna," *IRE Int. Conv. Rec.*, vol. 9, p. 6175, 1961.

[14] J. Carr, "Some variations in log-periodic antenna structures," *IRE Trans. Antennas Propag.*, vol. 9, no. 2, pp. 229–230, 1961.

[15] R. K. Mongia and P. Bhartia, "Dielectric resonator antennasa review and general design relations for resonant frequency and bandwidth," *Int. J. Microwave Millimeter-Wave Eng.*, pp. 230–247, Jul. 1994.

[16] A. Petosa, A. Ittipiboon, Y. Antar, D. Roscoe, and M. Cuhaci, "Recent advances in dielectric resonator antenna technology," *IEEE Antennas Propag Mag.*, vol. 40, pp. 35–48, 1998.

[17] R. D. Richtmeyer, "Dielectric resonators," *Journal of Applied physics*, vol. 15, pp. 391–398, 1939.

[18] A. Okaya and L. Barash, "The dielectric microwave resonator," *Proceedings of the IRE*, vol. 50, pp. 2081–2092, 1962.

[19] M. T. Sebastian, *Dielectric Materials for Wireless Communication*. Linacre House, Jordan Hill, Oxford, UK: Elsevier, 1st ed., 2008.

[20] S. Long, M. W. McAllister, and L. Shen, "The resonant cylindrical dielectric cavity antenna," *IEEE Transactions on Antenna and Propagations*, vol. 31, pp. 406–412, 1983.

[21] M. McAllister, G. L. Conway, and S. Long, "Rectangular dielectric-resonator antenna," *IEE Electronics Letters*, vol. 19, pp. 218–219, 1983.

[22] J. L. Volakis, *Antenna Engineering Handbook*. New York, Chicago: McGraw-Hill Education, 4th ed., 2007.

[23] R. Mongia and A. Ittipiboon, "Theoretical and experimental investigations on rectangular dielectric resonator antennas," *IEEE Transactions on Antennas and Propagation*, vol. 45, no. 9, pp. 1348–1356, 1997.

[24] G. P. Junker, A. A. Kishk, A. W. Glisson, and D. Kajfez, "Effect of an air gap around the coaxial probe exciting a cylindrical dielectric resonator antenna," *IEEE Electronics Letters*, vol. 30, pp. 177–178, Feb. 1994.

[25] G. P. Junker, A. A. Kishk, and A. W. Glisson, "Input impedance of dielectric resonator antennas excited by a coaxial probe," *IEEE Transactions on Antennas & Propagation*, vol. 42, pp. 960–966, Jul. 1994.

[26] R. A. Kranenburg and S. A. Long, "Microstrip transmission line excitation of dielectric resonator antennas," *Electronics Letters*, vol. 24, pp. 1156–1157, Sept. 1988.

[27] R. K. Mongia, A. Ittipiboon, and M. Cuhaci, "Experimental investigations on microstrip fed series dielectric resonator antenna array," *Symposium on Antenna Technology and Applied Electromagnetics ANTEM 94*, pp. 81–84, Aug. 1994.

[28] R. A. Kranenburg and S. A. Long, "Microstrip transmission line excitation of dielectric resonator antennas," *Electronics Letters*, vol. 24, pp. 1156–1157, Sept. 1988.

[29] J. T. H. S. Martin and Y. M. M. Antar, "Dielectric resonator antenna using aperture coupling," *Electronics Letters*, vol. 26, pp. 2015–2016, Nov. 1990.

[30] D. M. Pozar and B. Kaufmann, "Increasing the bandwidth of a microstrip antenna by proximity coupling," *Electron. Lett.*, vol. 23, pp. 368–369, 1987.

[31] H. G.Oltman and D. A. Huebner, "Electromagnetically coupled microstrip dipoles," *IEEE Trans. On Antennas and Propagation*, vol. AP-29, pp. 151–157, 1981.

[32] A. Petosa, R. K. Mongia, A. Ittipiboon, and J. S. Wight, "Investigation of various feed structures for linear arrays of dielectric resonator antennas," *IEEE Antennas & Propagation Symposium Digest AP-S 1995*, pp. 1982–1985, 1995.

[33] M. Wyville, A. Petosa, and J. S. Weight, "Dig feed for dra arrays," *IEEE Antennas & Propagation Symposium Digest AP-S 2005*, vol. 2b, pp. 176–179, 2005.

[34] M. Aras, M. Rahim, Z. Rasin, and M. A. Aziz, "An array of dielectric resonator antenna for wireless application," *IEEE International RF and Microwave Conference Proceedings*, pp. 459–463, Dec. 2008.

[35] K. Wong and C. H. Wu, "Wide-band omnidirectional square cylindrical metal-plate monopole antenna," *IEEE Transactions on Antennas and Propagation*, vol. 53, pp. 2758–2761, Aug. 2005.

[36] K. L. Lau and K. M. Luk, "A wide-band circularly polarized l-probe coupled patch antenna for dual-band operation," *IEEE Transactions on Antennas and Propagation*, vol. 53, pp. 2636–2644, Aug. 2005.

[37] W. S. Lee, D. Z. Kim, K. J. Kim, and J. W. Yu, "Wideband planar monopole antennas with dual band-notched characteristics," *IEEE Transactions on Microwave Theory and Techniques*, vol. 54, pp. 2800–2806, Jun. 2006.

[38] K. Ryu and A. Kishk, "Ultrawideband dielectric resonator antenna with broadside patterns mounted on a vertical ground plane edge," *IEEE Transactions on Antennas and Propagation*, vol. 58, no. 4, pp. 1047–1053, 2010.

[39] O. Ahmed, A. Sebak, and T. Denidni, "Compact uwb printed monopole loaded with dielectric resonator antenna," *Electronics Letters*, vol. 47, Jan. 2011.

[40] M. Abedian, S. K. A. Rahim, and M. Khalily, "Two-segments compact dielectric resonator antenna for uwb application," *IEEE Antennas and Wireless Propagation Letters*, vol. 11, pp. 1533–1536, 2012.

[41] R. Chair, A. A. Kishk, and K. F. Lee, "Wideband stair-shaped dielectric resonator antennas," *IET Microw. Antennas Propag.*, vol. 1, pp. 299–305, Apr. 2007.

[42] J. R. Costa, C. A. Fernandes, G. Godi, R. Sauleau, L. L. Coq, and H. Legay, "Compact ka-band lens antennas for leo satellites," *IEEE Transactions on Antennas and Propagation*, vol. 56, pp. 1251–1258, May 2008.

[43] E. Arnieri, L. Boccia, and G. Amendola, "Ka-band dual-frequency radiator for array applications," *IEEE Antennas and Wireless Propagation Letters*, vol. 8, pp. 894–897, 2009.

[44] T. Denidni and Q. Rao, "Design, analysis and measurement of a new dual-band compact hybrid resonator antenna," *Int J RF Microwave Comput Aided Eng.*, vol. 16, pp. 629–634, 2006.

[45] R. Kumari and S. Behera, "Ring dielectric resonator antenna for broadband applications," pp. 7–10, Nov. 2010.

[46] H. Khalil, S. Bila, M. Aubourg, D. Baillargeat, S. Verdeyme, F. Jouve, C. Delage, and T. Chartier, "Shape optimized design of microwave dielectric resonators by level-set and topology gradient methods," *Int J RF Microwave Comput Aided Eng.*, vol. 20, pp. 33–41, Jan. 2010.

[47] H. Khalil, M. A. S. Bila, D. Baillargeat, S. Verdeyme, F. Jouve, and T. Chartier, "Shape optimization of a dielectric resonator for improving its unloaded quality factor," *Int J RF Microwave Comput Aided Eng.*, vol. 21, pp. 120–126, Jan. 2011.

[48] R. Kumari and S. K. Behera, "Miniaturized dual band dielectric resonator antenna for ieee 802.16d fixed wimax applications," *Int. J RF Microwave Comput Aided Eng.*, vol. 22, pp. 682–689, Nov. 2012.

[49] R. Kumari and S. K. Behera, "Mushroom shaped dielectric resonator antenna for wimax applications," *Microwave Opt Technol Lett.*, vol. 55, pp. 1360–1365, Jun. 2013.

[50] R. Chair, A. A. Kishk, and K. Lee, "Wideband simple cylindrical dielectric resonator antenna," *IEEE Microwave and Wireless Components Lett.*, vol. 15, pp. 241–243, Apr. 2005.

[51] C. S. D. Young and S. A. Long, "Wideband cylindrical and rectangular dielectric resonator antennas," *IEEE Antennas and Wirel. Propag. Lett.*, vol. 53, pp. 126–129, 2006.

[52] S. H. Ong, A. A. Kishk, and A. W. Glisson, "Rod-ring dielectric resonator antenna," *Int J RF Microwave Comput Aided Eng.*, vol. 14, pp. 441–446, Aug. 2004.

[53] A. K. Bhattacharyya, "Effects of finite ground plane on the radiation characteristics of a circular patch antenna," *IEEE Transactions on Antennas Propag.*, vol. 38, pp. 152–159, Feb. 1990.

[54] T. H. Chang and J. F. Kiang, "Sectorial-beam dielectric resonator antenna for wimax with bent ground plane," *IEEE Transactions on Antennas and Propag.*, vol. 57, pp. 563–567, Feb. 2009.

[55] T. Chang and J. F. Kiang, "Sectorial-beam dielectric resonator antenna for wimax with bent ground plane," *IEEE Trans Antennas Propag.*, vol. 57, pp. 563–567, 2009.

[56] J. Huang, "The finite ground plane effect on the microstrip antenna radiation patterns," *IEEE Trans Antennas Propag.*, vol. 31, pp. 649–653, 1983.

[57] D. Guha and Y. M. M. Antar, "Four-element cylindrical dielectric resonator antenna for wideband monopole-like radiation," *IEEE Transactions on Antennas and Propagation*, vol. 54, pp. 2657–2662, Sept. 2006.

[58] A. Al-Zoubi, A. Kishk, and A. Glisson, "A linear rectangular dielectric resonator antenna array fed by dielectric image guide with low cross polarization," *IEEE Transactions on Antennas and Propagation*, vol. 58, pp. 697–705, Mar. 2010.

[59] R. Tian, V. Plicanic, B. K. Lau, and Z. Ying, "A compact six-port dielectric resonator antenna array: Mimo channel measurements and performance analysis," *IEEE Transactions on Antennas and Propagation*, vol. 58, pp. 1369–1379, Apr. 2010.

[60] A.G.Walsh, S.D.Young, and S.A.Long, "An investigation of stacked and embedded cylindrical dielectric resonator antennas," *IEEE Antennas and Wireless Propagation Letters*, vol. 5, pp. 130–133, 2006.

[61] A. A. Kishk, H. A. Auda, and B. C. Ahn, "Radiation characteristics of cylindrical dielectric resonator antenna with new applications," *IEEE Transactions Antennas Propagation. Soc. Newsletter*, vol. 31, pp. 6–16, Feb. 1989.

[62] A. A. Kishk, M. R. Zunoubi, and D. Kajfez, "A numerical study of a dielectric disk antenna above grounded dielectric substrate," *IEEE Transactions Antennas Propagation.*, vol. 41, pp. 813–821, Jun. 1993.

[63] A. A. Kishk, X. Zhang, A. Glisson, and D. Kajfez, "Numerical analysis of stacked dielectric resonator antenna excited by a coaxial probe for wideband applications," *IEEE Transactions Antennas Propag.*, vol. 51, p. 19962006, Aug. 2003.

[64] A. A. Kishk, B. Ahn, and D. Kajfez, "Broadband stacked dielectric resonator antennas," *Electronic Letter.*, vol. 25, pp. 1232–1233, Aug. 1989.

[65] M. H. A. Sharkawy, A. Z. Elsherbeni, and C. E. Smith, "Stacked elliptical dielectric resonator antennas for wideband," *IEEE Antennas and Propagation Society Int. Symposium*, vol. 2, pp. 1371–1374, Jun. 2004.

[66] K. Leung, "Conformal strip excitation of dielectric resonator antenna," *IEEE Transactions on Antennas and Propagation*, vol. 48, no. 6, pp. 961–967, 2000.

[67] T. A. Denidni, Q. Rao, and A. R. Sebak, "Broadband l-shaped dielectric resonator antenna," *IEEE Antennas and Wireless Propagation Letter*, vol. 4, pp. 453–454, 2005.

[68] T. H. Chang, Y. C. Huang, W. F. Su, and J. F. Kiang, "Wideband dielectric resonator antenna with a tunnel," *IEEE Antennas Wireless Propagation Letter*, vol. 7, pp. 275–278, Sept. 2008.

[69] W. Chang and Z. Feng, "Investigation of a novel wideband feeding technique for dielectric ring resonator antennas," *IEEE Antennas Wireless Propagation Letters*, vol. 8, pp. 348–351, 2009.

[70] Y. Pan and K. W. Leung, "Wideband circularly polarized trapezoidal dielectric resonator antenna," *IEEE Antennas Wireless Propagation Letters*, vol. 9, pp. 588–591, 2010.

[71] M. I. Sulaiman and S. K. Khamas, "A singly fed wideband circularly polarized dielectric resonator antenna using concentric open half-loops," *IEEE Antennas Wireless Propagation Letters*, vol. 10, pp. 1305–1308, 2011.

[72] X. S. Fang and K. W. Leung, "Designs of single-, dual-, wide-band rectangular dielectric resonator antennas," *IEEE Transactions on Antennas and Propagation*, vol. 59, pp. 2409–2414, Jun. 2011.

[73] Y. Ge, K. P. Esselle, and T. S. Bird, "Compact dielectric resonator antennas with ultrawide 60110Propagation, vol. 59, pp. 3445–3448, Sept. 2011.

[74] G. Drossos, Z. Wu, and L. E. Davis, "Four-element planar arrays employing probe-fed cylindrical dielectric resonator antennas," *Microw.Opt. Technol. Lett.*, vol. 18, no. 5, pp. 315–319, 1998.

[75] L. Moustafa and B. Jecko, "Design of a wideband highly directive ebg antenna using double-layer frequency selective surfaces and multi feed technique for application in the ku-band," *IEEE Antennas Wireless Propagation Letter*, vol. 9, pp. 342–346, 2010.

[76] A. Borji, D. Busuioc, and S. Safavi-Naeini, "Efficient, low-cost integrated waveguide-fed planar antenna array for ku-band applications," *IEEE Antennas Wireless Propagat. Lett.*, vol. 8, pp. 336–339, 2009.

[77] N. Ghassemi, K. Wu, S. Claude, X. Zhang, and J. Bornemann, "Compact coplanar waveguide spiral antenna with circular polarization for wideband applications," *IEEE Antennas Wireless Propagation Letter*, vol. 10, pp. 666–669, 2011.

[78] A. Buerkle, K. Sarabandi, and H. Mosallaei, "Compact slot and dielectric resonator antenna with dual-resonance, broadband characteristics," *IEEE Transactions on Antennas and Propagation*, vol. 53, pp. 1020–1027, Mar. 2005.

[79] T. W. Li and J. S. Sun, "Dual-frequency dielectric resonator antenna with inverse t-shape parasitic strip," *IEEE International conference on wireless communications and Applied Computational Electromagnetics*, p. 384387, Apr. 2005.

[80] P. Hall, "Multioctave bandwidth log-periodic microstrip antenna array," *IEE Proceedings*, vol. 133, pp. 127–136, Apr. 1986.

[81] S. H. Kim, J. H. Choi, J. W. Baik, and Y. S. Kim, "Cpw-fed log-periodic dumb-bell slot antenna array," *Electronics Letter*, vol. 42, pp. 436–438, 2006.

[82] S. Y. Chen, P. H. Wang, and P. Hsu, "Uniplanar log-periodic slot antenna fed by a cpw for uwb applications," *IEEE Antennas Wireless Propagation Letter*, vol. 5, pp. 256–259, 2006.

[83] D. E. Anagnostou, J. Papapolymerou, M. M. Tentzeris, and C. G. Christodoulou, "A printed log-periodic koch-dipole array (lpkda)," *IEEE Antennas and Wireless Propagation Letters*, vol. 7, pp. 456–460, 2008.

[84] Y. H. Baek, L. H. Truong, S. W. Park, S. J. Lee, Y. S. Chae, E. H. Rhee, H. Park, and J. K. Rhee, "94-ghz log-periodic antenna on gaas substrate using air-bridge structure," *IEEE Antennas and Wireless Propagation Letters*, vol. 8, pp. 909–911, 2009.

[85] J. Yang, "On conditions for constant radiation characteristics for log-periodic array antennas," *IEEE Transactions on Antennas and Propagation*, vol. 58, pp. 1521–1526, May 2010.

[86] J. R. Mruk, W. N. Kefauver, and D. S. Filipovic, "Band rejection methods for planar log-periodic antennas," *IEEE Transactions on Antennas and Propagation*, vol. 58, pp. 2288–2294, Jul. 2010.

[87] M. R. Hamid, P. S. Hall, and P. Gardner, "Frequency reconfigurable log periodic patch array," *Electronics Letters*, vol. 46, pp. 1648–1650, Dec. 2010.

[88] H. Jardon-Aguilar, J. A. Tirado-Mendez, R. Flores-Leal, and R. Linares-Miranda, "Reduced log-periodic dipole antenna using a cylindrical-hat cover," *IET Microwave Antennas Propagation*, vol. 5, pp. 1697–1702, Nov. 2011.

[89] C. Yu, W. Hong, L. Chiu, G. Zhai, C. Yu, W. Qin, and Z. Kuai, "Ultra wideband printed log-periodic dipole antenna with multiple notched bands," *IEEE Transactions on Antennas and Propagation*, vol. 59, pp. 725–732, Mar. 2011.

[90] U. H. Park, H. S. Noh, S. H. Son, K. H. Lee, and S. I. Jeon, "A novel mobile antenna for ku-band satellite communications," *ETRI Journal*, vol. 27, pp. 243–249, Jun. 2005.

[91] C. A. Balanis, *Antenna Theory: Analysis and Design*. Hoboken, New Jersey: John Wiley & Sons, Inc.,, 3rd ed., 2005.

[92] R. Mittra and K. Jones, "Theoretical brillouin (k-beta) for monopole and dipole arrays and their application to log periodic antennas," *IEEE Transactions on Antennas and Propagation*, vol. 12, pp. 533–540, Sept. 1964.

[93] E. Y. Jung, J. W. Lee, T. K. Lee, and W. K. Lee, "Siw-based array antennas with sequential feeding for x-band satellite communication," *IEEE Transactions on Antennas and Propagation*, vol. 60, pp. 3632–3639, Aug. 2012.

[94] S. H. Hsu, Y. J. Ren, and K. Chang, "A dual-polarized planar-array antenna for s-band and x-band airborne applications," *IEEE Antennas and Propagation Magazine*, vol. 51, pp. 70–78, Aug. 2009.

[95] C. K. Campbell, I. Traboulay, M. S. Suthers, and H. Kneve, "Design of a stripline log-periodic dipole antenna," *IEEE Transactions on Antennas and Propagation*, vol. 25, pp. 718–721, Sept. 1977.

[96] L. Juan, F. Guang, and Y. Lin, "Design of a dual-polarized wideband short backfire antenna with high gain," *IET Microwave Antennas Propag.*, vol. 7, no. 9, pp. 735–740, 2013.

[97] D. Zhou, R. Abd-Alhameed, C. See, A. Alhaddad, and P. Excell, "Compact wideband balanced antenna for mobile handsets," *IET Microwave Antennas Propag.*, vol. 4, no. 5, pp. 600–608, 2010.

[98] D. Paris and F. Hurd, *Basic Elctromagnetics Theory*. Newyork: McGraw-Hill, 1969.

[99] N. Bastos and J. P. A. Sadowski, *Electromagnetic Modeling by Finite Element Methods*. NewYork: Marcel Dekker, Inc, 2003.

[100] W. C. Gibson, *The Method of Moments in Electromagnetics*. Chapman & Hall/CRC, Taylor & Francis Group, 2008.

[101] A. Taflove and S. C. Hagness, *Computational Electrodynamics: The Finite-Difference Time-Domain Method*. Artech House, third edition ed., 2005.

[102] D. Swason, *Microwave Circuit Modeling using Electromagnetic Field Simulation*. ARTECH House, 2003.

[103] . User Manual for the CST. IMST GmbH, Germany

[104] M. Clements and T. Weiland, "Discrete electromagnetism with the finite integration technique," *Progress In Electromagnetics Research*, vol. 32, pp. 65–87, 2001.

Disseminations

Journal papers Published/Accepted

1. **Runa Kumari**, Santanu Kumar Behera, "Investigation on Log Periodic Dielectric Resonator Antenna Array for Ku band Applications", *Taylor Francis, Electromagnetics, 34(1):19-33, 2014.*

2. **Runa Kumari** and Santanu Kumar Behera, "Wideband Log Periodic Dielectric Resonator Array with Overlaid Microstrip Feed Line", *IET Microwave, Antenna and Propagation, 7(7):582-587, 2013.*

3. **Runa Kumari** and Santanu Kumar Behera, "Nine Element Frequency independent Dielectric Resonator Array for X- band Applications", *Microwave Opt. Technol. Lett.(MOTL Wiley), 55(2):400-403, 2013.*

4. **Runa Kumari** and Santanu Kumar Behera, "Design of Log Periodic Dielectric Resonator Array for NATO-K band Applications", *International Journal of Signal and Imaging Systems Engineering.* (Accepted)

5. **Runa Kumari** and Santanu Kumar Behera, "Mushroom Shaped Dielectric Resonator Antenna for WiMAX Applications", *Microwave Opt. Technol. Lett.(MOTL Wiley), 55(6):1360-1365, 2013.*

6. **Runa Kumari**, Santanu Kumar Behera, "Miniaturized Dual band Dielectric Resonator Antenna for IEEE 802.16d Fixed WiMAX Applications", *International Journal of RF and Microwave Computer Aided Engineering (Wiley) USA, 22(6):682-689 2012*

Conference papers Published/Accepted

1. **Runa Kumari**, S K Behera and S K Sharma, "Aperture Coupled Wideband Dielectric Resonator Antenna Array with Polarization Reconfiguration" *Applied Electromagnetic Conference (AEMC-2013), Bhubaneswar, India, Dec. 2013.*

2. **Runa Kumari** and S K Behera, "Mutual Coupling Reduction in C-shaped Dielectric Resonator Antenna array for MIMO Applications", *Annual IEEE India Conference (INDICON), Cochin, India, Dec 2012.*

3. **Runa Kumari** and S K Behera, "A Compact Dual Resonance Dielectric Resonator Antenna Array with partial ground plane", *IEEE International Conference on Recent Advances in Information Technology, (RAIT), Dhanbad, India, Mar 2012.*

4. **Runa Kumari**, Kapil Parmar and S K Behera, "A Dual band Triangular shaped DRA Array for WLAN/WiMAX Applications", *Annual IEEE India Conference (INDICON), Hyderabad, India, Dec 2011.*

5. **Runa Kumari**, and S K Behera, "Log Periodic Dielectric Resonator Antenna for Broadband Applications", *International Symposium on Devices MEMS Intelligent Systems and Communication (ISDMISC), Sikkim, India, Apr 2011.*

6. **Runa Kumari**, S K Behera and R K Mishra, "Log Periodic Dielectric Resonator Antenna for K and Ka-band Applications", *Procc. On International Conference on Electronic Systems, page 264-267, Rourkela, India, Jan 2011.*

7. **Runa Kumari**, Kapil Parmar and S K Behera, "Conformal Patch Fed Stacked Triangular Dielectric Resonator Antenna for WLAN Applications", *IEEE International conference on Emerging Trends in Robotics and Communication Technologies, (INTERACT), Chennei, India, Dec 2010.*

8. **Runa Kumari**, and S K Behera, "Ring Dielectric Resonator Antenna for Broadband Applications", *IEEE International Conference on Computational Intelligence and Communication Systems, (CICN), Bhopal, India, Nov 2010.*

Journal papers Communicated/To be communicated

1. **Runa Kumari** Santanu Kumar Behera, "Log Periodic Dielectric Resonator Antenna Array antenna with series fed microstrip line for X-band Applications", *Taylor Francis, Electromagnetics.* (To be communicated)

BIO-DATA

Runa Kumari

Date of Birth: 15^{st} July, 1981

Correspondence:
PhD Scholar, Department of Electronics and Communication Engineering,
National Institute of Technology Rourkela, India – 769 008.

Ph: +91 9778364955 (F)

e-mail: runakumari15@gmail.com

Qualification

- Ph.D. (Continuing)
  National Institute of Technology Rourkela, India
- M.Tech. (Electronics and Communication Engineering)
  National Institute of Science and Technology Berhampur,Odisha India [First division]
- B.E.
  Dhaneswar Rath Institute of Engineering and Management Studies, Odisha, India [First division]

Senior Lecturer, NIST, Berhampur, Odisha, India, May 2008 – Dec 2009

Lecturer, SIET, Dhenkanal, Odisha, India, Sept 2005 – Aug 2006

Publications

- 8 Journal articles;
- 1 Journal article to be communicated;
- 14 Conference articles.